



<https://theses.gla.ac.uk/>

Theses Digitisation:

<https://www.gla.ac.uk/myglasgow/research/enlighten/theses/digitisation/>

This is a digitised version of the original print thesis.

Copyright and moral rights for this work are retained by the author

A copy can be downloaded for personal non-commercial research or study,
without prior permission or charge

This work cannot be reproduced or quoted extensively from without first
obtaining permission in writing from the author

The content must not be changed in any way or sold commercially in any
format or medium without the formal permission of the author

When referring to this work, full bibliographic details including the author,
title, awarding institution and date of the thesis must be given

Enlighten: Theses

<https://theses.gla.ac.uk/>
research-enlighten@glasgow.ac.uk

THE NUMERICAL SOLUTION OF CERTAIN

DIFFERENTIAL EQUATIONS WHICH OCCUR

IN THEORETICAL PHYSICS

by

Arthur Compton Allison.

A Thesis submitted for the degree of
Doctor of Philosophy in the University of Glasgow.

C O N T E N T S

	<u>Page</u>
Chapter A	1
Chapter B	15
Chapter C	21
Chapter D	37
Chapter E	47
Chapter F	75
Chapter G	86
Chapter H	99
Chapter I	107
Chapter J	119
Chapter K	125

CHAPTER A

Introduction

This dissertation is concerned with the numerical solution of certain differential equations which occur very frequently in theoretical physics. The solution of any physical problem involves the setting up of a mathematical model and in the past this model has been solved by analytical methods or, in the many cases where no analytical solution can be found, by numerical methods. Better approximations lead to more complicated equations and to more difficult solutions. In recent years the advent of large fast automatic computers has made the solution of these complicated systems possible.

The solution of a system of equations is simplified by an understanding of the physical processes which give rise to the particular equations and these equations frequently exhibit some awkward numerical pitfalls. Therefore a background of the two disciplines, numerical analysis and theoretical physics is desirable.

Thus, this thesis is divided into two parts. The first is a description of the numerical techniques involved and thereafter a discussion of some of the numerical problems which were encountered; the second is an account of the physical problem, the derivation of the differential equations and a discussion of the results obtained.

We investigate the scattering of an incident point particle by a homonuclear diatomic molecule, the only inelastic process under consideration being excitation of the rotational levels of the molecule. The mathematical model we use to describe this collision is that of scattering by a rigid rotator. This model will only be valid if vibrational degrees of freedom are ignored and the molecule is in the ground electronic state, that is, if the component of electronic angular momentum along the internuclear axis is zero. For scattering problems of this type the relative motion in the various channels can be described in terms of "ingoing" waves and "outgoing" scattered waves. When the coefficient of the "ingoing" wave is normalised to unit flux, the coefficients of the "outgoing" waves form the scattering or S matrix (Wu and Ohmura 1962) which determines the cross section. This S matrix is unitary because of the requirement of conservation of flux and it is also symmetric as a consequence of the time reversal of the system. Two associated matrices, the reactance matrix R and the transition matrix T also occur. Their relation with the S matrix is given by the equations

$$R = \frac{1}{2} (I + S)^{-1} (I - S), \quad A1$$

$$T = I - S. \quad A2$$

From A1 it follows that R is a real symmetric matrix. It will be shown later (Chapter G) that the cross section for the excitation of the j^{th} rotational level to that level defined by rotational

quantum number j' is given by

$$\sigma(j'; j) = \frac{\pi}{(2j+1)k_{jj}^2} \sum_j (2j+1) \sum_l \sum_{l'} |T(jl; j'l')|^2, \quad A3$$

where k_{jj} is the channel wave number.

The Schrödinger equation describing this collision can be simplified to give a set of coupled, second order, ordinary differential equations in terms of the radial distance r . These equations may be written

$$\left[\frac{d^2}{dr^2} + k_i^2 - \frac{l_i(l_i+1)}{r^2} \right] u_{ij} = \sum_{k_i} V_{ik} u_{kj}, \quad A4$$

where k_i is again the channel wave number, l_i is a constant and V_{ik} is a matrix element depending on the interaction potential and the angular dependence of the incident particle and target. These equations are to be solved subject to the boundary conditions,

(a) u_{ij} is regular at the origin,

$$(b) \quad u_{ij} \sim \exp(-i[k_i r - \frac{1}{2} l_i \pi]) \cdot S_{ij} - \left(\frac{k_i}{k_j} \right)^{\frac{1}{2}} S_{ij} \exp(i[k_i r - \frac{1}{2} l_i \pi]), \quad A5$$

or, introducing the reactance matrix R to avoid the use of complex numbers,

$$(o) \quad u_{xy} \sim \sin(k_x r - \frac{1}{2} l_x \pi) \cdot S_{xy} \\ - \left(\frac{k_x}{k_y} \right)^{\frac{1}{2}} R_{xy} \cos(k_x r - \frac{1}{2} l_x \pi). \quad A6$$

Historical survey

The first mathematical treatment of collisions involving molecules was given by Zener (1931). His treatment, based on the distorted wave approximation, was restricted to collinear collisions between a diatomic molecule and an atom. He showed the inefficiency of interchange of translational, vibrational and rotational energy in molecular collisions, thus establishing the model of a rigid rotator for the consideration of rotational excitation of the molecule.

Nothing more was done for about twenty years until Takayanagi (1952) solved the equations A4 using his modified wave number method. In this approximation the centrifugal potential

$$l_i(l_i + 1) / r^2$$

is replaced by its value at a distance r_c , chosen to be of the order of the distance of closest approach, according to the classical theory, of the particles in a typical collision. The problem is thereby reduced to that of a one-dimensional collision with effective wave number k_{eff} given by

$$k'_l{}^2 = k_l{}^2 - \frac{l_l(l_l+1)}{r^2} .$$

A7

If the s-wave ($l_l = 0$) radial equations can be solved in closed form, the direct numerical solution of the radial equations is avoided and considerable simplification results. This method has been used by Schwarz and Herzfeld (1954) to calculate rotational transitions in hydrogen. However it has two main disadvantages. First, it is useful only within the very restricted range of potentials for which an analytical solution of the s-wave equation is known; second, the arbitrary parameter r_0 introduces an added uncertainty into the final cross section.

An approximate solution to equations A4 may be obtained by using the Born approximation (Mott and Massey 1949). This is obtained by first setting all u_{kj} equal to zero, k not equal to j , neglecting all V_{ii} and solving the remaining equations,

$$\left[\frac{d^2}{dr^2} + k_l{}^2 - \frac{l_l(l_l+1)}{r^2} \right] u_{ll} = 0 .$$

A8

The solutions of A8 which satisfy the boundary conditions are the spherical Bessel functions,

$$u_{ll} = k_l r y_l(k_l r) .$$

A9

The solutions A9 are then substituted back into the right hand side of A4 and the resultant uncoupled inhomogeneous differential

equations are solved for all the u_{ij} . This method will give a very poor result for the value of the cross section due to the poor approximation the Born functions make to the true u_{ij} close to the origin. In this region the true u_{ij} will go to zero much faster than the Born solutions A9.

A much better first approximation is obtained by leaving the diagonal terms V_{ii} in equation A8. Solving the equation,

$$\left[\frac{d^2}{dr^2} + k_r^2 - \frac{l_r(l_r+1)}{r^2} - V_{rr} \right] u_{rr} = 0, \quad A10$$

gives, not just the spherical Bessel functions, but rather, radial wave functions which are distorted by the diagonal matrix elements V_{ii} . If these solutions are then substituted back into the right hand side of A4 the solution of the resultant uncoupled inhomogeneous equations defines the distorted wave approximation. This is the method used by Roberts (1963), Davison (1963, 1964), Dalgarno and Henry (1965), Dalgarno, Henry and Roberts (1966).

This approximation was one of the most satisfactory ways of applying a straight forward numerical approach to the equations A4. However, since these last mentioned calculations were carried out, larger and faster automatic computers have become available and it is now practical to find the solutions of equations A4 when none of the off-diagonal matrix elements V_{ik} are neglected. This defines the close coupling approximation. This method has been used by Barnes, Lane and Lin (1965) for the calculation of electron

7
excitation cross sections in sodium.

To the best of the author's knowledge no calculations on the collisions between atoms and diatomic molecules have been carried out using this approximation and it will be an important part of this work to compare the distorted wave and close coupled approximations in several collisions of this type.

Another problem which is of current interest is resonant scattering. In practice, resonances are said to have occurred in scattering if the cross sections exhibit sharp maxima and minima. These resonances will only occur when an open channel is coupled to a closed channel, i.e. those channels for which $k_i^2 < 0$ in A4. Thus for the closed channel case we introduce the boundary condition,

$$u_{i,y} \sim K e^{-k_i r}$$

All

An extensive review article on resonant scattering has been given by Smith (1965).

Content of thesis

As mentioned before, this work divides into two parts. In the first, consisting of chapters B, C, D, E, F, the numerical treatment of the problem is considered; in the second, which includes

chapters G, H, I, J, K, the physical problem is described and the significance of the results discussed. For this reason the basic equations A4, together with the asymptotic boundary conditions A5, A6, have been included in this introduction so that in the numerical section we can consider these equations quite independently from the physical problem from which they were derived.

Chapter B consists of a simple resumé of the properties of a second order linear differential equation with the first derivative absent. Most of these properties can be found in the standard texts, e.g. Watson (1944), Mott (1952), Fox (1962), but it was thought worthwhile to include them here as constant reference is made to many of them in the following chapters.

The numerical solution of this type of differential equation is described in Chapter C. Several numerical methods are discussed and some of the numerical pitfalls associated with these methods are pointed out.

The distorted wave approximation is derived in Chapter D and the numerical scheme for the calculation of the cross section A3 is laid out. The chapter is concluded with a write-up, description and flow diagram of a program written for the English-Electric-Leo-Marconi KDF9 computer to perform these calculations. Similar programs have been written notably by Roberts (1963) on an I.B.M. 709 at Massachusetts Institute of Technology and Davison (1963) on the EDSAC2 at Cambridge.

Most of the original work involving the close coupling approximation is described in Chapter E. Several numerical techniques were tried on the computer and some investigation was done into critical values of the parameters. Several numerical snags were encountered each manifesting itself in a loss of symmetry of the R matrix. The write-up, description and flow diagram of a program to solve coupled differential equations and evaluate the reactance matrix R are included.

The last section of the numerical part, Chapter F, describes the problem of coupling an open channel equation to that representing a closed channel. Some numerical problems are encountered and it is thought that these will increase in complexity as more equations are coupled together. These problems need further investigation.

Chapter G begins the physical part with a derivation of the differential equations describing the scattering of a point particle by a rigid rotator (Arthurs and Dalgarno 1960). The distorted wave and close coupled approximations are now seen in context and the effect of the orientation dependence of the internuclear potential is treated mathematically.

The validity of the distorted wave approximation is studied in Chapter H with reference to a particular example. Numerical calculations show that, in the case of scattering of a hydrogen atom by a hydrogen molecule, the distorted wave approximation behaves and breaks down in precisely the manner predicted in the theoretical example.

Chapter I contains the majority of the numerical calculations in this thesis. In all, we consider the scattering of a hydrogen atom, a helium atom and a hydrogen molecule by a hydrogen molecule and also that of a hydrogen atom by a deuterium molecule, using both the distorted wave and close coupled approximations. These results have been summarised in a recent paper (Allison and Dalgarno 1967).

In Chapter J the numerical techniques developed in Chapter F are applied to the search for resonances in the collision of a hydrogen atom and a hydrogen molecule. No resonances were found in this case; a result predicted by Mott and Massey (1965).

Chapter K, which concludes this work, contains a description of the scattering of slow electrons by a hydrogen molecule. The programs developed in Chapter E have been modified to deal with this case. A short introduction is included at the beginning of the chapter.

Intermolecular potentials

The problem of finding a realistic intermolecular potential which describes the interaction between two colliding bodies forms one of the major difficulties in scattering theory to-day.

The non-empirical calculation of intermolecular potentials

from the first principles of quantum theory requires very complicated mathematics except for some pairs of the simplest molecules.

Empirical information comes from the scattering of molecular beams in gases, the second virial coefficient and the transport properties of gases.

There are various analytical expressions which have been used over the years to represent the interaction of the type shown in Fig 2. These are often written in the form

$$V(r) = \epsilon v(\rho),$$

where $\rho = r/\sigma$, and

where ϵ and σ are convenient scaling factors and $v(\rho)$ is a shape function which may or may not contain one or more parameters.

An empirical potential frequently used is (Hirschfelder, Curtiss and Bird 1954) the Lennard-Jones (12, 6) potential,

$$V(r) = 4\epsilon \left[\left(\frac{\sigma}{r} \right)^{12} - \left(\frac{\sigma}{r} \right)^6 \right],$$

A12

where ϵ is the maximum energy of attraction, i.e. the depth of the potential well which occurs at $r = 2^{1/6}\sigma$ and σ is the value of r for which $v(r)$ is zero. This potential gives a simple and realistic representation for non-polar molecules and while the inverse sixth power represents the attractive part fairly well the repulsive part is only an approximation.

Another form is the Buckingham (exp -6) potential (Bernstein et al 1963),

$$V(r) = A e^{-\alpha r} - \frac{B}{r^6}$$

A13

This function approximates the repulsive term by an exponential form. It is unrealistic in that the exponential term would lead to a meaningless maximum at a small value of r unless the function is arbitrarily made infinite for all r less than some value r_s (see Fig 2).

Frequently the long-range force has been neglected and implicit in this neglect of the attractive part of the potential is the assumption that the long-range force gives a so gradually varying force that the internal degrees of freedom adjust themselves adiabatically and so no quantum transition is expected with appreciable probability. As a result simple potentials such as an exponential function,

$$V(r) = A e^{-\alpha r}$$

A14

have been used (Roberts 1963).

Among other purely repulsive potentials is the one used by Zener (1931),

$$V(r) = \frac{a}{(r-b)^2} \quad r > b$$

$$= \infty \quad r < b$$

and the Morse potential (Davison 1963, 1964),

$$V(r) = D_e \left(\exp \left[-2\alpha (r - r_e) \right] - 2 \exp \left[-\alpha (r - r_e) \right] \right). \quad A15$$

This tractable function represents the actual potential at small distances much better than the Lennard-Jones or Buckingham potentials but at large distances it is less satisfactory. D_e is the energy at equilibrium separation r_e .

Although the attractive part of the potential does not seem to directly cause the inelastic processes with appreciable probability it affects the transition probabilities indirectly by accelerating the relative motion when an atom and a molecule approach each other. Hence long range forces must also be taken into account.

For an investigation of rotational transitions in three dimensional collisions the orientation dependence of the intermolecular potential is also required. This is often written in terms of the Legendre polynomials and for the atom-diatomic molecule case one may write

$$V(r, \theta) = V_{\text{rep}}(r) \sum_n b_n P_n(\cos \theta) + V_{\text{attr}}(r) \sum_n a_n P_n(\cos \theta), \quad A16$$

where θ is the angle between the internuclear axis of the molecule and the line connecting the centre of mass of the molecule with the atom. a_n and b_n are the asymmetry coefficients whose sign and

magnitudes are to be determined.

Usually only the leading terms are retained,

$$V_{\text{rep}}(r, \theta) = V_{\text{rep}}(r) \left[b_0 + b_2 \cdot P_2(\cos \theta) \right]$$

and

$$V_{\text{attr}}(r, \theta) = V_{\text{attr}}(r) \left[a_0 + a_2 \cdot P_2(\cos \theta) \right],$$

whence

$$V(r, \theta) = V_{\text{rep}}(r, \theta) + V_{\text{attr}}(r, \theta).$$

A17

The omitted term $P_1(\cos \theta)$ is zero for a homonuclear molecule and $V_{\text{rep}}(r)$ and $V_{\text{attr}}(r)$ are respectively the repulsive and attractive parts of the potential. Review articles on the subject of intermolecular potentials have been given by Buckingham (1960) and Dalgarno (1963).

CHAPTER B

Simple properties of differential equations

Consider the solution of the second-order linear differential equation

$$\left[\frac{d^2}{dr^2} + F(r) \right] u(r) = 0,$$

B1

where $F(r)$ is a known function of r . Since this is a second order equation it will have two independent solutions (u_1 and u_2 say) and the general solution can be written $Au_1 + Bu_2$, where A and B are constants.

The simplest case is when $F(r) = k^2$, where k is a constant. The general solution is then

$$\begin{aligned} u &= A \sin kr + B \cos kr \\ &= C \sin(kr + \eta). \end{aligned}$$

i.e. the solution is an oscillatory function and η is a real phase shift.

If $F(r)$ is constant and negative, $F(r) = -k^2$ say, then the two independent solutions are e^{-kr} and e^{+kr} with general solution

$$u = A e^{+kr} + B e^{-kr}$$

In the general case when $F(r)$ is not constant then if $F(r)$ is positive, u is an oscillatory function. This can be seen as follows.

Since $F(r)$ is positive then u and $\frac{d^2u}{dr^2}$ will have opposite signs, i.e. at a point at which u is positive the rate of change of the tangent to the curve is decreasing so the tangent will bend more and more steeply toward the axis. When the curve crosses the axis, i.e. u is negative, then the slope of the tangent will increase. This process continues to give an oscillatory function.

If, however, $F(r)$ is negative then u and $\frac{d^2u}{dr^2}$ will have the same sign and an exponential solution will result.

We will be interested in the case where $F(r)$ is initially negative and changes to being positive as r increases. In this case the solution will behave exponentially until $F(r) = 0$ and will then oscillate.

The form of $F(r)$ with this particular property will be taken as

$$F(r) = k^2 - \frac{l(l+1)}{r^2} - f(r),$$

B2

and we impose the additional requirement that $f(r)$ does not have a pole of order higher than one at the origin and $r f(r) \rightarrow 0$ as $r \rightarrow \infty$. l will be taken as constant for a particular equation. For large r , $F(r) \rightarrow k^2$ and the solution will have asymptotic form

$$u = C \sin(kr + \eta)$$

B3

where η is a real phase shift.

To investigate the behaviour of u , for small r , a series solution of the form

$$u = r^p \sum_{n=0}^{\infty} a_n r^n,$$

B4

is tried.

Substituting into the equation

$$\left[\frac{d^2}{dr^2} + k^2 - \frac{l(l+1)}{r^2} - f(r) \right] u(r) = 0$$

B5

and equating coefficients of r^{p-2} , there results the equation

$$[p(p-1) - l(l+1)] a_0 = 0.$$

Since $a_0 \neq 0$ then $p = -l$ or $l+1$.

By equating all other coefficients of r to zero, all the terms a_n , $n \gg 1$ may be obtained in terms of a_0 .

It is now required that the solution u is regular at the origin and so the solution with the requisite behaviour at the origin is

$$u = r^{l+1} \sum_{n=0}^{\infty} a_n r^n.$$

B6

This determines one of the arbitrary constants in the solution. The other constant provides an over-all normalisation.

To specify the solution uniquely some particular asymptotic form for the solution must be given. This will fix the normalisation.

The asymptotic form B3 will hold only in regions where

$$\frac{l(l+1)}{r^2} + f(r)$$

is negligible. Usually $f(r) \rightarrow 0$ much faster than $\frac{l(l+1)}{r^2}$ so the latter is the preponderating term. However the spherical Bessel functions

$$y_l(x) = \sqrt{\frac{\pi}{2x}} J_{l+\frac{1}{2}}(x), \quad \text{B7}$$

$$n_l(x) = (-1)^{l+1} \sqrt{\frac{\pi}{2x}} J_{-l-\frac{1}{2}}(x), \quad \text{B8}$$

satisfy the equation

$$\frac{d^2 y}{dx^2} + \frac{2}{x} \frac{dy}{dx} + \left(1 - \frac{l(l+1)}{x^2}\right) y = 0.$$

Thus $kr y_l(kr)$ and $kr n_l(kr)$ are the two independent solutions of the equation

$$\left[\frac{d^2}{dr^2} + k^2 - \frac{l(l+1)}{r^2} \right] u(r) = 0. \quad \text{B9}$$

The asymptotic solution of equation B5 may now be taken as

$$u(r) \sim kr \left(A y_e(kr) - B n_e(kr) \right) \quad \text{B10}$$

and this will be valid as soon as the effect of $f(r)$ has died away.

Equation B3 may be written, without loss of generality, as

$$u \sim C \sin \left(kr - \frac{1}{2} l \pi + \eta \right), \quad \text{B11}$$

so that $\eta = 0$ when $f(r) = 0$.

Comparing B10 and B11 gives

$$B = C \sin \eta,$$

$$A = C \cos \eta,$$

and these may be used to determine η uniquely. Thus the solution is completely determined by

- (a) the phase shift η ,
- (b) the normalisation C .

For computational purposes B10 is written in the form

$$u \sim D kr \left(y_e(kr) - \tan \eta \cdot n_e(kr) \right), \quad \text{B12}$$

and taking two distinct points r_a, r_b in the asymptotic region, allows D to be eliminated to give

$$\tan \eta = \frac{u_b r_a y_e(kr_a) - u_a r_b y_e(kr_b)}{u_b r_a n_e(kr_a) - u_a r_b n_e(kr_b)}, \quad \text{B13}$$

whence

$$D = \frac{\mu_a}{k \tau_a \left(y_e(k \tau_a) - \tan \eta \cdot n_e(k \tau_a) \right)} \quad \text{B14}$$

Unfortunately the value of η calculated from B13 by a standard computer subroutine is given in the range $-\frac{\pi}{2} < \eta \leq \frac{\pi}{2}$ so η will be arbitrary by an amount π , which will affect the sign of D.

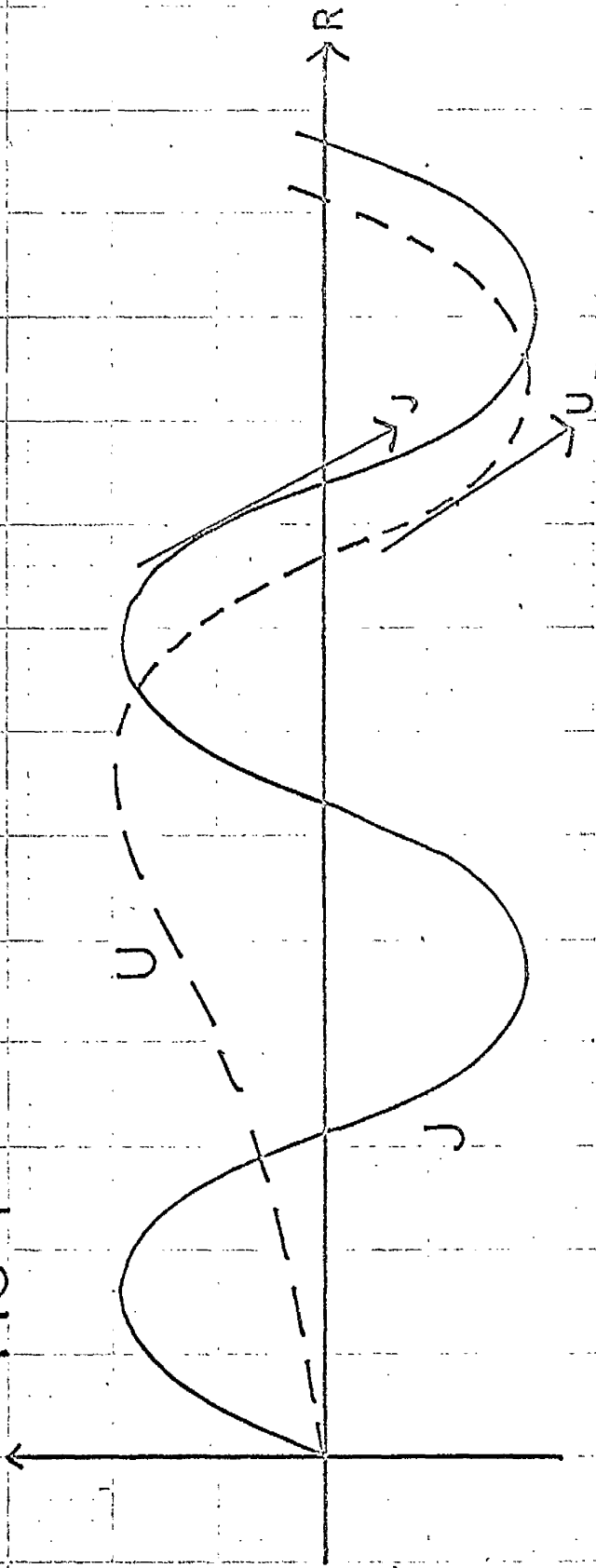
The correct sign can be determined by ensuring that the directions of the solution u and the corresponding spherical Bessel function are the same in the asymptotic region.

i.e. the phase shift η is obtained by comparing that solution of B9, which is regular at the origin, viz. $k \tau y_e(k \tau)$, with that solution of B5, with the same initial condition, which has asymptotic form B10 (see Fig 1).

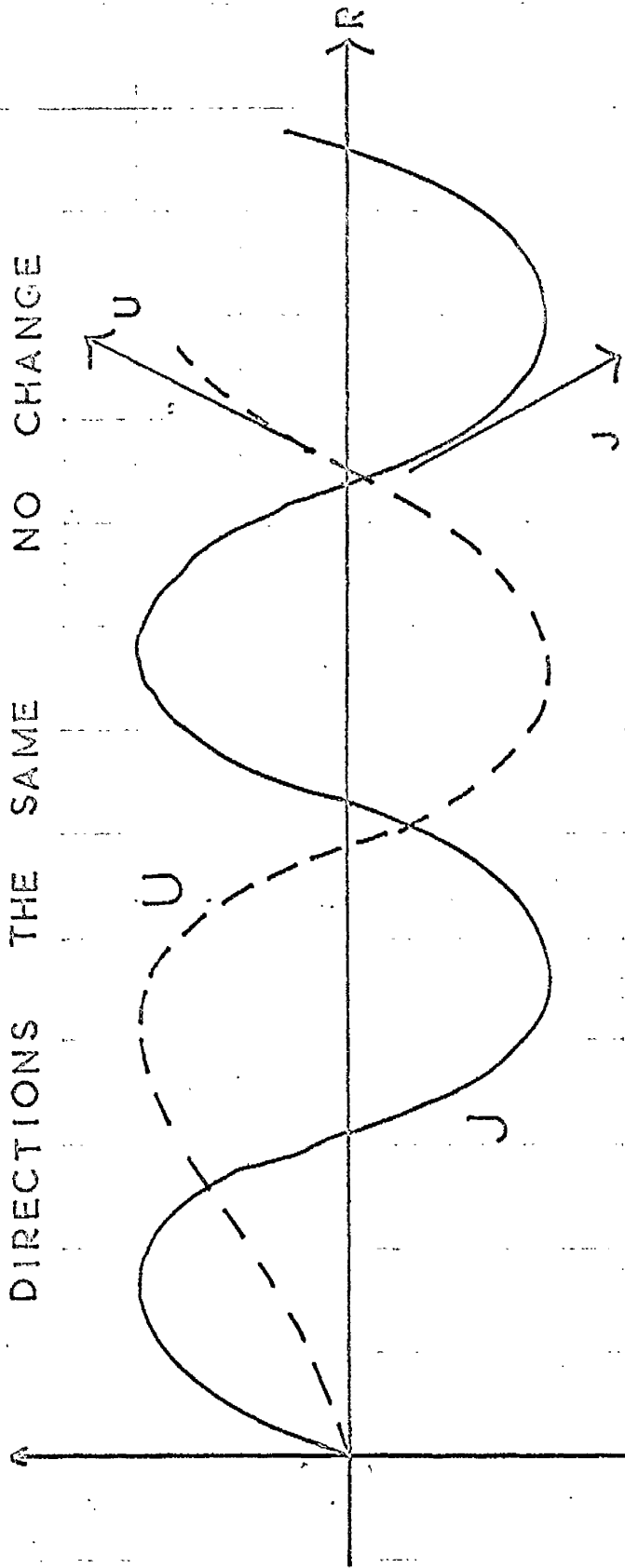
FIGURE 1

Comparison of solutions U with $J_1(kr)j_1(kr)$ to determine sign of normalisation.

FIG 1



DIRECTIONS THE SAME NO CHANGE



DIRECTIONS DIFF. CHANGE SIGN OF D

CHAPTER C

Numerical Solution

Two numerical methods for the solution of equation B5 will be considered. The first is the Runge-Kutta method (Kopal 1955) which solves a set of coupled first-order differential equations.

If a differential equation of any order is of such a form that the highest derivative can be expressed as a function of lower derivatives and the two variables, then, by simple substitution, it can be expressed as a set of coupled first-order equations.

Thus the Runge-Kutta method is applicable to a differential equation of any order with this property.

Runge-Kutta Method

The differential equations can be written

$$y^{i'} = f^i(x, y^1, y^2, \dots, y^m), \quad 1 \leq i \leq m, \quad C1$$

then defining

$$k_{r0} = h \cdot f^r(x_r, y_r^1, y_r^2, \dots, y_r^m),$$

$$k_{r1} = h \cdot f^r(x_r + \frac{1}{2}h, y_r^1 + \frac{1}{2}k_{r0}, \dots, y_r^m + \frac{1}{2}k_{r0}),$$

$$k_{12} = h f^{\wedge} \left(x_r + \frac{1}{2} h, y_r^i + \frac{1}{2} k_{11}, \dots, y_r^m + \frac{1}{2} k_{m1} \right),$$

$$k_{13} = h f^{\wedge} \left(x_r + h, y_r^i + k_{12}, \dots, y_r^m + k_{m2} \right),$$

gives

$$y_{r+1}^i = y_r^i + \frac{1}{6} (k_{10} + 2k_{11} + 2k_{12} + k_{13}). \quad 02$$

The integration is started by assuming initial conditions $y^i = y_0^i$ at the point $x = x_0$, where x_0 and the set y_0^i are known.

Equation B5 may be written, by putting $v = \frac{du}{dr}$,

$$\frac{du}{dr} = v,$$

$$\frac{dv}{dr} = - \left[k^2 - \frac{l(l+1)}{r^2} - f(r) \right] u, \quad 03$$

and in this form the Runge-Kutta method is immediately applicable.

Thus by choosing initial conditions, say $u = 0$ and $v = \frac{du}{dr} = a$ at $r = 0$, a step by step process may be set up giving values of u at successive points, interval h apart. Here a is an arbitrary constant.

These equations are derived from a comparison with the Taylor Series expansion up to and including terms in h^4 .

This is the most commonly used method for the solution of differential equations on an automatic computer. It is relatively easy to programme-- absence of a starting procedure helps here -- and as large, complicated and even non-linear sets of equations can

be handled with little extra effort it is not surprising that this method is so popular. Also changes in interval involve no complication, a situation which requires special treatment in finite difference methods.

The main disadvantage is that each function has to be calculated four times per step and this increases the time of computation. Also estimation of the truncation error is difficult so that the best that can be done is to make use of the fact that the local truncation error is of the order of h^5 in the process described.

Recurrence Formulae

The second method that will be described is a finite difference method known alternatively as Numerov's method (Hartree 1957) or second order Fox-Goodwin recurrence relation (Fox and Goodwin 1949). It is based on the finite difference formula

$$\delta^2 y_r = \left(1 + \frac{1}{12} \delta^2 - \frac{1}{240} \delta^4 \dots \right) h^2 y_r'' \quad \text{C4}$$

This formula is applied to the equation

$$y'' + f(x) y = g(x), \quad \text{C5}$$

i.e. a second order linear differential equation with the first derivative absent.

Truncating formula C4 after term in δ^2 and substituting into C5 gives the recurrence formula

$$\begin{aligned} \left(1 + \frac{1}{12} h^2 f_{x+1}\right) y_{x+1} - \left(2 - \frac{10}{12} h^2 f_x\right) y_x + \left(1 + \frac{1}{12} h^2 f_{x-1}\right) y_{x-1} \\ = \frac{1}{12} h^2 \left(y_{x+1} + 10 y_x + y_{x-1} \right). \end{aligned} \quad C6$$

If values of the solution are known at two points then this relation may be used to generate further values of y .

A disadvantage is that a starting procedure is usually required to evaluate two initial values. Also changing the interval requires special treatment, especially reducing the interval, in which case some means of estimating an intermediate value is necessary. This can be done by interpolation or, in the case of halving the interval, by simple elimination.

However the functions $g(x)$ and $f(x)$ need only to be calculated once per step and due to the very small truncation error, which has leading term

$$\frac{1}{240} \delta^4 h^2 y'' \equiv \frac{1}{240} \delta^6 y_x \equiv \frac{1}{240} h^6 y^{(6)},$$

a larger value of h may be chosen than in the previous case. This fact, together with the recurrence formula C6 will mean that this method will run very much faster on an automatic computer than will the Runge-Kutta method.

It is generally true that a method which is tailor-made for a

particular differential equation, in this case, second order, linear, first derivative absent, will be more efficient than a general method such as Runge-Kutta.

Another example of this statement is that a second order, non-linear differential equation with the first derivative absent will be more efficiently solved by the De Vogelaere method (De Vogelaere 1955) than by Runge-Kutta. In the former method the function values are only calculated twice per step.

Returning to equation C6 if we substitute

$$Y_r = \left(1 + \frac{1}{12} h^2 f_r\right) y_r - \frac{1}{12} h^2 g_r,$$

then the recurrence formula becomes

$$Y_{r+1} = 2 Y_r + h^2 (g_r - f_r y_r) - Y_{r-1}. \quad C7$$

In this form the number of arithmetic operations per step is reduced and is very suitable for programming an automatic computer. A slight disadvantage is that the mechanism for changing the interval becomes more complicated. For example, to increase the interval size by a factor p the scheme is :

(a) Equation C6.

Set $h = p \times h$ and replace y_r by y_{r-p} .

(b) Equation C7.

Set $h = p \times h$.

Add $\frac{3}{12} h^2 \{ f(r-h \times h) \times y_{r-h} - g(r-h \times h) \}$

to Y_{r-h} .

Add $\frac{3}{12} h^2 \{ f(r) \times y_r - g(r) \}$ to Y_r .

However since this routine would be entered very seldom compared with the number of steps required we prefer to use the recurrence formula as given by C7.

Stability

There are two types of stability connected with these equations and the two numerical methods.

(a) Inherent Instability

If in equation B1, $F(r) = -k^2$ then the solution will be

$$u = Ae^{+kr} + Be^{-kr}$$

C8

Even if our initial conditions require A to be zero, rounding errors will introduce a small multiple of the unwanted solution which will eventually swamp the true solution. When this type of equation is solved, with the above initial requirement, it is necessary to integrate backwards in which case the unwanted solution is decreasing and will not affect the true solution. This type of

instability is a function of the differential equation.

(b) Partial Instability

Consider the equation

$$y'' = -A^2 y, \text{ which has solution}$$

$$y = B e^{iAx} + C e^{-iAx}.$$

C9

(a) Runge-Kutta

When the Runge-Kutta method is used to integrate equation C9 the solution is represented by

$$y_{r+1} = E y_r,$$

where

$$E = 1 + ihA - \frac{1}{2} h^2 A^2 - \frac{1}{6} h^3 A^3 + \frac{1}{24} h^4 A^4. \quad \text{C10}$$

For this solution to converge to the true solution of the differential equation requires the condition $|E| < 1$ which, in turn, implies $h^2 A^2 < 8$.

(b) Recurrence Formula

Applying the recurrence formula C6 to the equation C9 gives

$$\left(1 + \frac{1}{12} h^2 A^2\right) E^2 - \left(2 - \frac{10}{12} h^2 A^2\right) E + \left(1 + \frac{1}{12} h^2 A^2\right) = 0, \quad \text{C11}$$

where again $y_{r+1} = E y_r$.

Now the set y_r is to represent an oscillatory solution so E must be complex.

Thus

$$\left(1 - \frac{5}{12} h^2 A^2\right)^2 - \left(1 + \frac{1}{12} h^2 A^2\right)^2 < 0,$$

or $h^2 A^2 < 6.$

C12

Thus the stability condition is very similar for both methods. Comparing equations C9 and B1 shows that these results may be applied to B1 if A^2 is some measure of the upper bound of the function $F(r)$.

An example illustrating this condition is given at the end of the chapter.

Choice of interval

There are two criteria that have to be considered before a choice of interval h is made.

- (a) The truncation error must be made negligible.
- (b) The stability condition must be satisfied.

The function $f(r)$, which we consider, will have its largest value at small r and tend to zero as r increases.

The stability condition for the equation C9 using the recurrence relation was $A^2 h^2 < 6.$

Thus if Λ^2 is taken as an upper bound for f at initial value of r . then this condition will allow a bound for the initial value of h to be chosen.

e.g. $f = 10 + 4$ at $r = r_0$,

then $h^2 < 6_{10} - 4$, whence h may be taken as 0.02 (say).

Further, asymptotically the solution will oscillate as $\sin(kr + \eta)$.

Truncation error for recurrence formula is, neglecting terms in h^8 and higher,

$$\frac{1}{240} h^6 y^{(vi)} = \frac{h^6 k^6}{240} \sin(kr + \eta). \quad C13$$

h must be chosen such that

$$\frac{h^6 k^6}{240} \text{ is negligible.}$$

For example if we require overall accuracy of four figures in the solution the integration should be carried out to six figures and the local truncation error is then allowed to be $5_{10} - 7$.

i.e. $\frac{(hk)^6}{240} < 5_{10} - 7,$

or $hk < 0.22.$

Thus combining these two examples, and assuming $k = 1$, a suitable choice of initial interval would be 0.02. The interval could be increased smoothly, depending on how quickly f dies away, up to

a final value of 0.2.

At this stage it is interesting to note that the next term in the correction from this recurrence relation is $\frac{13}{15120} \delta^8$. Assuming the sixth differences were included in a modified recurrence relation the same example gives

$$\frac{13}{15120} h^8 k^8 < 5 \cdot 10^{-7},$$

$$h \cdot k < 0.39.$$

Thus including the eighth differences we could choose a value of h about 1.7 times larger than the interval required to give the same accuracy with only the sixth differences included. It is unlikely that the extra work involved in evaluating the much more complicated recurrence formula would compensate for this reduction in interval.

Choice of initial condition

In chapter B the equation considered had boundary conditions

$$u = 0 \quad \text{at} \quad r = 0,$$

$$u \sim C \sin(kr + \eta).$$

The phase shift η is determined from the first condition and the second condition provides the normalisation factor C . The problem may be transformed into an initial value one by assuming some quite

arbitrary condition at the beginning of the range such as

$$\begin{aligned} u' &= a \quad \text{at} \quad r = 0, \\ \text{or} \quad u &= b \quad \text{at} \quad r = h. \end{aligned}$$

Choosing the first condition allows the Runge-Kutta method to commence its step, while the recurrence formula can be applied immediately if the second condition is used. The solution may then be integrated into the asymptotic region and the normalisation calculated.

A difficulty may arise when the recurrence formula C7 is used at the point $r = h$ as the term $f_0 u_0$ appears in the equation and f_0 may be infinite.

Robertson (1956) points out that this term may be replaced by $\lim_{r \rightarrow 0} fu$. Using B2 this is zero in all cases except for $\ell = 1$ when it contributes an amount $2a_0$ where a_0 is the leading term in the Frobenius expansion B6. In practice he found that retaining the first term in B6 was sufficient thus giving $a_0 = h^{-2}$.

This trouble only arises if integration is started at the origin.

It was further shown in chapter B that equation B5 had two solutions which behave for small r as

$$\begin{aligned} u_1 &= a_0 r^{\ell+1} \\ u_2 &= a_0 r^{-\ell} \end{aligned}$$

Theoretically the starting condition $u = 0$ at $r = 0$ must be taken

to get rid of the unwanted solution u_2 which tends to infinity as r tends to zero. However numerically we can obtain all of the required solution by choosing completely arbitrary initial values at a suitable small value of r .

The most general solution of equation B5 is given by

$$u = Au_1 + Bu_2,$$

where A and B are constants.

Then if r_0 is chosen such that the unwanted solution u_2 is very much greater than u_1 , the integration starting from r_0 will consist only of the wanted solution u_1 .

i.e. since u_2 tends to infinity as r tends to zero then r_0 can be chosen such that B is zero, to the accuracy with which one is working.

Two choices of starting conditions that can be used are

$$(a) \quad u = a \quad \text{at} \quad r = r_0, \quad C14$$

$$u = a \quad \text{at} \quad r = r_0 + h;$$

$$(b) \quad u = 0 \quad \text{at} \quad r = r_0, \quad C15$$

$$u = a \quad \text{at} \quad r = r_0 + h;$$

where a is an arbitrary (usually small) number. This effect is demonstrated by an example.

Ex. Consider the equation

$$\left[\frac{d^2}{dr^2} + k^2 - \frac{l(l+1)}{r^2} \right] u = 0, \quad C16$$

which has solution

$$u = A \text{ker } y_\ell(\text{ker}) + B \text{ker } n_\ell(\text{ker}).$$

We wish to find that solution of C16 which is regular at the origin, i.e. $B = 0$.

Working to five figure accuracy in the solution, taking

$$k = 1, \quad \ell = 3$$

$$r_0 = 0.2, \quad h = 0.1,$$

$$u_0 = u_1 = 10^{-5},$$

and integrating out past 7.1, where the first zero of $y_3(r)$ lies, gives a phase shift $\eta = 0$ showing that only the solution which is regular at the origin is present.

This can be seen by using very approximate values of the spherical Bessel functions

$$\text{at } r = 0.2, \quad y_3(r) = 8 \cdot 10^{-5}, \quad n_3(r) = 9 \cdot 10^{+3};$$

$$\text{at } r = 0.3, \quad y_3(r) = 2.5 \cdot 10^{-4}, \quad n_3(r) = 2 \cdot 10^{+3};$$

Thus $B \approx (3 \cdot 10^{-9})$ and since $r n_3(r)$ does not build up as r increases it can never affect the solution.

Repeating the example with $r_0 = 0.7$ instead of 0.2 gave a value of $\eta = 0.0001$ which shows that some of the unwanted solution must be present.

Again

$$\text{at } r = 0.7, \quad \gamma_3(r) = 3 \cdot 10^{-3}, \quad n_3(r) = 6.5 \cdot 10^+1;$$

$$\text{at } r = 0.8, \quad \gamma_3(r) = 4 \cdot 10^{-3}, \quad n_3(r) = 3.9 \cdot 10^+1;$$

gives $B \approx \frac{1}{3} (3 \cdot 10^{-4})$ which is not zero to the required accuracy.

As r increases the unwanted solution oscillates in a similar way and with similar magnitude to the required solution. Thus if any error is present at the first zero of $\gamma_\ell(kr)$ it will be carried through to the asymptotic region. In the latter example some of the unwanted solution would be present throughout the whole range.

An exactly similar situation occurs if initial conditions C15 had been used instead of C14. However C14 cannot be used in the case $\ell = 0$ when the solution is $A \sin kr + B \cos kr$ as in this case only the unwanted solution B will appear. This is because that solution is finite at the origin. Initial conditions C15 will give a correct result in this case if r_0 is of the order 10^{-6} .

Example of Instability

The previous example was successful with choice of $r_0 = 0.2$, $h = 0.1$, for $\ell = 3$. It might seem reasonable to make the same choice for $\ell = 10$. If this is done the calculated function values

increase very rapidly until the numbers become too large for the computer ($10 + 39$ in this case).

This has occurred because a violent instability has been introduced by the choice of initial conditions.

It was shown earlier in this chapter that the stability condition for the recurrence relation was $A^2 h^2 < 6$.

C12

In the previous example $A^2 \approx 3 \cdot 10^{+2}$,

$$A^2 h^2 = 3 \cdot 10^{+2} \cdot 10^{-2} < 6.$$

In this example $A^2 \approx 25 \cdot 10^{+2}$,

$$A^2 h^2 = 25 > 6.$$

Thus this solution is unstable. The interval should have been about 0.02 to get a correct representation of the solution.

Form of $f(r)$

A form of the function $f(r)$ which will be used is given by

$$f(r) = a e^{-br} - c/r^b.$$

As mentioned in Chapter A this function is not defined for small r as it does not obey the condition that $r f(r)$ is finite as r tends to zero.

The shape of the function is shown in Fig 2. A spurious maximum occurs at some value of r and this affects the shape back to some point r_s .

The function f is now modified to have the behaviour

$$f(r) = a e^{-br} - c/r^6 \quad \text{for } r > r_0.$$

For $r < r_s$, $f(r)$ can have any shape which, at worst, goes off as $\frac{1}{r}$, as r tends to zero, and has a continuous join with the former part at $r = r_s$. If these conditions are obeyed the solution is treated as being effectively zero for $r < r_s$.

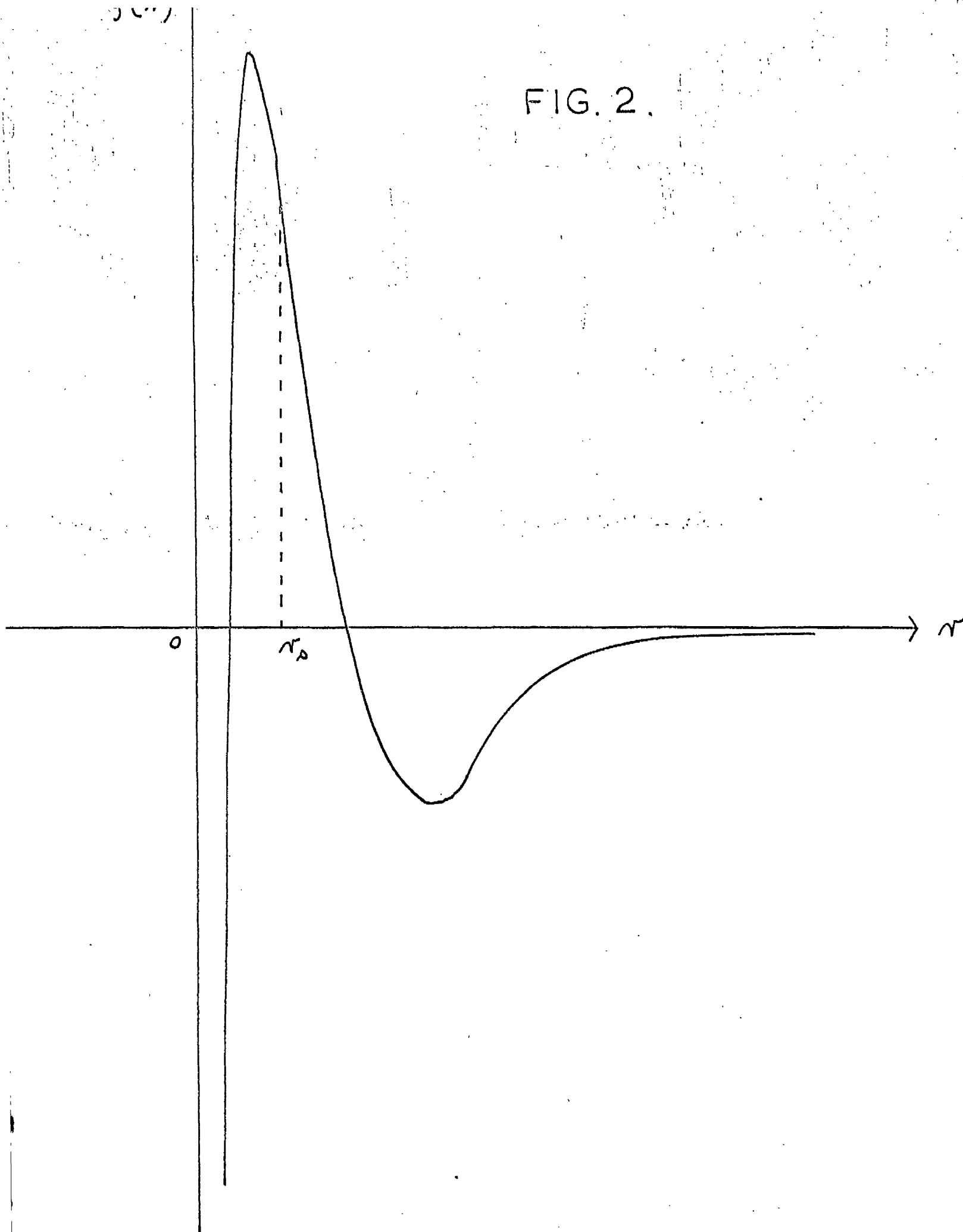
The values of the parameters a , b , c in $f(r)$ are such as to make the value of $f(r_s)$ of the order of 10^{-4} .

If the integration is started at r_s and also at several values of r greater than r_s the phase shift is found to be unchanged, i.e. there is a region greater than r_s in which the unwanted solution is very much greater than the wanted solution and in this region starting conditions can be chosen quite arbitrarily. Clearly this range will increase for increasing values of l and, in practice, the initial value r_0 can be moved out to save computing time.

FIGURE 2

Typical shape of function of the form $ae^{-br} - \frac{c}{r^6}$.

FIG. 2.



Distorted Wave Approximation

If it can be assumed that the non-diagonal matrix elements V_{ij} , $i \neq j$, are small compared with other terms so that all products on the right hand side of A4 except $V_{ii} u_i$ and $V_{li} u_i$, which involves the incident wave, can be neglected, then the equations A4 become

$$\left[\frac{d^2}{dr^2} + k_l^2 - \frac{l_l(l_l+1)}{r^2} - V_{ll} \right] u_l = 0, \quad D1$$

$$\left[\frac{d^2}{dr^2} + k_l^2 - \frac{l_l(l_l+1)}{r^2} - V_{ll} \right] u_l = V_{li} u_i, \quad l \neq i, \quad D2$$

Defining w_l to be that solution of

$$\left[\frac{d^2}{dr^2} + k_l^2 - \frac{l_l(l_l+1)}{r^2} - V_{ll} \right] w_l = 0, \quad D3$$

such that

$$w_l \sim \sin \left(k_l r - \frac{1}{2} l_l \pi + \eta_l \right) \quad D4$$

and v_l that solution of the same equation such that

$$v_l \sim \frac{1}{k_l} \exp i \left(k_l r - \frac{1}{2} l_l \pi + \eta_l \right), \quad D5$$

then

$$u_i \sim \sin(k_i r - \frac{1}{2} l_i \pi + \eta_i) \quad D6$$

and the solution of equation D2 is (Mott and Massey 1949)

$$u_i = -v_i \int_0^r w_i V_{i1} u_i dr + w_i \int_r^\infty v_i V_{i1} u_i dr, \quad D7$$

which behaves, for large r , as

$$u_i \sim -\frac{1}{k_i} \exp i(k_i r - \frac{1}{2} l_i \pi + \eta_i) \int_0^\infty w_i V_{i1} u_i dr. \quad D8$$

Matching these asymptotic forms with the boundary conditions A5

gives

$$S_{11} = \exp(2i\eta_1), \quad D9$$

$$S_{i1} = \exp i(\eta_1 + \eta_i) \left(\frac{k_i}{k_1}\right)^{\frac{1}{2}} 2i\beta_i, \quad i \neq 1, \quad D10$$

where

$$\beta_i = \frac{1}{k_i} \int_0^\infty w_i V_{i1} u_i dr. \quad D11$$

Thus with this approximation the S matrix elements can be obtained

in terms of the solutions of the uncoupled homogeneous differential equations D3.

Formula A3 for the elastic and inelastic cross sections given by $j = 0, j' = 2$ becomes

$$\sigma(0;0) = \frac{4\pi}{k_1^2} \sum_{J=0}^{\infty} (2J+1) \sin^2 \eta_1, \tag{D12}$$

$$\sigma(2;0) = \frac{4\pi}{k_1^2} \sum_{J=0}^{\infty} (2J+1) \sum_{\lambda} \left(\frac{k_{\lambda}}{k_1} \right)^{\frac{1}{2}} \beta_{\lambda}^2. \tag{D13}$$

where λ takes the values $n, n-1 \dots$ corresponding to values of l' .

A program has been written to apply this approximation to certain cases to be described.

It solves M differential equations of the form

$$\left[\frac{d^2}{dr^2} + k_{\lambda}^2 - \frac{l_{\lambda}(l_{\lambda}+1)}{r^2} - V_{\lambda\lambda}^s(r) \right] u_{\lambda}^s(r) = 0,$$

where M can take the values $4, 9, 16 \dots$, l_1 is

given by

J		
$J - 2$	J	$J + 2$
$J - 4$	$J - 2$	$J \dots \dots \dots$

and

$$V_{\lambda\lambda}^s(r) = B_0 \left\{ N_0(r) \cdot \delta_{\lambda\lambda} + f_2^s(r, \lambda) N_2(r) \right\},$$

where f_2 is given by the formulae in Bernstein et al (1963) and

$$v_\mu(r) = a_\mu e^{-b_\mu r} - \frac{c_\mu}{r^6} \quad \mu = 0, 2.$$

The integration is carried into a region where the potential $V_{ij}^J(r)$ is negligible and the β -integrals are formed from a knowledge of the normalised solutions u_i ,

$$\beta_i^J = \frac{B_0}{k_i} f_2^J(1, \mu) \int_0^\infty u_i^J v_2(r) u_i^J dr.$$

The calculations are repeated for consecutive values of J until the contribution from the β -integrals has died away. The elastic and inelastic cross sections are then calculated from the formulae D12 and D13.

Data required is,

M (the number of equations),

$B_0, a_0, b_0, c_0, a_2, b_2, c_2$ (parameters for $v_0; v_2$),

$I_1, I_2, I_3, p_1, p_2,$

$r_0, h, y_1,$

$k_1, k_2, \dots, k_M,$

$j, j', \text{ initial } J, -1, \text{ eps, bool.}$

The integration begins at r_0 and takes $I_1 + 1$ steps of interval h . The interval is changed to $h \times p_1$ and I_2 steps are taken. The range is completed by adding I_3 steps of interval $h \times p_1 \times p_2$.

41

The value of all solutions u_1 is assumed zero at r_0 and equal to y_1 at $r_0 + h$. $j = 0$ for the cases considered and $j' = 2 (\sqrt{M} - 1)$.

The initial value of J was usually 0 and J was stepped successively by 1 until the β -integrals had fallen off by a factor ϵ usually taken to be 10^{-3} .

`bool` was a boolean marker set false if angular distribution was required and true otherwise (see equation 13).

The data is read in and at this stage the maximum storage requirement of the program is known.

Since the two functions $v_0(r)$ and $v_2(r)$ appear in all the $V_{ij}^J(r)$ elements it is more efficient to calculate these functions at all the tabular points and store them as two vectors. This would be especially true if $v_\mu(r)$ were more complicated.

When the value of J is known the values of l may be set up and also, the constants $f_2(i, j)$ calculated from the reference. The equations are integrated as described in chapter C. The integration is terminated as soon as the phase shift has settled down to a steady value usually taken when two successive phase shifts differ by less than 0.0001. The phase shift is calculated from formula B13 which involves the spherical Bessel functions. It would be wasteful of computer time to test the phase shift too soon so a marker X_s is set within the program such that for values of r less than X_s the phase shift routine is ignored.

In the region for r greater than X_s the solutions are os-

oscillatory and the phase shift is calculated each time any solution crosses the axis. As a safeguard to determine whether the phase shift has converged or the end of the range has been reached, the final value of r is printed out together with the phase shifts.

The value of the normalisation is then calculated from B14, averaged over several points, and the correctly normalised solutions are stored. This information allows the β -integrals D11 to be evaluated.

Three numerical methods of integration were tried.

First the well-known Simpson's rule was used

$$\int_{x_0}^{x_{2m}} f(x) dx = \frac{h}{3} \left\{ y_0 + 4y_1 + 2y_2 + \dots \dots \dots + 4y_{2m-1} + y_{2m} \right\}, \quad D14$$

and secondly, two forms of Gregory's formula

$$\int_{x_0}^{x_m} f(x) dx = h \left\{ \frac{1}{2} y_0 + y_1 + \dots \dots \dots + y_{m-1} + \frac{1}{2} y_m \right\} + \frac{h}{12} (\nabla y_m - \Delta y_0) - \frac{h}{24} (\nabla^2 y_m - \Delta^2 y_0) + \dots, \quad D15$$

given by neglecting second differences and again by neglecting fifth differences (Modern Computing Methods 1961).

The integration was taken over the tabular points of the solution of the differential equation and hence the integrand split into three parts. There was little to choose between these three methods considering the accuracy required but in the case of Simpson's Rule

I_1 has to be odd and I_2 even. Probably the Gregory formula with second difference ignored, i.e. the Trapezoidal Rule with end correction, is the most convenient to apply in practice.

The phase shifts are calculated by comparison with the spherical Bessel functions. The next section describes the calculation of these functions based on the method given in "Tables of spherical Bessel functions", N.B.S. (1947).

Spherical Bessel Functions

Bessel functions of order ν satisfy the differential equation

$$x^2 \frac{d^2 y}{dx^2} + x \frac{dy}{dx} + (x^2 - \nu^2) y = 0. \quad D16$$

One solution of D16 is $J_\nu(x)$ defined by the series

$$J_\nu(x) = \sum_{k=0}^{\infty} (-1)^k \frac{(x/2)^{\nu+2k}}{k! \Gamma(\nu+2k+1)}. \quad D17$$

For $\nu = n + \frac{1}{2}$, where n is an integer, the general solution of D16 is

$$A J_{n+\frac{1}{2}}(x) + B J_{-n-\frac{1}{2}}(x),$$

where A and B are constants.

The well-known asymptotic expansion of $J_{n+\frac{1}{2}}(x)$ is (Watson 1944),

$$\sqrt{\frac{\pi}{2x}} J_{n+\frac{1}{2}}(x) = \frac{1}{x} \left\{ P_{n+\frac{1}{2}}(x) \cos\left(x - \frac{\pi}{2}(n+1)\right) - Q_{n+\frac{1}{2}}(x) \sin\left(x - \frac{\pi}{2}(n+1)\right) \right\}, \quad D18$$

where

$$P_{n+\frac{1}{2}}(x) = \sum_{k=0}^{\lfloor \frac{n}{2} \rfloor} \frac{(-1)^k (n+2k)!}{(2x)^{2k} (2k)! (n-2k)!},$$

$$Q_{n+\frac{1}{2}}(x) = \sum_{k=0}^{\lfloor \frac{n-1}{2} \rfloor} \frac{(-1)^k (n+2k+1)!}{(2x)^{2k+1} (2k+1)! (n-2k+1)!}.$$

The functions $J_\nu(x)$ satisfy the recurrence relation

$$J_{\nu+1}(x) + J_{\nu-1}(x) = \frac{2\nu}{x} J_\nu(x). \quad D19$$

The closely related function

$$\Lambda_\nu(x) = \frac{\Gamma(\nu+1)}{(x/2)^\nu} \cdot J_\nu(x), \quad D20$$

may be shown to satisfy the relations

$$\Lambda_\nu(x) = \Lambda_{\nu-1}(x) + \frac{x^2}{4\nu(\nu+1)} \cdot \Lambda_{\nu+1}(x), \quad D21$$

$$\Lambda_{\nu-1}(x) = \left[1 - \frac{x^2}{4\nu(\nu+1)} \right] \Lambda_{\nu+1}(x) - \frac{x^2}{4(\nu+1)(\nu+2)} \Lambda_{\nu+2}(x), \quad \text{D22}$$

For $\nu = n + \frac{1}{2}$,

$$\Lambda_{n+\frac{1}{2}}(x) = \sum_{k=0}^{\infty} a_k \frac{(2n+1)!}{n!} x^{2k}, \quad \text{D23}$$

where

$$a_k = \frac{(-1)^k (n+k)!}{k! (2n+2k+1)!}$$

$$= \frac{-1}{2k(2n+2k+1)} a_{k-1}, \quad \text{D24}$$

which gives

$$\sqrt{\frac{\pi}{2x}} J_{n+\frac{1}{2}}(x) = (2x)^n \sum_{k=0}^{\infty} a_k x^{2k}. \quad \text{D25}$$

The simple recurrence relation D19 may be used to generate function values either by a forward or backward recurrence relation provided $\frac{(2n+1)}{x}$ is less than unity. When $\frac{(2n+1)}{x}$ is greater than unity the error in the generated values may increase rapidly and it becomes impractical to use D19 for computing.

purposes. However $\Lambda_{n+\frac{1}{2}}(x)$ may be conveniently generated by a forward relation when $\frac{(2n+1)(2n+3)}{x^2}$ is less than unity and by a backward relation when this factor is greater than unity.

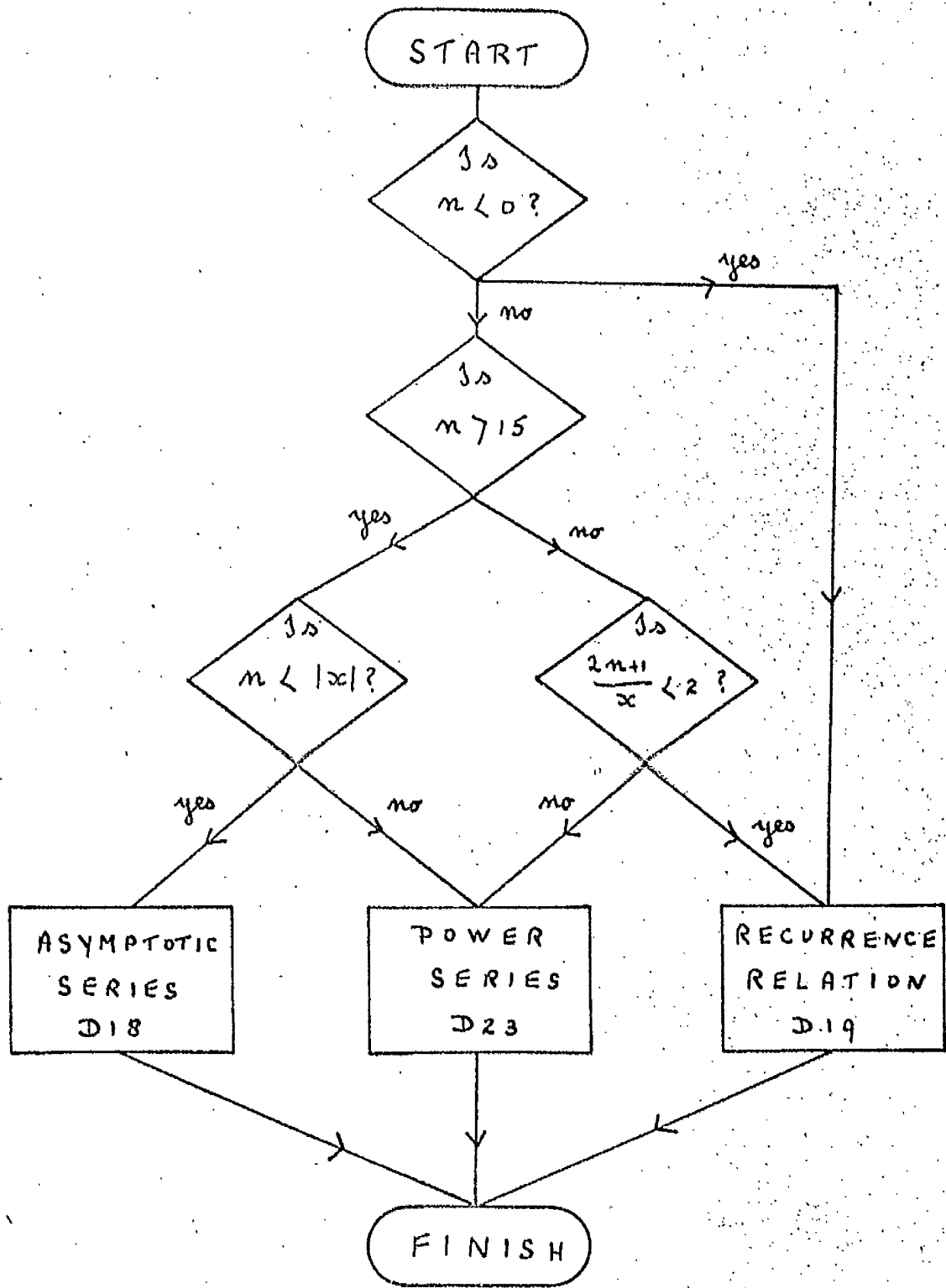
Hence we restricted use of recurrence formula D19 to values of n less than fifteen and in this range direct evaluation of $\sqrt{\frac{\pi}{2x}} J_\nu(x)$ from the power series D25 was valid whenever the recurrence formula broke down.

For values of n greater than fifteen and for values of x greater than n the asymptotic expansion D18 was used. The most awkward range is when n is greater than fifteen and x less than n and in this range we used the functions $\Lambda_{n+\frac{1}{2}}(x)$.

These values were calculated from the power series D23. A block diagram showing the organisation of the various functions used, is given.

BLOCK DIAGRAM

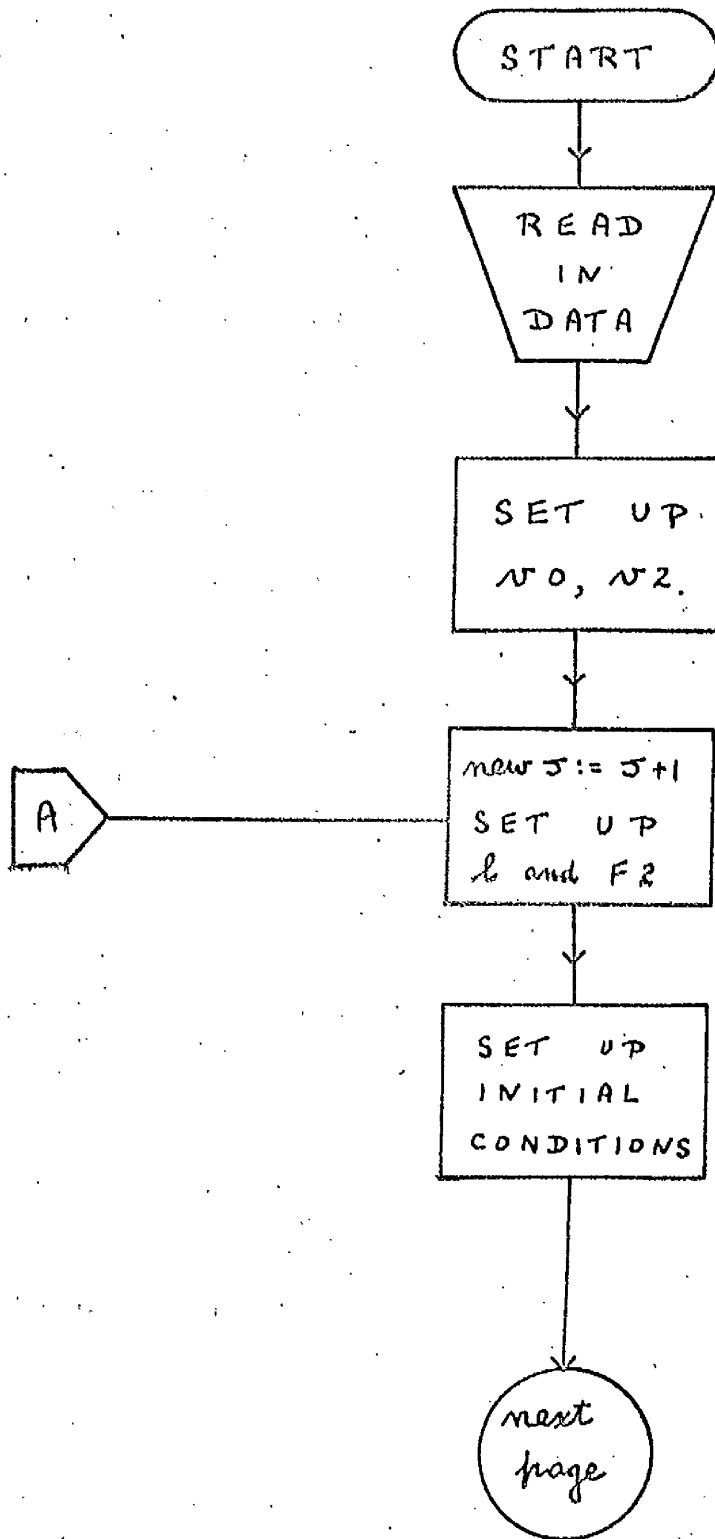
SPHERICAL BESSEL FUNCTIONS

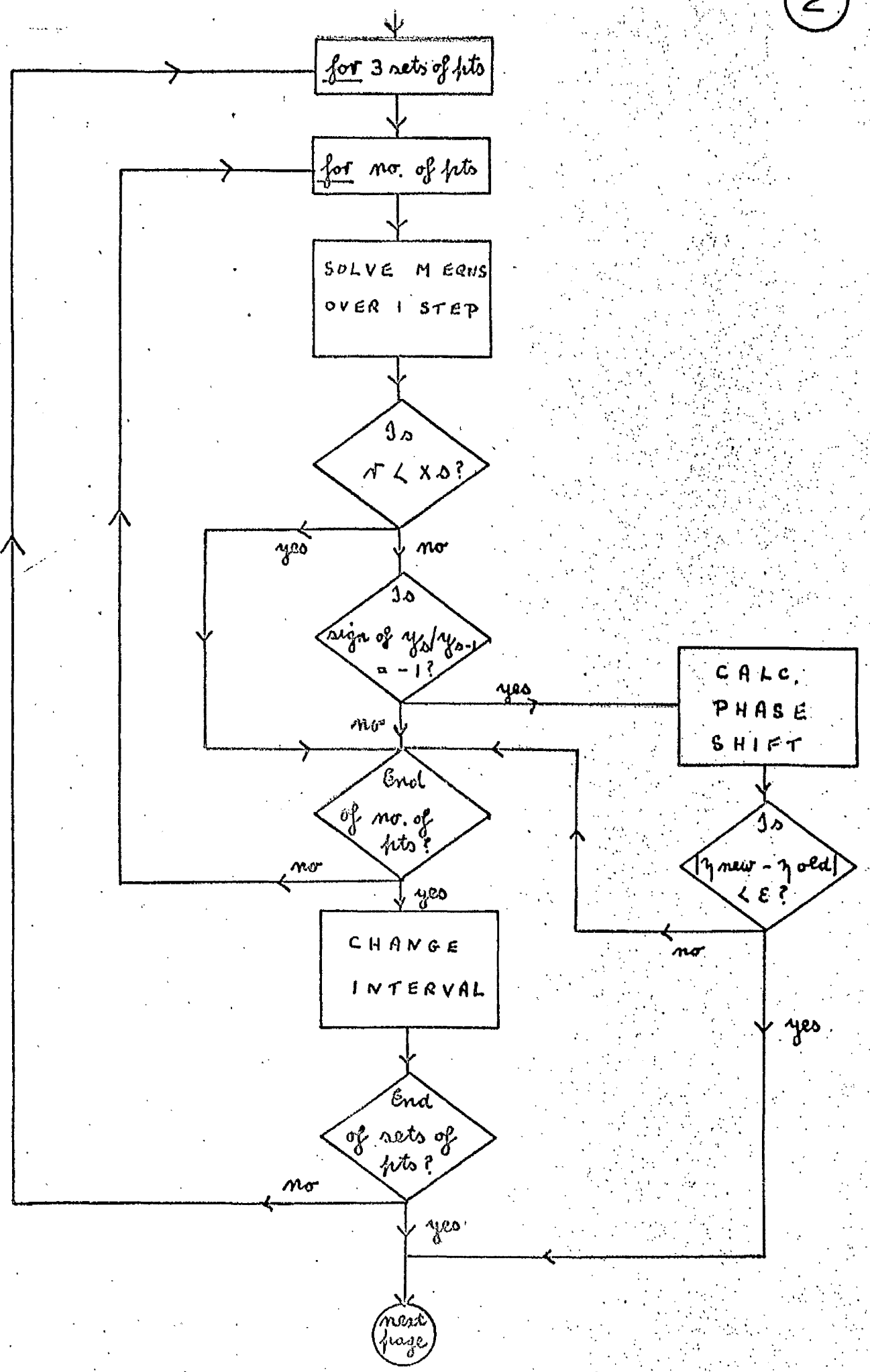


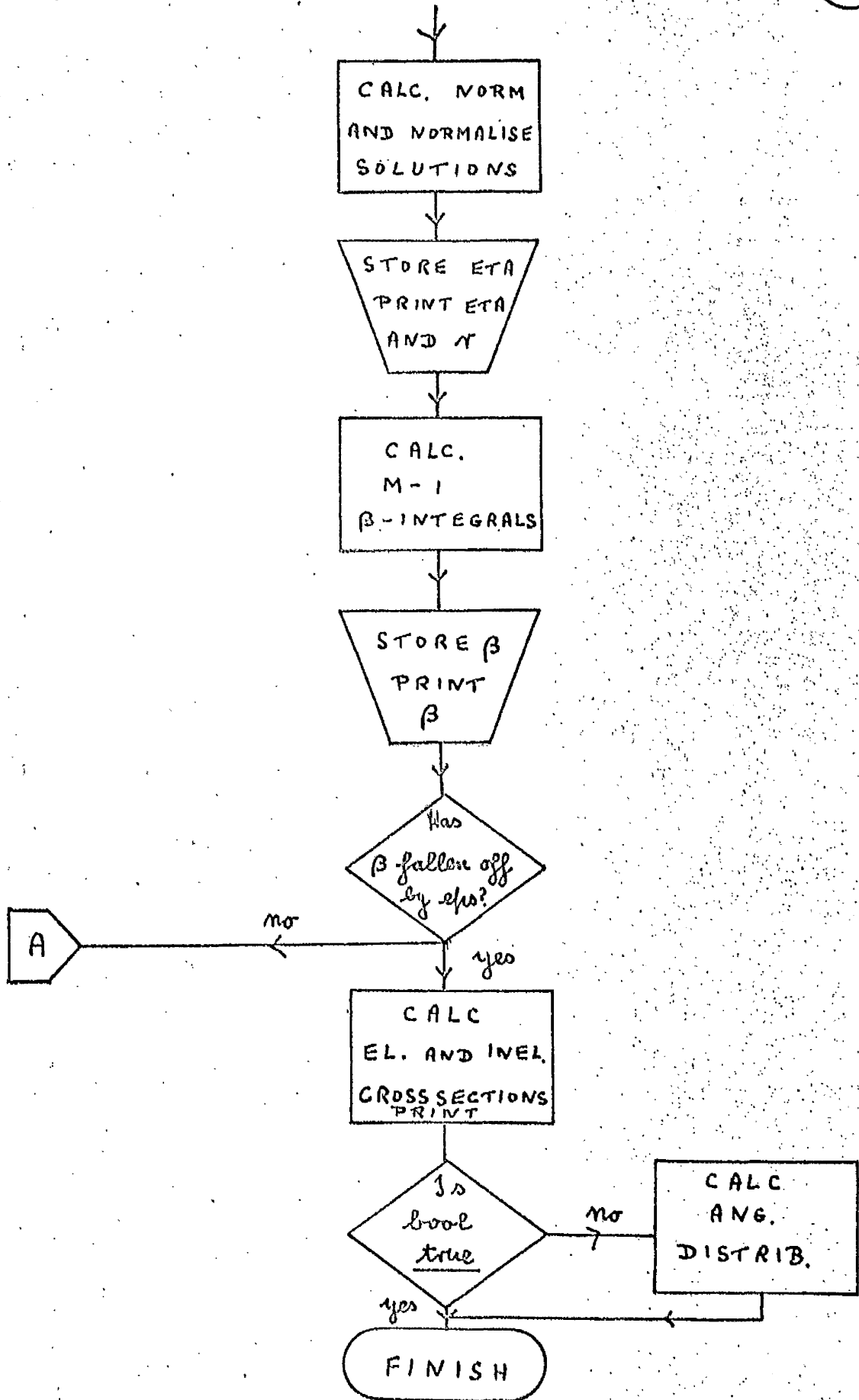
BLOCK DIAGRAM

1

DISTORTED WAVE PROGRAM







CHAPTER E

Close coupling Approximation

If none of the off-diagonal matrix elements in equation A4 can be neglected then no analytical solution of the coupled equations can be found and it is necessary to proceed numerically.

A method of solving these equations has been given by Barnes, Lane and Lin (1965). It involves solving the coupled equations into the asymptotic region and there matching the solutions to the boundary conditions.

The equations are

$$\left[\frac{d^2}{dr^2} + k_i^2 - \frac{l_i(l_i+1)}{r^2} - V_{ii} \right] u_{iy} = \sum_{\substack{k=1 \\ k \neq i}}^n V_{ik} u_{ky}, \quad \text{E1}$$

for $1 \leq i \leq n$, $1 \leq j \leq n$.

To avoid use of complex numbers the boundary conditions given in terms of the R matrix are used,

$$u_{iy} = 0 \quad \text{at} \quad r = r_0,$$

$$u_{iy} \sim k_i r \gamma_l(k_i r) \delta_{iy} + \left(\frac{k_i}{k_j} \right)^{\frac{1}{2}} R_{ij} k_i r n_l(k_i r). \quad \text{E2}$$

Since the S matrix contains all the elements of the R matrix

this set of equations must be solved n times using the n sets of boundary conditions.

If the matrix elements V_{ij} have no singularities of order two or higher at the origin then, for small r , the solutions of E1 which satisfy E2 are given by

$$w_{xy} = \alpha_{xy} r^{l_x+1}, \quad \text{E3}$$

where α is a matrix of constants. The solutions thus obtained will not, in general, satisfy the asymptotic boundary conditions.

Thus n linearly independent solutions of equation E1 must be found and then a suitable linear combination can be matched to the correct asymptotic form.

The criterion for linearly independent solutions of this equation is that the phase shifts obtained must themselves be markedly different and ~~strongly~~ independent. This has been noted by Buckingham (1962). We make the assumption that if the rows of α are linearly independent then the respective asymptotic forms will also be linearly independent. This choice of α is of great importance and may certainly not be chosen in an entirely arbitrary manner as mentioned by Barnes, Lane and Lin (1965).

Thus the solutions u_{ij} may be expanded as

$$u_{xy} = \sum_{k=1}^n w_{xk} c_{ky}, \quad \text{E4}$$

or
$$\underline{u} = \underline{w} \cdot \underline{c} .$$

The solutions \underline{u} may be matched to the boundary conditions at two values of r (say r_a, r_b), large enough such that the potential terms V_{ij} have died away. Then, defining a matrix R' and diagonal matrices M^r, N^r by

$$R'_{ij} = \left(\frac{k_x}{k_y} \right)^{\frac{1}{2}} R_{ij}, \quad \text{E5}$$

$$M_{ij}^r = k_x r \gamma_e(k_x r) \cdot \delta_{ij}, \quad \text{E6}$$

$$N_{ij}^r = k_x r n_e(k_x r) \cdot \delta_{ij}, \quad \text{E7}$$

the matching process becomes

$$\underline{w}^a \cdot \underline{c} = M^a + R' \cdot N^a, \quad \text{E8}$$

$$\underline{w}^b \cdot \underline{c} = M^b + R' \cdot N^b, \quad \text{E9}$$

whence

$$R' = \left(\underline{w}^b \cdot N^a - \underline{w}^a \cdot N^b \right)^{-1} \cdot \left(M^b \cdot \underline{w}^a - M^a \cdot \underline{w}^b \right), \quad \text{E10}$$

The R, S and T matrices defined in A1 and A2 may be easily found since

$$T = 2 \left(I + R^2 \right)^{-1} \cdot R^2 + 2 \cdot \left(I + R^2 \right)^{-1} \cdot R \quad \text{E11}$$

and $S = I - T,$ E12

where I is the unit matrix.

The recurrence relation may be applied to these equations in terms of matrix operations.

$$\text{Defining } F_{xy} = \left(\frac{e_x(e_x+1)}{r^2} - k_x^2 \right) \delta_{xy} + V_{xy}, \quad \text{E13}$$

equation E1 becomes

$$U'' = F \cdot U \quad \text{E14}$$

and substituting in C6 gives

$$U_{m+1} = \left(I - \frac{1}{12} h^2 F_{m+1} \right)^{-1} \left\{ \left(2I + \frac{10}{12} h^2 F_m \right) U_m - \left(I - \frac{1}{12} h^2 F_{m-1} \right) U_{m-1} \right\} \quad \text{E15}$$

i.e. to advance the solution of the differential equation E14 one step involves a matrix inversion.

If equation E14 is solved using recurrence relation E15 then a matrix inversion, or in practice, a solution of simultaneous equations, is necessary at each step. This matrix,

$$I - \frac{1}{12} h^2 F_{m+1},$$

where F_{n+1} is defined by E13,

is strongly diagonally dominant except for small r . Indeed as r increases it will tend to a diagonal matrix. Iterative methods

are very useful when dealing with matrices of this type and this gives two choices

- (a) to invert the matrix at each step which would be wasteful in the region where the coupling has died away, or
- (b) to use an iterative method.

We decided to use the latter. Also one can examine more closely the nature of the solution and the effect of coupling if the equations are solved in this way. By this method the equations must be solved n times taking successive columns of $\underline{\alpha}$ as initial conditions.

Three iterative methods are considered.

Method A

A method of solving E1, used by Buckingham and Massey (1942) and Robertson (1956) to solve a single integro-differential equation, is to solve the equation by successive approximation.

In the following scheme the suffix j refers to a column of $\underline{\alpha}$ and remains fixed for each set of n equations. If initially u_{ij}^0 is set equal to zero an iterative scheme may be defined as follows :

$$\left[\frac{d^2}{dr^2} + k_n^2 - \frac{l_n(l_n+1)}{r^2} - V_{nn} \right] u_{ny}^{n+1} = \sum_{k < l} V_{lk} u_{ny}^{n+1} + \sum_{k > l} V_{lk} u_{ny}^n$$

and iteration may be carried out on some final value of the successive solutions,

e.g. the value of the solutions at the matching points. Note that this method involves iterating on the complete solution of the differential equation.

The next two methods take the iteration at each step.

Method B

Truncating formula C4 after the term in δ^2 gives

$$y_{r+1} = 2y_r - y_{r-1} + \frac{1}{12}h^2 \{ y''_{r+1} + 10y''_r + y''_{r-1} \} \quad \text{E17}$$

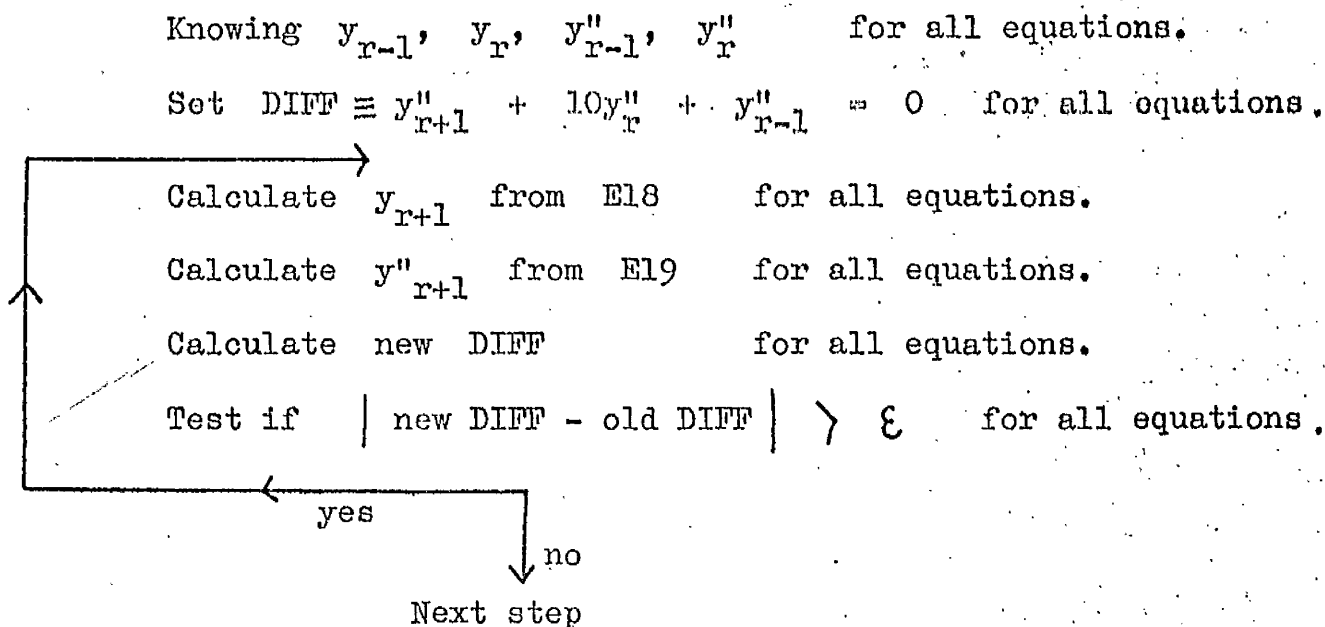
and an iterative scheme could be set up as

$$y_{r+1}^{m+1} = 2y_r - y_{r-1} + \frac{1}{12}h^2 \{ y''_{r+1} + 10y''_r + y''_{r-1} \}^m, \quad \text{E18}$$

where, from C5,

$$y''_r = g_r - f_r y_r. \quad \text{E19}$$

The flow diagram is as follows :



Method C

In C7 the recurrence formula is written

$$Y_{r+1} = 2 Y_r + h^2 (g_r - f_r y_r) - Y_{r-1}, \quad \text{E20}$$

where $y_r = \frac{Y_r + \frac{1}{12} h^2 g_r}{1 + \frac{1}{12} h^2 f_r}$. E21

This is a particularly suitable form for an iterative process as the calculation of Y_{r+1} using E20 is independent of the coupling terms on the right hand side of E1. They only arise through the term g_r in E21.

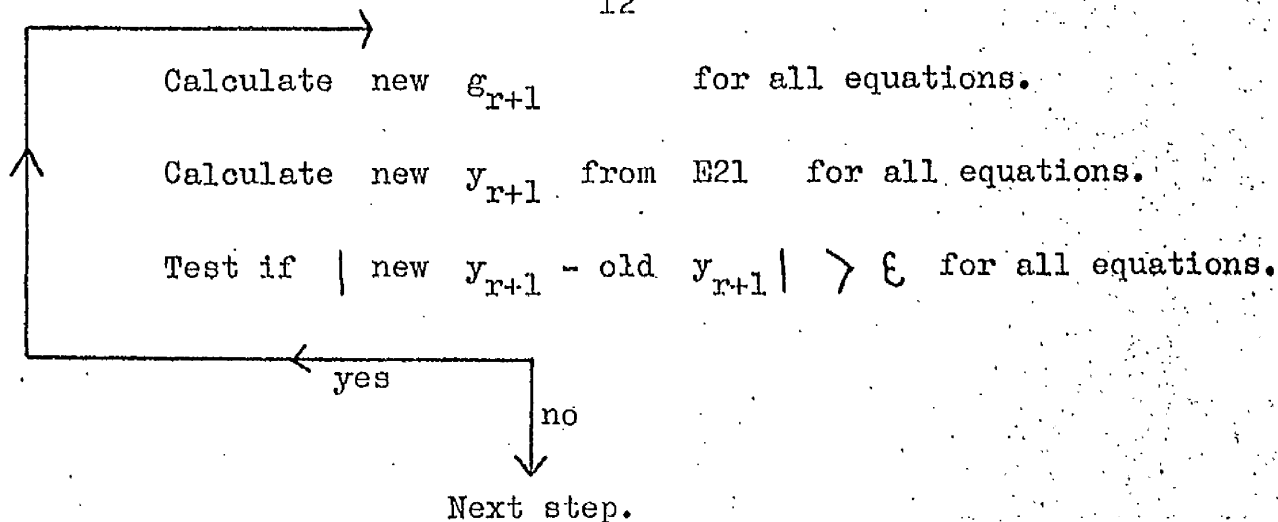
The flow diagram is as follows :

Knowing Y_r, Y_{r-1}, y_r for all equations.

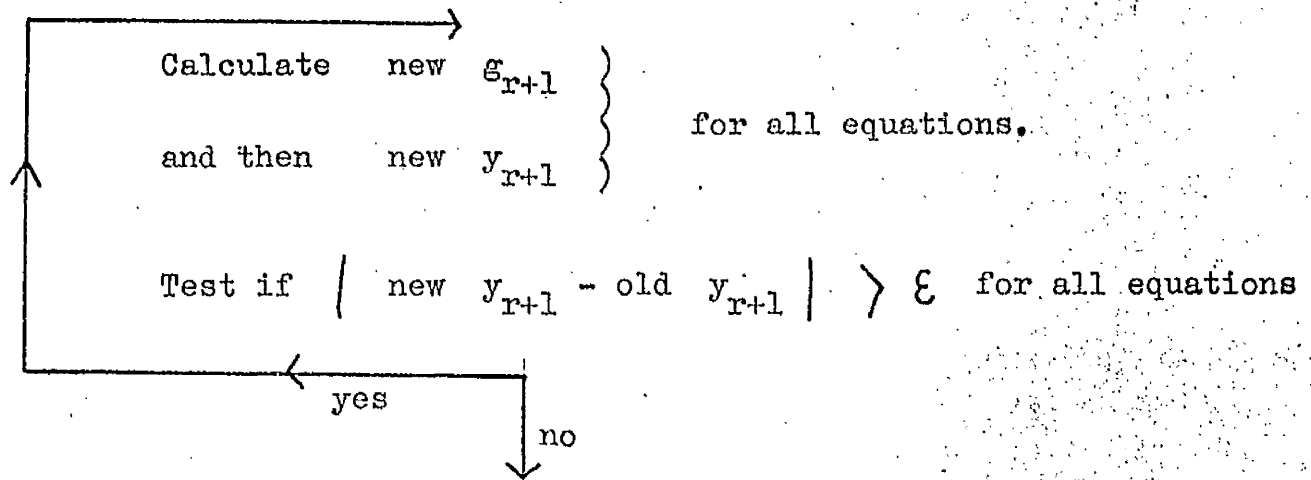
Calculate $h^2 g_r - h^2 f_r y_r$ for all equations.

Calculate Y_{r+1} from E20 for all equations,

and $y_{r+1} = \frac{Y_{r+1}}{1 + \frac{1}{12} h^2 f_r}$ for all equations.

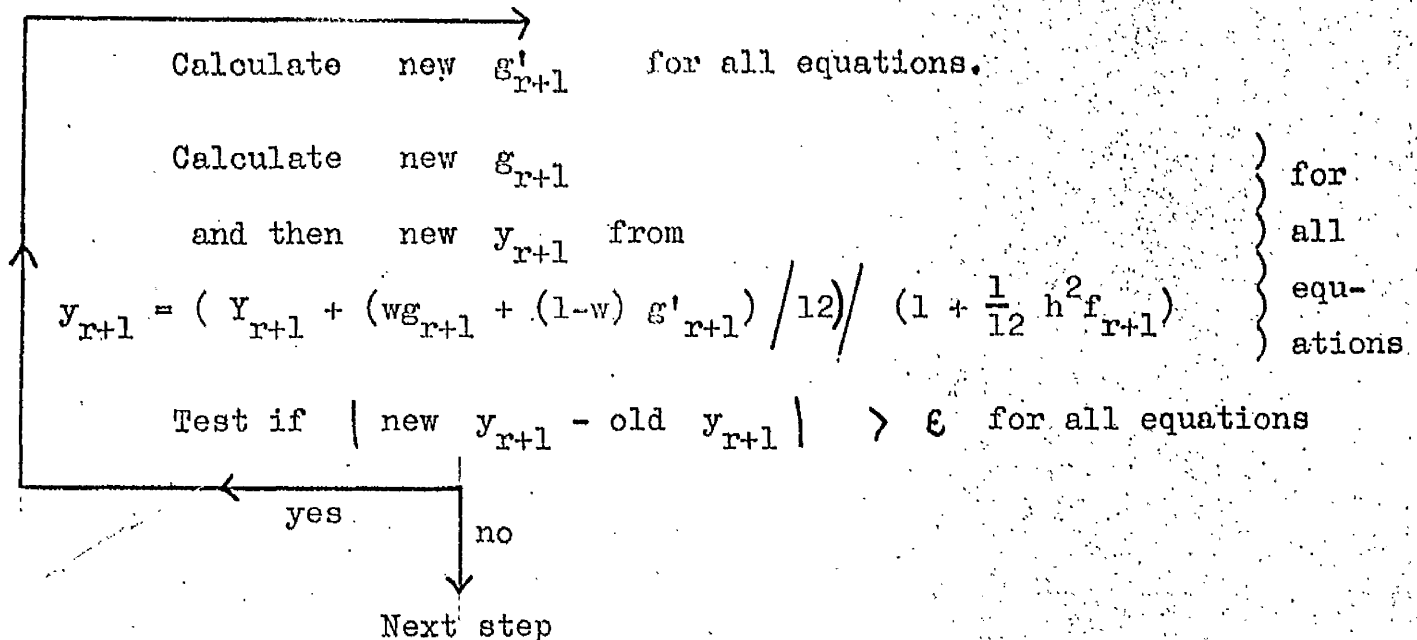


This scheme gives rise to Jacobi type iteration but if the last few lines are modified to be



then Gauss-Seidel iteration will result.

These two may be combined to give Successive Over-Relaxation by modifying the same few lines to give



However the number of equations considered and the number of iterations involved are small enough for the extra work involved to be not worthwhile. For a large number of coupled equations this approach might be worth considering. The Gauss-Seidel scheme was

the one chosen for method C.

Methods B and C were compared by integrating the two coupled equations given by E1 with

$$\underline{k} = \begin{bmatrix} 10 \\ 1 \end{bmatrix}, \quad \underline{l} = \begin{bmatrix} 4 \\ 2 \end{bmatrix}, \quad \underline{v} = \begin{bmatrix} 0 & 100 \\ 100 & 0 \end{bmatrix},$$

over ten points with interval 0.05.

The number of iterations taken per step was output and the following was the result.

Method B

4 steps with 7 iterations each.

6 steps with 6 iterations each.

Method C

10 steps with 4 iterations each.

They were also compared by choosing an example with four coupled equations given by

$$\underline{k} = \begin{bmatrix} 16 \\ 2 \\ 2 \\ 2 \end{bmatrix}, \quad \underline{l} = \begin{bmatrix} 2 \\ 0 \\ 2 \\ 4 \end{bmatrix}, \quad \underline{v} = \begin{bmatrix} 0 & 100 & 100 & 100 \\ 1000 & 0 & 100 & 100 \\ 1000 & 100 & 0 & 100 \\ 1000 & 100 & 100 & 100 \end{bmatrix}$$

taken over 140 points at interval 0.05.

Method B

2 steps with 9 iterations each.

11 steps with 8 iterations each.

27 steps with 7 iterations each

100 steps with 2 iterations each.

Method C

35 steps with 5 iterations each.

5 steps with 4 iterations each.

100 steps with 1 iteration each.

These results show that method C is much more efficient than method B. As well as having less iterations throughout the chosen range method C gives the correct result straight away when the coupling has died away whereas method B will still iterate twice.

We therefore adopt method C and compare it with method A. Three typical cases, with four coupled equations, were taken,

$$\underline{k} = \begin{bmatrix} 16 \\ 1.5 \\ 1.5 \\ 1.5 \end{bmatrix}, \quad \underline{l} = \begin{bmatrix} J \\ J-2 \\ J \\ J+2 \end{bmatrix}, \quad J = 0, 2, 8;$$

and \underline{V} a matrix with elements of the form $ae^{-bx} - c/x^6$ where a, b, c are constants.

In all cases method A took about twelve iterations until the relative error between the matching points of successive iterates was 10^{-4} and the time taken for one column of $\underline{\alpha}$ was approximately two minutes.

The results from method \underline{B}^C are summarised in Table 1 for two choices of initial value r_0 . For all four columns of $\underline{\alpha}$ the time taken was about two minutes. Thus method C runs four times faster than method A and so method C is used in the following work.

As can be seen from Table 1 the average number of iterations was two and this being the case the iterative scheme will probably be better than that of E15 using matrix inversion. However as the number of equations increases the matrix method will become more efficient as the time required to do the house-keeping of the matrices becomes a less proportion of the time required to do the arithmetic operations.

Table 1 also demonstrates the way in which the coupling affects the numerical solution of equations E1. It can be seen whether or not the integration has proceeded far enough for the coupling to be considered negligible for, if this is the case, we would expect the number of iterations to be one.

Choice of iteps

iteps is a small number representing the relative error between successive iterates of method C.

If it is assumed that we require the solutions of these differential equations correct to four figures in the asymptotic region then we should try to keep six figures in the solution at each step and hence the relative error, $\text{iteps} = 5 \cdot 10^{-7}$ is a satisfactory choice in these conditions. This was checked by repeating the calculations with $\text{iteps} = 5 \cdot 10^{-9}$ and ascertaining that there was no difference in the final solution.

Choice of matching points

The matching points r_a and r_b must be chosen so that substitution into B13 for all equations will give a sensible numerical result for the phase shift. This would not be the case if an unfortunate choice, such as $r_b - r_a$ equal to a period of the function $\approx 2\pi/k_i$ in the asymptotic region, were made. However there is nothing in the given algorithm which restricts the choice of matching points to be the same for each equation. Thus in each case if r_b is fixed then r_a may be obtained by subtracting (say) $\pi/2k_i$ from it,

$$\text{i.e. } r_b - r_a = \frac{\pi}{2k_i}$$

r_b is taken around that value of r for which the phase shifts had converged in the distorted wave approximation. This only occurs when the potential V_{ii} has died away and, since the behaviour of V_{ij} is similar to V_{ii} this criterion will hold at the same value of r in the coupled case.

Choice of matrix α

In most of the cases considered four coupled differential equations require to be solved. Thus α is a four by four matrix and we make the choice

$$\underline{\alpha} = \begin{bmatrix} 1 & 1 & 1 & 1 \\ 1 & -1 & -1 & 1 \\ -1 & 1 & -1 & 1 \\ 1 & 1 & -1 & -1 \end{bmatrix} .$$

E22

The rows of this matrix are linearly independent and further they are orthogonal. This type of matrix gives a good chance of the corresponding phase shifts being independent. It is easy to set up a matrix of this form for four equations but for more than four it becomes increasingly more difficult. This difficulty has been overcome by Smith, Henry and Burke (1966) who use the Runge-Kutta method to integrate from r_0 to r_0+h . This allows an initial matrix $\underline{\alpha}'$ to be chosen with reference to the value of the derivatives at r_0 instead of the function values at r_0+h . They found in these circumstances that $\underline{\alpha} = I$ (unit matrix) was a satisfactory choice and this reasoning will hold for any number of equations. Knowing the function values at r_0 and r_0+h allows the recurrence formula to be used immediately.

This is a particularly attractive numerical calculation to carry out since one of the quantities which is evaluated is the R matrix which, as mentioned in chapter A, is symmetric. This condition of symmetry is dependent on the physical model, the equations of which we are solving, and has not been assumed at any stage in the calculation. This gives an excellent in-built check on the accuracy of our working. Thus if the symmetry of the R matrix breaks down it is an indication of something going wrong with that calculation and further investigation is necessary. We

have come across two cases in which this occurs.

Symmetry trouble 1

The symmetry of the R matrix breaks down for high values of l but the breakdown is much more pronounced for correspondingly low values of k . This situation is a direct result of the different magnitudes of the various solutions which result from the fact that the solutions increase exponentially until $F_1(r)$, defined in B2 as

$$F_l(r) = k_l^2 - \frac{l_l(l_l+1)}{r^2} - f_l(r) \quad \text{E23}$$

is zero.

Consider the example $n = 2$, $k = \begin{bmatrix} 16 \\ 1.5 \end{bmatrix}$, $l = \begin{bmatrix} 6 \\ 8 \end{bmatrix}$

and f_1 some function which is small compared with k^2 for $r > 2$ (say).

Then $F_1(r)$ has a zero about r equal to 2.5 and the corresponding solution $u(r)$ will oscillate for larger r with approximately the same amplitude. But $F_2(r)$ does not have its zero until about r equal to 7.0 and over the range between 2.5 and 7.0 solution $u_2(r)$ is increasing exponentially while solution $u_1(r)$ is oscillating. Thus the oscillatory solution $u_2(r)$ will have a very much greater amplitude than solution $u_1(r)$ for r greater than 7.0. In the example quoted solution $u_1(r)$ had an

amplitude of 10^{+4} while the corresponding value of solution $u_2(r)$ was 10^{+10} . Thus cancellation will occur when these function values are substituted in a relation such as E10.

Since solution $u_2(r)$ is very much greater than solution $u_1(r)$ over most of the range then, for small r , the coupling of solution $u_1(r)$ with solution $u_2(r)$ will be so small that it will have very little effect on the phase shift of solution $u_2(r)$. Hence this phase shift will be almost independent of the starting conditions and we will not be able to get linearly independent values of solution $u_2(r)$. For this reason values of the phase shifts for each column of $\underline{\alpha}$ were printed out together with the R matrix, showing quite clearly that the breakdown in symmetry of the R matrix occurs when the phase shifts of solution $u_2(r)$ are very nearly equal.

This type of situation suggests that the initial values $\underline{\alpha}$ should be scaled to compensate for the differing magnitudes.

However the following two choices of scaling the columns of $\underline{\alpha}$,

$$\underline{a} \quad \begin{bmatrix} 1 \\ 10^{-2} \\ 10^{-3} \\ 10^{-4} \end{bmatrix} ,$$

$$\underline{b} \quad \begin{bmatrix} 1 \\ 10^{-10} \\ 10^{-10} \\ 10^{-10} \end{bmatrix} ,$$

were made for a set of four equations and there was no improvement in the symmetry of the R matrix.

The third choice

$$\underline{c} \begin{bmatrix} 1 \\ 10^{+4} \\ 1 \\ 10^{-4} \end{bmatrix},$$

corresponding to values proportional to h^{l_i+1} for $h = 0.01$ is the most realistic but this gave no improvement over straightforward use of the matrix $\underline{\alpha}$ given in E22.

It was mentioned at the end of chapter C that the initial value r_0 could be chosen in a certain range determined by the constancy of the phase shift. As a means of improving the present situation it is essential that r_0 is taken as large as possible in this range, thus cutting down the range of r for which the solutions are building up exponentially. An illustration of this effect is shown in Table 2.

As l_i increases the position of the zeros of the functions $F_i(r)$ increases so it was decided to automatically increase the starting value r_0 .

Symmetry Trouble 2

It is of interest to study the effect on the solutions of an increase in the size of the coupling terms. This was done by introducing a parameter λ_R into the right hand side of E16. The equations are now

$$\left[\frac{d^2}{dr^2} + k_l^2 - \frac{l_l(l_l+1)}{r^2} - V_{ll} \right] u_{ly} = \sum_{\substack{k=1 \\ k \neq l}}^m \lambda_k V_{lk} u_{ky} \quad \text{E23}$$

As λ_k is increased from its realistic value of unity we find that the symmetry of the R matrix breaks down badly.

To investigate this we consider the analytical solution of two coupled equations for small values of r. The two equations are

$$\left[\frac{d^2}{dr^2} + k_1^2 - F_1 \right] u_1 = \lambda_2 F_0 u_2,$$

$$\left[\frac{d^2}{dr^2} + k_2^2 - \frac{6}{r^2} - F_2 \right] u_2 = \lambda_1 F_0 u_1, \quad \text{E24}$$

We shall assume $\frac{1}{F_0}$, $\frac{1}{F_1}$, $\frac{1}{F_2}$ to be small, for small r.

Eliminating u_2 from E24 gives

$$\left(\left[D^2 + k_2^2 - \frac{6}{r^2} - F_2 \right] F_0^{-1} \left[D^2 + k_1^2 - F_1 \right] - \lambda_1 \lambda_2 F_0 \right) u_1 = 0.$$

i.e.

$$\begin{aligned} & \left[D^2 (F_0^{-1} D^2) + k_1^2 D^2 (F_0^{-1}) - D^2 (F_0^{-1} F_1) - F_2 F_0^{-1} D^2 \right. \\ & + \left(k_2^2 - \frac{6}{r^2} \right) F_0^{-1} D^2 + \left(k_2^2 - \frac{6}{r^2} \right) k_1^2 F_0^{-1} - k_1^2 F_2 F_0^{-1} \\ & \left. - \left(k_2^2 - \frac{6}{r^2} \right) F_0^{-1} F_1 + F_2 F_0^{-1} F_1 - \lambda_1 \lambda_2 F_0 \right] u_1 = 0. \end{aligned}$$

Neglecting terms of the order of Γ^{-1} the equation becomes

$$\left[D^2 (F_0^{-1} F_1) + F_2 F_0^{-1} D^2 + k_1^2 F_2 F_0^{-1} + \left(k_2^2 - \frac{6}{r^2} \right) F_0^{-1} F_1 - F_2 F_0^{-1} F_1 + \lambda_1 \lambda_2 F_0 \right] \mu_1 = 0.$$

In the cases which we are considering Γ_1 and Γ_2 depend on two similar functions v_0 and v_2 while Γ_0 depends only on the function v_2 . Thus we make the substitution

$$F_1 = \mathcal{N}_0 + \mathcal{N}_2,$$

$$F_2 = \mathcal{N}_0 + \mathcal{N}_2,$$

$$F_0 = \mathcal{N}_2,$$

and the equation becomes

$$\left[D^2 \left(1 + \frac{\mathcal{N}_0}{\mathcal{N}_2} \right) + \left(1 - \frac{\mathcal{N}_0}{\mathcal{N}_2} \right) D^2 + k_1^2 \left(1 + \frac{\mathcal{N}_0}{\mathcal{N}_2} \right) + \left(k_2^2 - \frac{6}{r^2} \right) \left(1 + \frac{\mathcal{N}_0}{\mathcal{N}_2} \right) - \frac{(\mathcal{N}_0 + \mathcal{N}_2)^2}{\mathcal{N}_2} + \lambda_1 \lambda_2 \mathcal{N}_2 \right] \mu_1 = 0,$$

or

$$\left[D^2 + \frac{1}{2} \frac{\mathcal{N}_0}{\mathcal{N}_2} D^2 + \frac{1}{2} D^2 \left(\frac{\mathcal{N}_0}{\mathcal{N}_2} \right) + \frac{1}{2} \left(k_1^2 + k_2^2 - \frac{6}{r^2} \right) \times \left(1 + \frac{\mathcal{N}_0}{\mathcal{N}_2} \right) - \frac{1}{2 \mathcal{N}_2} \left(\{ \mathcal{N}_0 + \mathcal{N}_2 \}^2 - \lambda_1 \lambda_2 \mathcal{N}_2^2 \right) \right] \mu_1 = 0.$$

This analysis shows that the effect of increasing lambda from its realistic value of unity is to reduce the size of the quantity, corresponding to $f(r)$ in B2. Thus the effect of coupling is

diminished. This manifests itself in a loss of linear independence of the phase shifts and a corresponding loss of symmetry in the R matrix.

Three numerical examples have been taken to demonstrate this effect, each example with a typical value of $f(r)$.

$$(a) \quad \underline{k} = \begin{bmatrix} 16 \\ 1.5 \end{bmatrix}, \quad \underline{l} = \begin{bmatrix} 0 \\ 2 \end{bmatrix}.$$

With this choice of \underline{k} and \underline{l} the zero of the functions $f(r)$ of B2 given in E23 occur at approximately $r = 2.5$ and 7.0 respectively.

As λ increases these zeros are moved closer to the origin and symmetry breaks down at $\lambda = 4.5$.

$$(b) \quad \underline{k} = \begin{bmatrix} 80 \\ 66 \end{bmatrix}, \quad \underline{l} = \begin{bmatrix} 0 \\ 2 \end{bmatrix}.$$

In this case the zeros of the functions are much closer to the origin initially than in (a) and symmetry is lost for a lower value of λ , in this case 2.4 .

$$(c) \quad \underline{k} = \begin{bmatrix} 80 \\ 66 \end{bmatrix}, \quad \underline{l} = \begin{bmatrix} 25 \\ 27 \end{bmatrix}.$$

Again the zeros occur at larger values of r than in either (a) or (b) and λ can be increased to 5 before symmetry is lost.

The algorithm set up at the beginning of this chapter to solve

coupled differential equations requires linearly independent phase shifts to be calculated. This is not possible in the present situation and so the method becomes inaccurate. No way round this difficulty was found but a check on the values of the phase shifts will show whether or not linear independence is being lost.

Dependence of phase shift on k^2

A comparison between the distorted wave approximation and the close coupling approximation will be left until a later chapter. At this stage we investigate a peculiar numerical situation which arises in the close coupling approximation.

Consider the two coupled differential equations

$$\left[\frac{d^2}{dr^2} + k_1^2 - V_{11} \right] u_1 = \lambda_2 V_{21} u_2, \tag{E25}$$

$$\left[\frac{d^2}{dr^2} + k_2^2 - \frac{6}{r^2} - V_{22} \right] u_2 = \lambda_1 V_{12} u_1, \tag{E26}$$

with the usual initial conditions (E2).

The algorithm for solving coupled equations makes use of the fact that linearly independent solutions of the above equations can be found. These equations may be represented asymptotically by

$$u_{11} = A_{11} \sin(k_1 r + \eta_{11}),$$

$$u_{12} = A_{12} \sin(k_1 r + \eta_{12}),$$

$$u_{21} = A_{21} \sin(k_2 r + \eta_{21}),$$

$$u_{22} = A_{22} \sin(k_2 r + \eta_{22}).$$

E27

The difference between η_{11} and η_{12} , η_{21} and η_{22} will give a guide to the strength of linear independence of the phase shifts. These asymptotic solutions are matched in turn to the boundary conditions obtained by permuting the initial channels.

i.e.

$$U_1 \sim \sin(k_1 r) + R_{11} \cos(k_1 r),$$

$$U_2 \sim -\left(\frac{k_2}{k_1}\right)^{\frac{1}{2}} R_{12} \cos(k_2 r),$$

and

$$U_1 \sim \left(\frac{k_1}{k_2}\right)^{\frac{1}{2}} R_{21} \cos(k_1 r),$$

$$U_2 \sim -\sin(k_2 r) - R_{22} \cos(k_2 r);$$

E28

E29

and $R_{11} = \tan \eta_1$, $R_{22} = \tan \eta_2$ where η_1 and η_2 are the required phase shifts of U_1 and U_2 .

Taking a linear combination of E27 and matching to E28 gives

$$c_1 A_{11} \sin(k_1 r + \eta_{11}) + c_2 A_{12} \sin(k_1 r + \eta_{12}) \\ = \sin(k_1 r) + R_{11} \cos(k_1 r),$$

$$c_1 A_{21} \sin(k_2 r + \eta_{21}) + c_2 A_{22} \sin(k_2 r + \eta_{22}) \\ = -\left(k_2/k_1\right)^{\frac{1}{2}} R_{21} \cos(k_2 r),$$

whence, using the substitution

$$X = A_{11} A_{22} \cos \eta_{11} \cos \eta_{22} - A_{12} A_{21} \cos \eta_{21} \cos \eta_{12},$$

we obtain

$$c_1 = A_{22} \cos \eta_{22} / X,$$

$$c_2 = -A_{21} \cos \eta_{21} / X;$$

$$R_{11} = (A_{11} A_{22} \sin \eta_{11} \cos \eta_{22} - A_{12} A_{21} \sin \eta_{12} \cos \eta_{21}) / X, \quad \text{E30}$$

$$R_{12} = \left(k_1/k_2\right)^{\frac{1}{2}} A_{21} A_{22} \sin(\eta_{22} - \eta_{21}) / X; \quad \text{E31}$$

Similarly matching to E30 leads to the equations

$$R_{22} = (A_{11} A_{22} \cos \eta_{11} \sin \eta_{22} - A_{12} A_{21} \cos \eta_{12} \sin \eta_{21}) / X, \quad \text{E32}$$

$$R_{21} = \left(k_2/k_1\right)^{\frac{1}{2}} A_{11} A_{12} \sin(\eta_{11} - \eta_{12}) / X. \quad \text{E33}$$

Also since R is symmetric,

$$A_{11} A_{12} k_1 \sin(\gamma_{11} - \gamma_{12}) = A_{21} A_{22} k_2 \sin(\gamma_{21} - \gamma_{22}). \quad E34$$

We now define a relation between k_1 and k_2 in terms of a variable E , s.t.

$$k_1^2 = BO \times E,$$

$$k_2^2 = BO (E - hi),$$

where BO and hi are constants.

If E is increased then the phase shifts should change smoothly.

For convenience the phase shift is tabulated in the range

$-\pi/2 < \gamma \leq \pi/2$ and thus there are effective discontinuities when γ passes through a multiple of $\pi/2$. This behaviour is

observed in the distorted wave approximation obtained by setting

λ_2 equal to zero in E25 and using boundary conditions E28 to give γ_1 , or setting λ_1 equal to zero in E26 and using boundary condition E29 to give γ_2 .

In the first case $\gamma_{11} = \gamma_{12} = \gamma_1$ and E30 simplifies to

$$R_{11} = \tan \gamma_1 \quad \text{as expected.}$$

Similarly in the second case $\gamma_{22} = \gamma_{21} = \gamma_2$ and E32 gives

$$R_{22} = \tan \gamma_2.$$

In the following numerical work the parameters taken were

$$BO = 321.82,$$

$$hi = 0.045384,$$

$$V_{11} = BO \times v_0,$$

$$V_{22} = B_0 \times (v_0 + \frac{2}{7} v_2),$$

$$V_{12} = V_{21} = B_0 \times \frac{1}{\sqrt{5}} v_2 ; \quad \text{where}$$

$$v_0 = 511.09 \exp (-3.59r) - 5.523 / r^6,$$

$$v_2 = 346.66 \exp (-3.779r) - 0.612 / r^6,$$

and E is varied between 0.05 and 0.25.

The graphs of η_1 versus E and η_2 versus E from the distorted wave approximation are plotted as dotted lines in Figs 2A and 2B.

The close coupling approximation is used over the same range and we found that at various points throughout the range discontinuities occur, in that the phase shift suddenly jumps by an amount π .

Considering the graph of η_1 versus E we find that these discontinuities occur at values of E shown in Table 3.

Now on the graph of η_2 versus E, η_2 passes through the value $\pi/2$ at exactly the same values of E. The reciprocal process is also true; i.e. there are discontinuities in η_2 at the same values of E that η_1 takes the value $\pi/2$. That this should happen numerically can be seen by considering the equations E30 and E32 for R_{11} and R_{22} . If η_2 passes through the value $\pi/2$ then R_{22} will be infinite or, in practice, numerically very large. The value of X at this point will be zero. This has the effect of causing all the R matrix elements to be infinite and hence η_1 will take the value $\pi/2$ immediately giving rise to a

discontinuity of the type shown in Figs 2A and 2B.

However the matrix T given by

$$T = 2R^2 (I + R^2)^{-1} + 2iR (I + R^2)^{-1},$$

remains finite as all the elements of the R matrix become numerically large and the cross-sections as calculated from A_3 vary smoothly as the phase shifts pass through the value $\pi/2$. This is shown in Table 4. Thus although the shape of the graph of η_1 versus E looks rather alarming as given by the close coupling approximation, we can integrate with confidence over this region to obtain realistic cross sections.

Program to solve coupled differential equations

Four coupled differential equations of the type

$$\left[\frac{d^2}{dr^2} + k_i^2 - \frac{l_i(l_i+1)}{r^2} - V_{ii} \right] u_{ij} = \sum_{\substack{k=1 \\ k \neq i}}^4 \lambda_k V_{ik} u_{kj},$$

where $1 \leq i \leq 4$, $1 \leq j \leq 4$.

are solved subject to the boundary conditions

$$u_{ij} = 0 \quad \text{at} \quad r = r_0,$$

$$u_{ij} \sim k_i r \gamma_l(k_i r) \delta_{ij} + \left(\frac{k_i}{k_j} \right)^{\frac{1}{2}} R_{ij} k_i r n_l(k_i r).$$

l takes the values $J, J-2, J, J+2,$

and

$$V_{\mu\gamma}^J = B_0 \left\{ v_0(r) \cdot \delta_{\mu\gamma} + f_2^J(\mu, \gamma) v_2(r) \right\},$$

where f_2^J is given by formulae in Bernstein et al. (1963) and

$$v_\mu(r) = a_\mu e^{-b_\mu r} - \frac{c_\mu}{r^b}, \quad \mu = 0, 2.$$

The R matrix is calculated and the T matrix, giving the elastic and inelastic cross sections from A3, is found.

Data

$B_0, a_0, b_0, c_0, a_2, b_2, c_2,$

$I_1, I_2, I_3, p_1, p_2,$

$r_0, h, y_1,$

$k_1^2, k_2^2, k_3^2, k_4^2,$

$0, 2, \underline{\alpha}$ (4 x 4 matrix),

initial $J = 1, \max J, \text{bool}, \text{eps}, \text{iteps},$

$sa, sb, ra, rb,$

any number of sets of $\lambda,$

999.

The program is designed to be used in conjunction with the program for the distorted wave approximation described in chapter D. The initial parameters are defined there. This latter program contains

an automatic test on convergence of the phase shift which indicates if the functions V_{1j} are negligible. This occurs at a particular value of r and this is the value of r which is taken to terminate the coupled equations program since, at this point, the coupling will have disappeared which is the criterion required for use of the boundary conditions.

As before the values of the potential $v_0(r)$, $v_2(r)$ are calculated and stored at all the tabular points.

The value of J is stepped by one and r_0 advanced a small distance each time. From a knowledge of J a matrix F_2 is set up consisting of the required values $f_2^J(i,j)$. The equations are solved over the entire range using consecutive columns of $\underline{\alpha}$ given by E22.

The values of the function at the matching points r_a , r_b which correspond to tabular points s_a , s_b are stored.

Matrix operations are used to calculate

- (a) the phase shifts for each column of $\underline{\alpha}$ from a modification of B13,
- (b) the matrix \underline{c} given by

$$\underline{c} = \left(w^b \cdot N^a - w^a \cdot N^b \right)^{-1} \left(M^b \cdot N^a - M^a \cdot N^b \right),$$

a formula similar to E10, and

- (c) the matrix R from E10. The T matrix follows from E11, the real and imaginary parts (TA , TB) being stored separately.

These operations are repeated for successive values of J up to J_{\max} when the elastic and inelastic cross-sections are calculated from A3.

If the boolean marker `bool` is set equal to `true` then the various matrices TA , TB , for all values of J , are output onto magnetic tape.

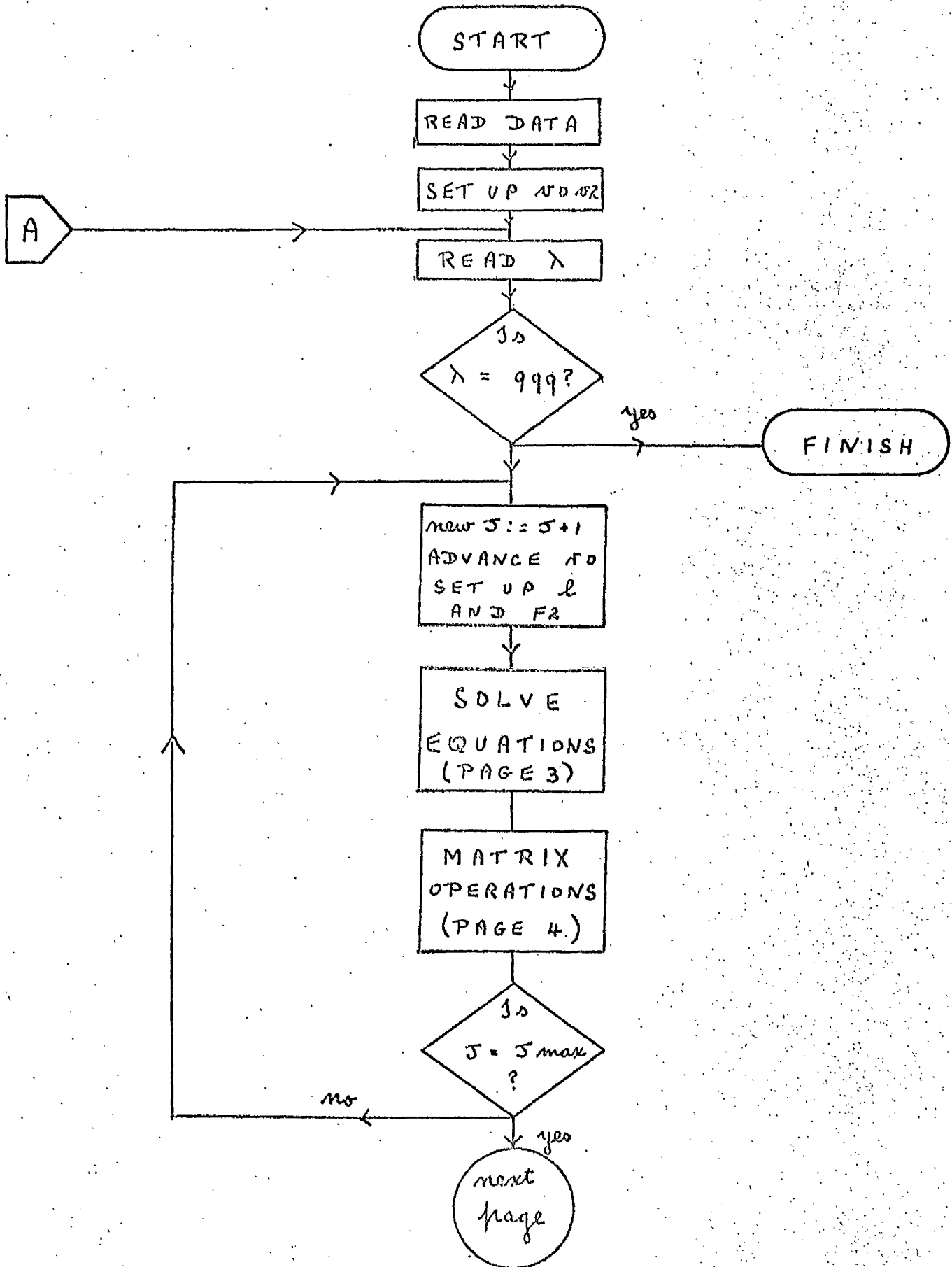
The following matrices are output :-

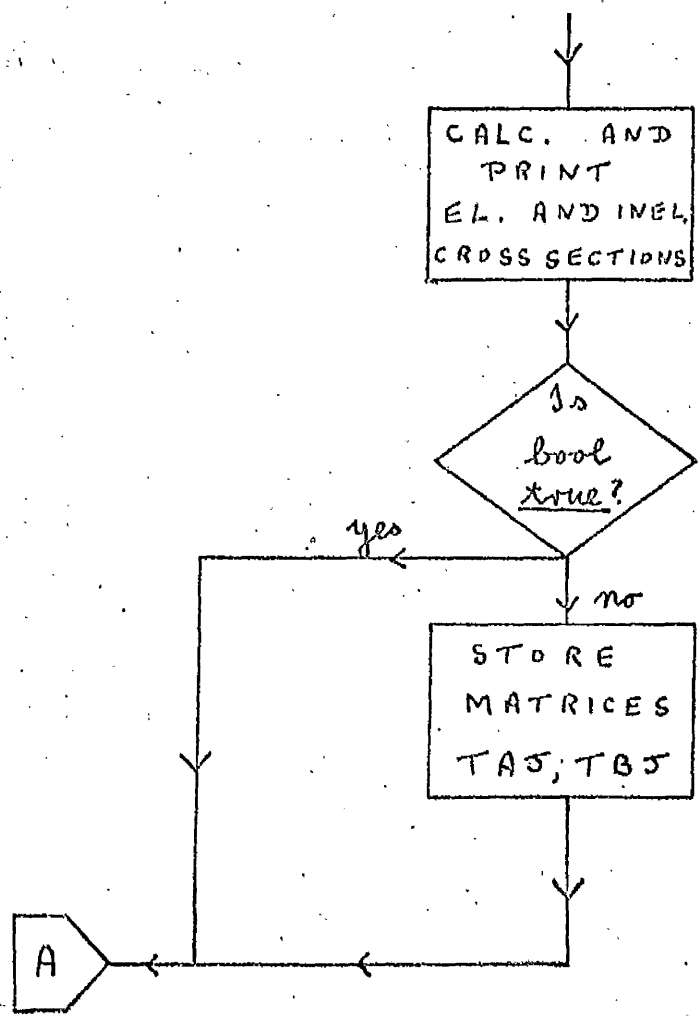
matrix of phase shifts, $\underline{\alpha}$, R , TA , TB for each value of J and then the value of the elastic cross-section ($j = 0 \rightarrow j' = 0$) and the inelastic cross-section ($j = 0 \rightarrow j' = 2$).

BLOCK DIAGRAM

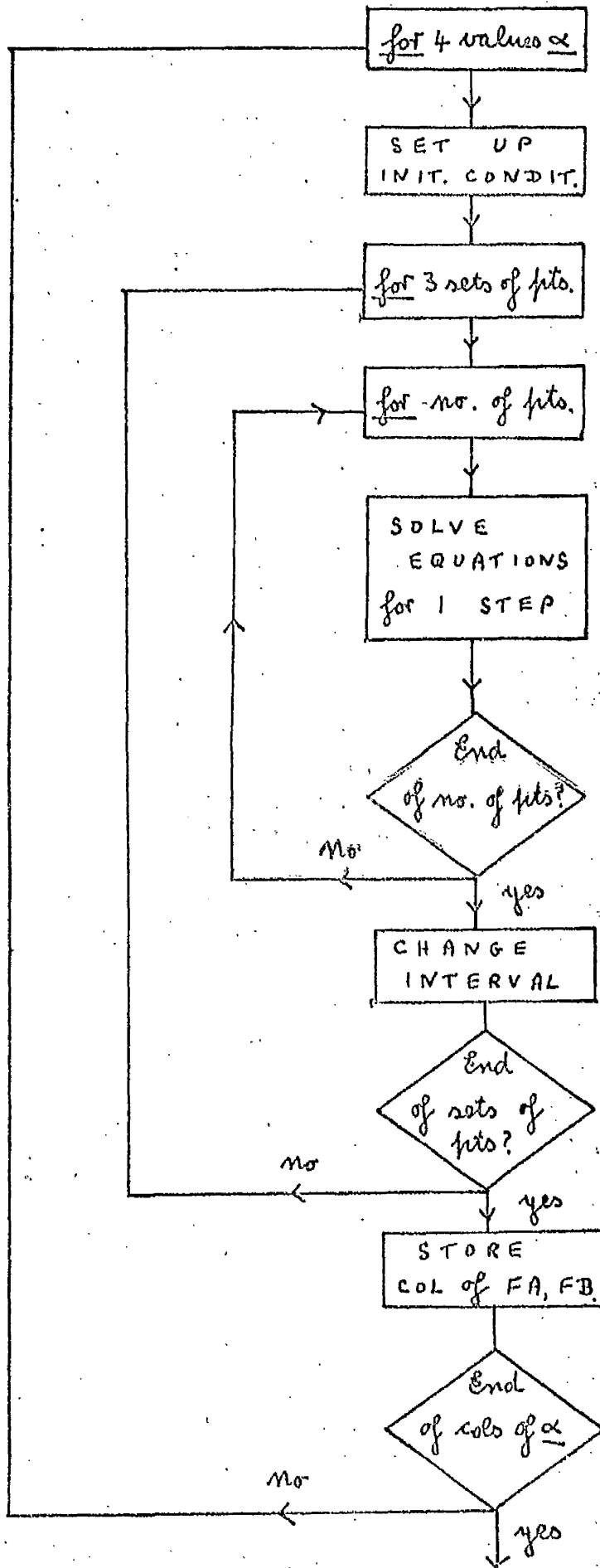
1

CLOSE COUPLING PROGRAM





SOLVE EQUATIONS



MATRIX OPERATIONS

4

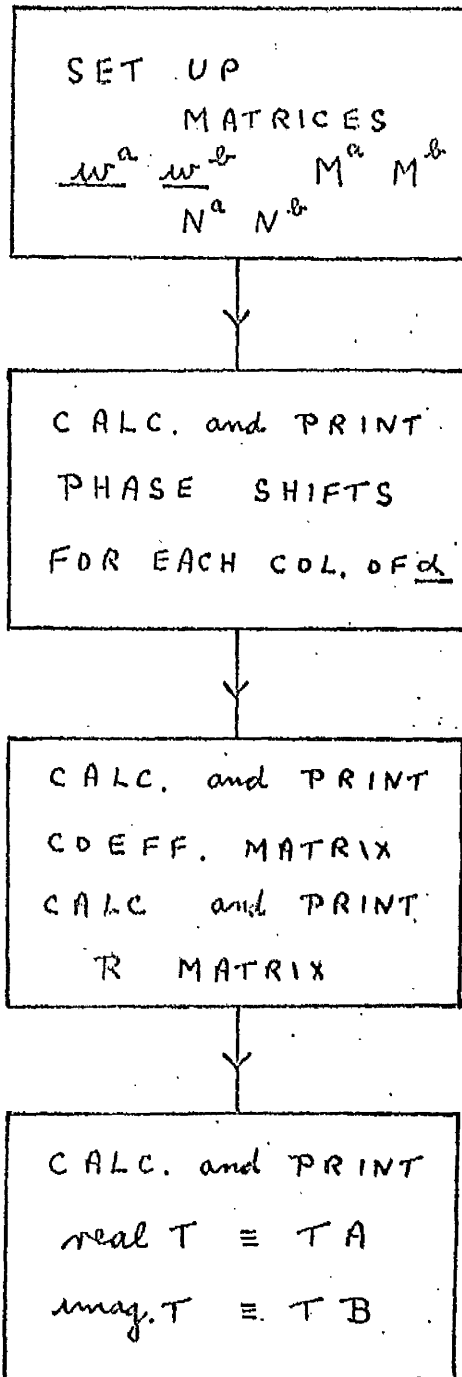


TABLE 1

J value 2.
 Initial interval 0.01

Initial value $r_0 = 1.0$		Initial value $r_0 = 1.5$	
No. of ITERATIONS	No. of POINTS	No. of ITERATIONS	No. of POINTS
3	63	3	8
2	124	2	19
1	3	3	3
2	70	2	132
1	1	1	3
2	28	2	91
1	5	1	1
2	5	2	27
1	2	1	5
2	5	2	5
1	5	1	2
2	1	2	5
1	7	1	4
2	1	2	2
1	7	1	7
2	1	2	1
1	30	1	7
2	1	2	1
1	291	1	30
		2	1
		1	196

TABLE 2

In a typical case

$r_0 = 1.0$

	4.5330	-0.0649	0.0043	-0.0002
R matrix	-0.0649			
	0.0041			
	0.0013			

$r_0 = 2.0$ same case

	4.5196	-0.0643	0.0043	-0.0002
R matrix	-0.0643			
	0.0043			
	-0.0002			

TABLE 3

E(e.v.)	0.054	0.068	0.073	0.107	0.123	0.158	0.203	0.231
$\eta_1(\text{rads})$	*	$\frac{\pi}{2}$	*	*	$\frac{\pi}{2}$	*	$\frac{\pi}{2}$	*
$\eta_2(\text{rads})$	$\frac{\pi}{2}$	*	$\frac{\pi}{2}$	$\frac{\pi}{2}$	*	$\frac{\pi}{2}$	*	$\frac{\pi}{2}$

* - discontinuity

TABLE 4

$E(\text{e.v.})$	η_{11}	η_{22}	R_{11}	R_{22}	$\sigma(0 \leftarrow 0)$	$\sigma(2 \leftarrow 0)$
0.070	0.835	-1.170	11.75	-0.82	0.535	0.0107
0.071	0.765	-1.299	5.62	-1.90	0.521	0.0109
0.072	0.695	-1.425	3.24	-3.32	0.504	0.0112
0.073	0.626	-1.552	1.18	-7.34	0.482	0.0114
0.074	0.555	1.469	91.1	356.2	0.457	0.0116
0.075	0.487	1.351	3.87	7.55	0.430	0.0118

Phase shift in radians and cross section in \AA^2 .

FIGURE 2A

Graph of η_1 (rads) versus energy E (e.V.) showing discontinuities at those values of E for which $\eta_2 = \frac{\pi}{2}$ in Fig 2B.

FIG. 2A.

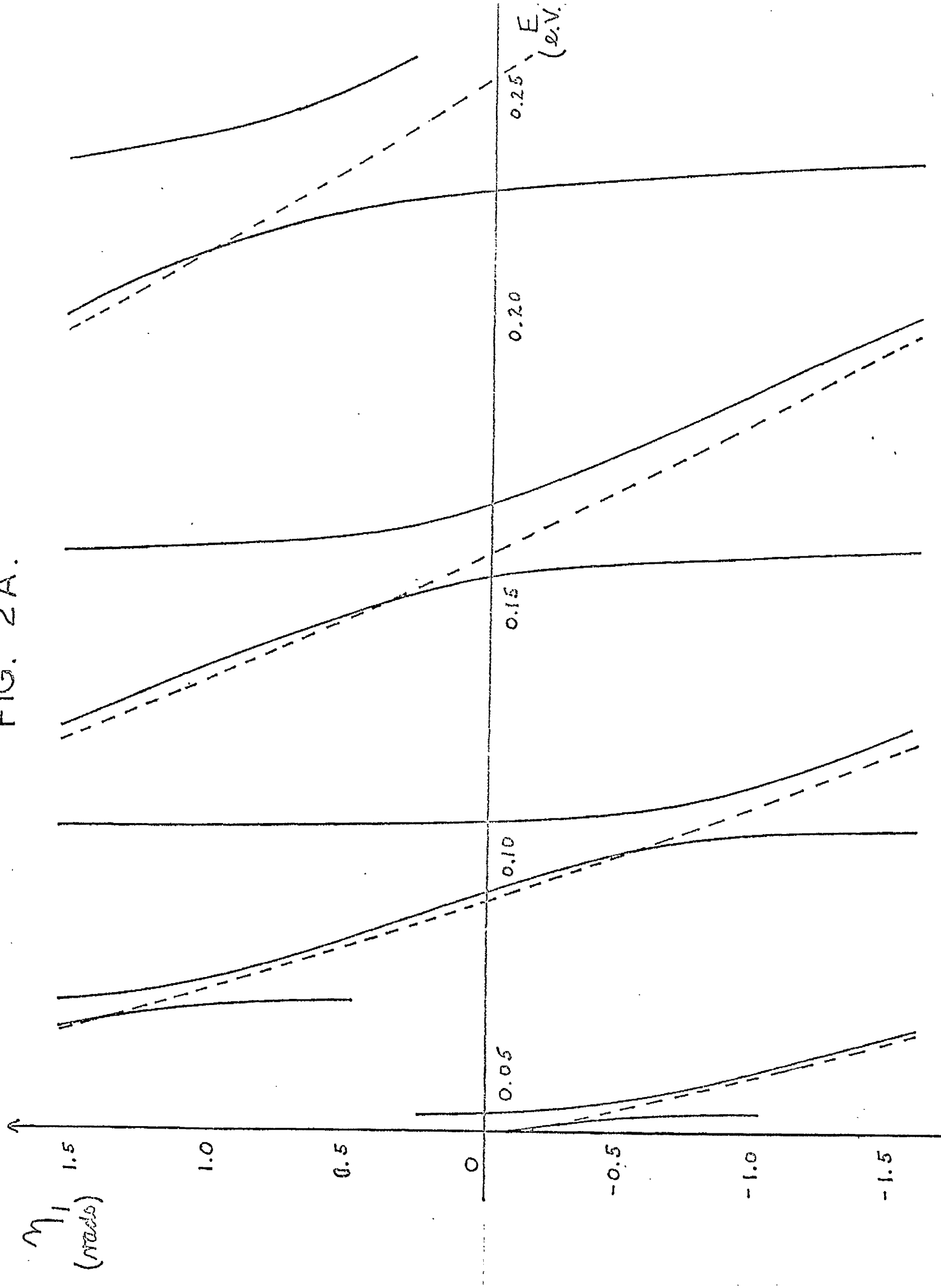
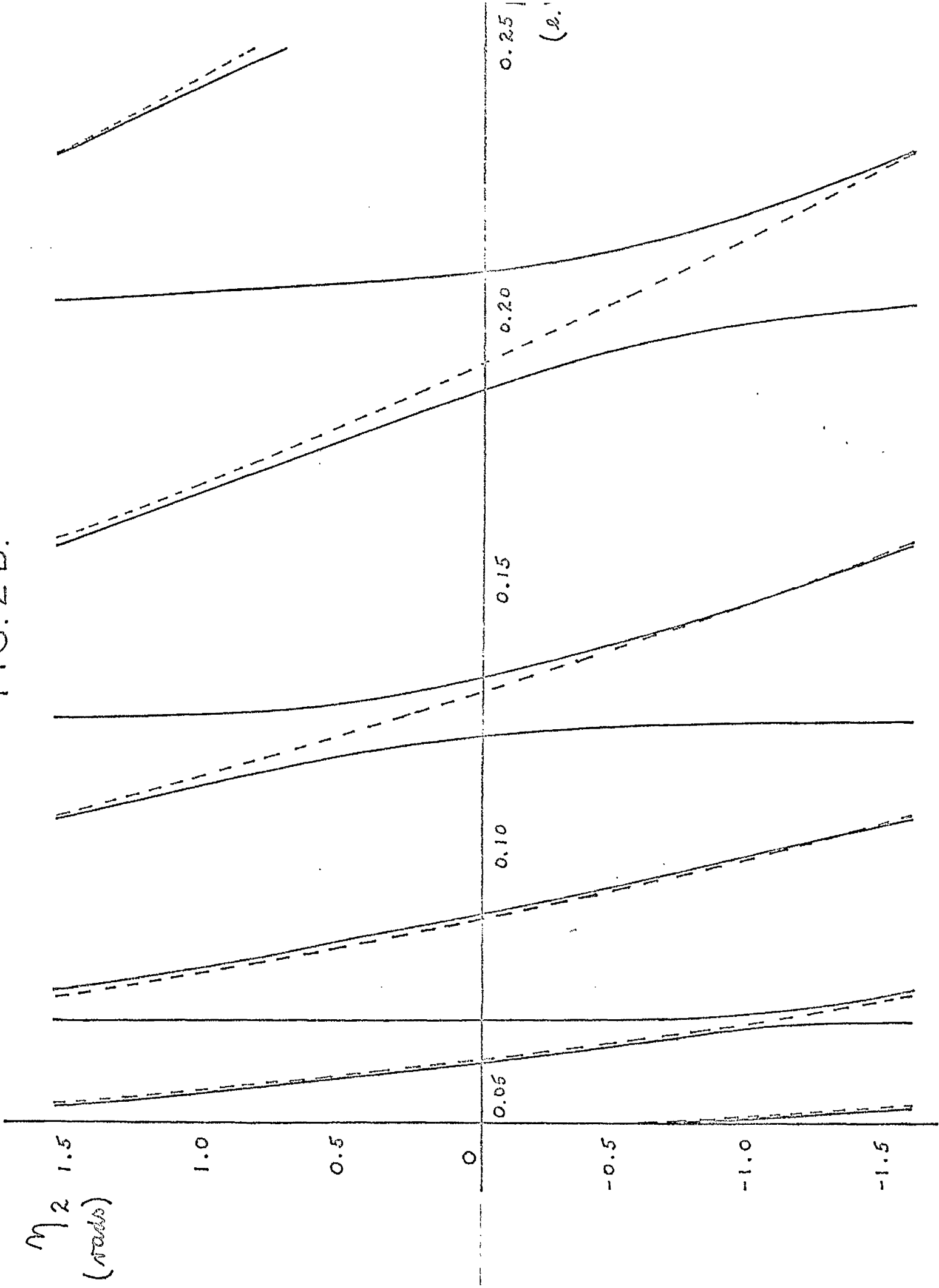


FIGURE 2B

Graph of η_2 (rads) versus energy E (e.V.) showing discontinuities at those values of E for which $\eta_1 = \frac{\pi}{2}$ in Fig 2A.

FIG. 2B.



CHAPTER F

Decaying boundary condition

Introduction

If, in equations B2 and B1, k^2 is replaced by $-k^2$ the equations become

$$\left[\frac{d^2}{dr^2} - k^2 - \frac{l(l+1)}{r^2} - f(r) \right] u(r) = 0, \quad \text{F1}$$

and, as mentioned in chapter B, the asymptotic form of the solution will be

$$u(r) \sim A e^{+kr} + B e^{-kr} \quad \text{F2}$$

If the boundary conditions

$$u = 0 \quad \text{at} \quad r = 0,$$

$$u \sim e^{-kr}, \quad \text{F3}$$

are imposed then it is only for certain values of k , the eigenvalues, that a solution of F1 can be obtained. However there is a solution of the equation

$$\left[\frac{d^2}{dr^2} - k^2 - \frac{l(l+1)}{r^2} - f(r) \right] u(r) = g(r), \quad \text{F4}$$

which satisfies the boundary conditions F3.

This is given by Mott and Massey (1949) to be :

(a) if k is not an eigenvalue,

$$u = \frac{1}{2} \left[u_1 \int_{\infty}^r q u_2 dr - u_2 \int_0^r q u_1 dr \right], \quad \text{F5}$$

where u_1 is that solution of Fl such that

$$u_1 = 0 \quad \text{at} \quad r = 0,$$

and u_2 that solution of Fl such that

$$u_2 \sim \frac{1}{k} e^{-kr}.$$

(b) if k is an eigenvalue,

$$u = \frac{1}{2} \left[u_1 \int_a^r q u_2 dr - u_2 \int_0^r u_1 q dr \right], \quad \text{F6}$$

where u_1 is that solution of Fl such that

$$u_1 = 0 \quad \text{at} \quad r = 0,$$

implying that also $u_1 \sim e^{-kr}$, and u_2 that solution of

Fl such that

$$u_2 \sim \frac{1}{k} e^{kr}.$$

Description of two coupled equations

We now consider the two coupled differential equations

$$\left[\frac{d^2}{dr^2} + k_1^2 - V_{11} \right] u_1 = \lambda_2 V_{12} u_2, \quad \text{F7}$$

$$\left[\frac{d^2}{dr^2} - k_2^2 - \frac{b}{r^2} - V_{22} \right] u_2 = \lambda_1 V_{21} u_1, \quad \text{F8}$$

and impose the boundary conditions

$$u_i = 0 \quad \text{at} \quad r = 0,$$

$$u_1 \sim \sin k_1 r + R \cos k_1 r,$$

$$u_2 \sim B e^{-kr}.$$

F9

Equation F8 is in the same form as F4 so it will be possible to find solutions of F7 and F8 satisfying F9.

Numerical solution

Equation F8 will have asymptotic form F2 but only the decaying exponential is required. This equation is inherently unstable as described in chapter C. Thus forward integration is impossible in this region and we must integrate backwards, in the direction of decreasing r .

Again, for small r , the independent series solutions of F8 are

$$u = r^3 \sum_n a_n r^n \quad \text{and} \quad r^{-2} \sum_n b_n r^n,$$

and since we want to suppress the second of these, forward integration, in the direction of increasing r , is necessary.

The only choice left is to integrate forwards for small r , integrate backwards for large r , and match the solution in the middle, at some point where neither unwanted solution dominates.

Matching implies the equations

$$u_f = u_b \quad \text{and} \quad u'_f = u'_b \quad \text{at} \quad r = r_0, \quad \text{F10}$$

$$\text{or} \quad u_f = u_b \quad \text{at} \quad r = r_c \quad \text{and at} \quad r = r_0 + h, \quad \text{F11}$$

where the suffix f or b denotes forward or backward integration respectively.

Equation F10 is more suitable for use with the Runge-Kutta method while F11 applies more easily to the recurrence relation. We use F11.

Burke and Smith (1962) have described a method of solving these equations.

For the forward integration only two conditions, $u_1 = 0$, $u_2 = 0$ at $r = 0$, are known so two further values are required to specify the solution. These can be obtained by taking two linearly independent solutions and combining them to give the exact solution.

Let these solutions be u_{11}^f , u_{12}^f , u_{21}^f , u_{22}^f , the first index referring to the equation and the second to the choice of initial value.

In the asymptotic region the only condition which can be separated out is $u_2 \sim Be^{-k_2 r}$. In this case three further conditions are required so three linearly independent solutions must be found. These will be represented by u_{ij}^b , $i = 1, 2$; $j = 1, 2, 3$.

A linear combination of these solutions is now matched at the appropriate points,

i.e.

$$(a) \quad c_1 u_{11}^f + c_2 u_{12}^f = c_3 u_{11}^b + c_4 u_{12}^b + c_5 u_{13}^b \quad \text{F12}$$

$$(b) \quad c_1 u_{21}^f + c_2 u_{22}^f = c_3 u_{21}^b + c_4 u_{22}^b + c_5 u_{23}^b$$

at the point $r = r_c$, and two similar equations F12 (c) and (d) at the point $r = r_c + h$.

Dividing by c_5 and taking all values of c_i to left hand side of F12 gives the matrix equation

$$\begin{bmatrix} U^f(r_c) & -U^b(r_c) \\ U^f(r_c+h) & -U^b(r_c+h) \end{bmatrix} \begin{bmatrix} \underline{C} \\ \underline{C} \end{bmatrix} = \begin{bmatrix} U_3^b(r_c) \\ U_3^b(r_c+h) \end{bmatrix} \quad \text{F13}$$

where $U^f(r)$ is a (2×2) matrix u_{ij}^f ,

$U^b(r)$ is a (2×2) matrix u_{ij}^b ,

$U_3^b(r)$ is a (2×1) vector u_{3j}^b , $i = 1, 2$; $j = 1, 2$,

and \underline{C} is a (4×1) vector $\frac{c_k}{c_5}$, $k = 1, 2, 3, 4$.

This gives the correct combination of the arbitrary computed solutions required to fit the given boundary conditions. The phase

shift can now be found by matching the asymptotic solution of F7,

$$u_1 \sim C_3 u_{11}^b + C_4 u_{12}^b + u_{13}^b,$$

to the corresponding condition F9.

Choice of matching point

The choice of matching point is not critical for a single equation with a decaying exponential boundary condition since the only requirement is that integration in either direction should not suffer unduly through unstable accumulation of error (Mayers 1962). In practice we choose the value of r for which V_{22} , given in equation F8, is a minimum.

Forward integration

There is no problem with the forward integration. We choose the matrix $\begin{bmatrix} 1 & 1 \\ +1 & -1 \end{bmatrix}$ as values at the second tabular point and integrate as in chapter E out to the matching point $r_c + h$.

Backward integration

The situation in the asymptotic region is not so straightforward. If the backward integration is started far out at some point r_f and initial conditions

$$u_1(r_f) = \mathcal{O}(1),$$

$$u_2(r_f) = \mathcal{O}(1),$$

F14

are taken, where $\mathcal{O}(1)$ represents some quantity of the order of one, then the second solution will increase very rapidly with respect to the first, until the effect of the coupling term on the right hand side of F7 will dominate the equation and the true solution will be lost.

On the other hand, if initial conditions

$$u_1(r_f) = \mathcal{O}(1),$$

$$u_2(r_f) = \mathcal{O}(10^{-10})$$

F15

are taken, then the magnitude of the coupling on the right hand side of F8 would swamp the correct solution. This difficulty can be overcome if the backward integration is divided into two parts.

First equation F7 is integrated, by itself, backwards from r_f to some point r_e where we might reasonably expect the numerical value of the solution of F8 to be significant.

Then the coupled equations F7 and F8 are integrated backwards

from r_e to the matching point r_c . A suitable choice of r_e will avoid the severe cancellation which occurs in situations defined by asymptotic conditions F14 and F15. To keep a check on this the values of both sides of F12 were printed out.

An example is given which demonstrates the effect of the choice of r_e .

Equations F7 and F8 were solved using

$$\underline{k}^2 = \begin{bmatrix} 16.091 \\ 1.609 \end{bmatrix}$$

and the matrix V was taken as in the example at the end of chapter E.

The function V_{22} has a minimum about $r = 3.8$ and the matching points were chosen to be 4.01 and 4.11. The results, summarized in Table 5, were used to find a criterion for the choice of r_e . This is essential if a program is to be written with automatic calculation of r_e .

Table 5 shows that the phase shift $\gamma_1 = \tan^{-1}(R)$ is very insensitive to the value of r_e although accuracy is lost as r_e increases. If we assume that the decaying exponential behaviour begins around the point r_c , an estimate of the value of r_e can be obtained by taking a value of r for which the quantity $e^{-k_2 r}$ has fallen off by some factor (say p) from its value at the point r_c .

i.e.

$$\frac{e^{-k_2 r_c}}{e^{-k_2 r_e}}$$

p ,

$$\text{i.e.} \quad r_e - r_o < \frac{1}{k_2} P,$$

where $P = \log_e p$.

Using the values, from Table 5, of $r_e = 8.01$ and $r_o = 4.01$ gives $P \approx 5$, so the criterion used in the program was

$$r_e - r_o < 5.0/k_2.$$

This was found to be satisfactory over most of the range

$0 < k_1^2 < 16$, $16 > k_2^2 > 0$, although the accuracy diminished for very small values of k_1^2 .

Description of program

Two coupled differential equations of the form

$$\left[\frac{d^2}{dr^2} + k_1^2 - V_{11} \right] u_1 = \lambda_2 V_{12} u_2,$$

$$\left[\frac{d^2}{dr^2} - k_2^2 - \frac{b}{r^2} - V_{22} \right] u_2 = \lambda_1 V_{21} u_1,$$

are solved, subject to the boundary conditions

$$u_i = 0 \quad \text{at} \quad r = r_o; \quad i = 1, 2,$$

$$u_1 \sim \sin k_1 r + R \cos k_1 r,$$

$$u_2 \sim B e^{-kr}.$$

V_{ij} is the same as in previous programs. The program calculates and prints the value of R .

Data

BO, hi,

a0, b0, c0, a2, b2, c2,

I₁, I₂, I₃, p1, p2,

r0, h, y1,

0, 2, α (2 x 2 matrix), α' (3 x 3 matrix),

initial J-1 (set equal to -1 in this case),

J max (set equal to 0),

λ₁, λ₂, e1, e2, e3.

k₁² is given by BO x e while

k₂² is given by BO (e - hi),

where e takes values e1 (e2) e3.

The matching points are chosen to be the tabular points given by

I₁ + I₂ and I₁ + I₂ + 1.

The two equations are integrated forwards to this point, using the matrix α as initial values.

The first equation is integrated backwards from tabular point

I₁ + I₂ + I₃ + 1 to the point r_e defined by criterion F16. Now

the coupled equations are integrated backwards to the matching points

where the forward and backward solutions are matched. The vector

of coefficients C is calculated and, to keep a check on the acc-

uracy of the matching the left hand side and the right hand side of

equation F12 are printed.

Finally the phase shift η given by $\arctan(R)$ is evaluated from boundary condition for u_1 at the tabular points given by $I_1 + I_2 + I_3$ and $I_1 + I_2 + I_3 + 1$.

TABLE 5

r_e	R.H.S Fl2(b)	L.H.S Fl2(b)	R.H.S Fl2(d)	L.H.S Fl2(d)	η
8.01	-1.8976	-1.8976	-1.6442	-1.6443	0.095
10.01	-1.8981	-1.9066	-1.6446	-1.6545	0.095
12.01	-1.9015	-1.9932	-1.6476	-1.7536	0.095

CHAPTER G

Derivation of radial equations

The formalism of Arthurs and Dalgarno (1960) is used to consider rotational excitation of a diatomic molecule by an incident point particle. The model which is taken to represent the molecule is that of a rigid rotator.

Let $\hat{\underline{x}} \equiv (\theta, \phi)$ specify the direction of motion of the incident particle, distant r from the centre of mass of the rotator, and let $\hat{\underline{x}}' \equiv (\theta', \phi')$ specify the orientation of the internuclear axis with respect to some axis fixed in space.

The Hamiltonian for the entire system is

$$H = H_{rot} - \frac{\hbar^2}{2\mu} \nabla_r^2 + V(r, \theta - \theta'), \quad G1$$

where $-\frac{\hbar^2}{2\mu} \nabla_r^2$ is the kinetic energy operator for the scattered particle, H_{rot} is the Hamiltonian for a free rotator in space and $V(r, \theta - \theta')$ is the interaction potential of the colliding systems. The wave functions describing the rotational states of the molecule are the spherical harmonics $Y_{\gamma m_{\gamma}}(\hat{\underline{x}}')$ defined in Condon and Shortley (1935), which satisfy

$$H_{rot} Y_{\gamma m_{\gamma}}(\hat{\underline{x}}') = \frac{\hbar^2}{2I} \gamma(\gamma+1) Y_{\gamma m_{\gamma}}(\hat{\underline{x}}'), \quad G2$$

where I is the moment of inertia of the rotator, $\underline{j} \hbar$ is its rotational angular momentum and $m_j \hbar$ its projection on the z axis.

Let $\underline{l} \hbar$ be the orbital angular momentum of the incident particle, $m_l \hbar$ its projection and consider the wave function defined by

$$Y_{j\gamma l}^M(\hat{r}, \hat{r}') = \sum_{m_l} \sum_{m_j} (\gamma l m_j m_l | \gamma l J M) Y_{l m_l}(\hat{r}) Y_{j m_j}(\hat{r}'), \quad G3$$

where $(j l m_j m_l | j l J M)$ is the Clebsch-Gordan coefficient.

$Y_{j\gamma l}^M(\hat{r}, \hat{r}')$ describes a system of total angular momentum $\underline{J} \hbar$ and projection $M \hbar$, where

$$\underline{J} = \underline{j} + \underline{l},$$

and it includes the entire angular dependence of the incident particle and target.

If E is the kinetic energy of the incident particle, measured in the centre of mass system, the total energy of the system, when the rotator is in the state specified by rotational quantum number j , is given by

$$E_\gamma = E + \frac{\hbar^2}{2I} \gamma(\gamma+1). \quad G4$$

Eigenfunctions of H , corresponding to total angular momentum quantum numbers J and M and appropriate to the entrance channel defined by quantum numbers (j, l) may be expanded in terms of $Y_{j\gamma l}^M(\hat{r}, \hat{r}')$ as

$$\Psi_{j\ell}^{JM}(\underline{r}, \hat{\underline{r}}') = \sum_{j'} \sum_{\ell'} \frac{1}{r} u_{j'\ell'}^{j\ell}(\tau) y_{j'\ell'}^M(\hat{\underline{r}}, \hat{\underline{r}}'), \quad G5$$

where $u_{j'\ell'}^{j\ell}(\tau)$ are functions to be determined such that

$$H \Psi_{j\ell}^{JM}(\underline{r}, \hat{\underline{r}}') = E_j \Psi_{j\ell}^{JM}(\underline{r}, \hat{\underline{r}}'). \quad G6$$

Using the previous equations, the resulting set of coupled differential equations is

$$\left[\frac{d^2}{dr^2} + k_{j'\ell'}^2 - \frac{\ell'(\ell'+1)}{r^2} \right] u_{j'\ell'}^{j\ell}(\tau) \quad G7$$

$$= \frac{2\mu}{\hbar^2} \sum_{j''} \sum_{\ell''} \langle j'\ell'; \tau | V | j''\ell''; \tau \rangle u_{j''\ell''}^{j\ell}(\tau),$$

where $k_{j'\ell'}^2$ is the channel wave number given by

$$k_{j'\ell'}^2 = \frac{2\mu}{\hbar^2} \left[E_j - \frac{\hbar^2}{2I} \ell'(\ell'+1) \right] \quad G8$$

and

$$\langle j'\ell'; \tau | V | j''\ell''; \tau \rangle = \int y_{j'\ell'}^{M*} V y_{j''\ell''}^M d\hat{\underline{r}} \cdot d\hat{\underline{r}}'. \quad G9$$

The scattering matrix $S^J(j\ell; j'\ell')$ is defined by the requirement that asymptotically

$$u_{j'l'}^{j\gamma l}(\tau) \sim \delta_{jj'} \delta_{ll'} \exp\left[-i(k_{j\gamma} \tau - \frac{1}{2} l \pi)\right] - \left(\frac{k_{j\gamma}}{k_{j'\gamma}}\right)^{\frac{1}{2}} S^j(\gamma l; j'l') \exp\left[+i(k_{j'\gamma} \tau - \frac{1}{2} l' \pi)\right]. \quad \text{G10}$$

Derivation of cross section

Total wave functions $\Psi_{\gamma}(\tau, \hat{n}, \hat{n}')$, having the asymptotic form of a plane wave multiplying the initial target wave function plus a linear combination of products of outgoing waves and final target wave functions, are defined by Blatt and Biedenharn (1952) to be

$$\Psi_{\gamma}(\tau, \hat{n}, \hat{n}') = \frac{i(\pi)^{\frac{1}{2}}}{k_{j\gamma}} \sum_{J=0}^{\infty} \sum_{M=-J}^{+J} \sum_{l=|J-\gamma|}^{J+\gamma} i^l (2l+1)^{\frac{1}{2}} \times (\gamma l m_{\gamma} 0 | \gamma l J M) \Psi_{\gamma l}^{JM}(\tau, \hat{n}'). \quad \text{G11}$$

Equation G11 has asymptotic form

$$\begin{aligned} \Psi_{\gamma}(\tau, \hat{\underline{r}}, \hat{\underline{r}}') &\sim \exp(i k_{\gamma\gamma} \cdot \underline{r}) Y_{\gamma m_{\gamma}}(\hat{\underline{r}}') \\ &+ \sum_{\gamma'} \frac{i}{k_{\gamma\gamma}} \left(\frac{k_{\gamma\gamma}}{k_{\gamma'\gamma}} \right)^{\frac{1}{2}} r^{-1} \exp(i k_{\gamma'\gamma} \tau) \\ &\times \sum_{m_{\gamma'}} q(\gamma' m_{\gamma'}; \gamma m_{\gamma}) Y_{\gamma' m_{\gamma'}}(\hat{\underline{r}}'), \end{aligned} \quad \text{G12}$$

where $q(j' m_{j'}; j m_j)$ is the reaction amplitude given by

$$\begin{aligned} q(\gamma' m_{\gamma'}; \gamma m_{\gamma}) &= \sum_{\mathcal{J}} \sum_{M} \sum_{l} \sum_{l'} \sum_{m_{e'}} i^{l-l'} \pi^{\frac{1}{2}} (2l+1)^{\frac{1}{2}} \\ &\times (Y_{l m_{\gamma}} | Y_{l \mathcal{J} M}) (Y_{l' m_{\gamma'} m_{e'}} | Y_{l' \mathcal{J} M}) T^{\mathcal{J}}(\gamma l; \gamma' l') Y_{l' m_{e'}}(\hat{\underline{r}}), \end{aligned} \quad \text{G13}$$

$T^{\mathcal{J}}(j l; j' l')$ being an element of the transition matrix defined by

$$T^{\mathcal{J}}(\gamma l; \gamma' l') = \delta_{\gamma\gamma'} \delta_{ll'} - S^{\mathcal{J}}(\gamma l; \gamma' l'). \quad \text{G14}$$

The differential scattering cross section for excitation from the (j, m_j) state of the rotator to the $(j', m_{j'})$ state is given by

$$d\sigma(\gamma' m_{\gamma'}; \gamma m_{\gamma} | \hat{\underline{r}}) = \frac{1}{k_{\gamma\gamma}^2} |q(\gamma' m_{\gamma'}; \gamma m_{\gamma})|^2 d\hat{\underline{r}}. \quad \text{G15}$$

Since most scattering experiments do not distinguish between the

different states m_j or $m_{j'}$ of the rotator, we average over the m_j and sum over the $m_{j'}$, to give $d\sigma(j'; j | \hat{x})$, the differential scattering cross section for the $j - j'$ transition.

From equations G12, G13, G15 and by making use of the algebra of the Clebsch-Gordan and Racah coefficients (Biedenharn, Blatt and Rose 1952, Racah 1942) the following equation for the differential scattering cross section was obtained,

$$\frac{d\sigma(j'; j | \hat{x})}{d\hat{r}} = \frac{(-1)^{j-j'}}{4(2j+1)k_{jy}^2} \sum_{\lambda=0}^{\infty} A_{\lambda} P_{\lambda} \left(\frac{\hat{k}_{jy}}{k_{jy}} \cdot \frac{\hat{k}_{j'y}}{k_{j'y}} \right), \quad \text{G16}$$

where P_{λ} is the Legendre polynomial of order λ and

$$A_{\lambda} = \sum_{j_1=0}^{\infty} \sum_{j_2=0}^{\infty} \sum_{l_1=|j_1-j|}^{j_1+j} \sum_{l_2=|j_2-j|}^{j_2+j} \sum_{l_1'=|j_1-j'|}^{j_1+j'} \sum_{l_2'=|j_2-j'|}^{j_2+j'} Z(l_1, j_1, l_2, j_2; j, \lambda) \times Z(l_1', j_1, l_2', j_2'; j', \lambda) T^{j_1}(j', l_1'; j, l_1) T^{j_2'}(j', l_2'; j, l_2), \quad \text{G17}$$

where

$$Z(a, b, c, d; e, f) = (-1)^{\frac{1}{2}(f-a+c)} \left[(2a+1)(2b+1)(2c+1)(2d+1) \right]^{\frac{1}{2}} \times (a, c, 0, 0 | a, c, f, 0) W(a, b, c, d; e, f). \quad \text{G18}$$

The total cross section for the $j - j'$ transition takes the form

$$\sigma(j'; j) = \frac{\pi}{(2j+1)k_{jy}^2} \sum_{j=0}^{\infty} \sum_{l=|j-j|}^{j+j} \sum_{l'=|j-j'|}^{j+j'} (2j+1) \left| T^j(j', l'; j, l) \right|^2. \quad \text{G19}$$

Distorted wave approximation

If the coupling terms in G7 are ignored there results the set of uncoupled equations

$$\left[\frac{d^2}{dr^2} + k_{\delta\delta}^2 - \frac{l'(l'+1)}{r^2} - \frac{2\mu}{\hbar^2} \langle \delta'l'; \mathcal{V} | \delta'l'; \mathcal{V} \rangle \right] u_{\delta'l'}^{\mathcal{J}\delta l}(\tau) = 0. \quad G20$$

Defining $w_{\delta'l'}^{\mathcal{J}\delta l}(\tau)$ to be that solution of G20 which behaves asymptotically as

$$w_{\delta'l'}^{\mathcal{J}\delta l}(\tau) \sim \sin(k_{\delta\delta}\tau - \frac{1}{2}l'\pi + \eta_{\delta'l'}^{\mathcal{J}\delta l}), \quad G21$$

where $\eta_{\delta'l'}^{\mathcal{J}\delta l}$ is a real phase shift, the equation

$$u_{\delta'l'}^{\mathcal{J}\delta l}(\tau) = S_{\delta\delta'} S_{e'e'} w_{\delta l}^{\mathcal{J}\delta l}(\tau) \quad G22$$

is taken as the zero order approximation in an iteration procedure. The first order approximation is then those equations discussed in chapter D, the results of which are, changing the notation,

$$S^{\mathcal{J}}(\delta l; \delta l) = \exp(2i\eta_{\delta'l'}^{\mathcal{J}\delta l}), \quad G23$$

$$S^{\mathcal{J}}(\delta l; \delta'l') = 2i \left(\frac{k_{\delta\delta'}}{k_{\delta\delta}} \right)^{\frac{1}{2}} \beta_{\delta'l'}^{\mathcal{J}\delta l} \exp \left[i(\eta_{\delta l}^{\mathcal{J}\delta l} + \eta_{\delta'l'}^{\mathcal{J}\delta l}) \right], \quad G24$$

where

$$\beta_{\gamma' l'}^{\gamma l} = \frac{2\mu}{\hbar^2 k_{\gamma'}^2} \int_0^{\infty} w_{\gamma' l'}^{\gamma l}(r) \langle \gamma' l'; \sigma | V | \gamma l; \sigma \rangle w_{\gamma l}^{\gamma' l'}(r) dr. \quad G25$$

The elastic cross section becomes, in this approximation,

$$\sigma(\gamma; \gamma) = \frac{\pi}{(2\gamma+1) k_{\gamma}^2} \sum_{\sigma=0}^{\infty} (2\sigma+1) \left[\sum_l \sin^2(\eta_{\gamma l}^{\sigma}) + \sum_l \sum_{l' \neq l} (\beta_{\gamma' l'}^{\gamma l})^2 \right], \quad G26$$

while the inelastic cross section yields

$$\sigma(\gamma'; \gamma) = \frac{\pi}{(2\gamma+1) k_{\gamma}^2} \left(\frac{k_{\gamma'}^2}{k_{\gamma}^2} \right) \sum_{\sigma=0}^{\infty} (2\sigma+1) \sum_{l=|\sigma-\gamma|}^{\sigma+\gamma} \sum_{l'=|\sigma-\gamma'|}^{\sigma+\gamma'} (\beta_{\gamma' l'}^{\gamma l})^2. \quad G27$$

The distorted wave approximation violates the conservation requirement as expressed in the unitarity of the scattering matrix,

$$\sum_{\gamma' l'} |S^{\sigma}(\gamma l; \gamma' l')|^2 = 1. \quad G28$$

Now from G23, G24, G25,

$$\sum_{\gamma' l'} |S^{\sigma}(\gamma l; \gamma' l')|^2 = 1 + \sum_{\gamma' l'} \frac{k_{\gamma'}^2}{k_{\gamma}^2} \left(2 \beta_{\gamma' l'}^{\gamma l} \right)^2, \quad G29$$

so the distorted wave weak coupling approximation is only useful

when

$$\Delta_{\gamma'}^{\gamma\ell} = \sum_{\gamma'\ell'} \frac{k_{\gamma'\gamma}}{k_{\gamma\gamma}} \left(2 \beta_{\gamma'\ell'}^{\gamma\ell} \right)^2, \quad \text{G30}$$

is small compared with unity.

When it is not small, violation of the conservation requirement can be avoided by the introduction of a reactance matrix or phase matrix (Percival 1960, Seaton 1961). Another method of approach, used by Bernstein et al (1963), is to renormalise the matrix elements by multiplying them by a correcting factor.

$$C_{\gamma'}^{\gamma\ell} = \left(1 + \Delta_{\gamma'}^{\gamma\ell} \right)^{-\frac{1}{2}}. \quad \text{G31}$$

However, for practical computations, the quantity $\Delta_{\gamma'}^{\gamma\ell}$ is tested and when it becomes too large compared with unity, greater than 0.5 (say), the distorted wave approximation is no longer used. This is the criterion adopted by Roberts (1963) and Dalgarno, Henry and Roberts (1966) in their calculations using the distorted wave approximation.

Close coupling approximation

If none of the coupling terms in G7 are ignored then no analytical solution of these equations can be found so it is necessary

to proceed numerically as in chapter B.

The asymptotic condition

$$u_{j'l'}^{j'l} \sim \delta_{ll'} \delta_{jj'} \sin(k_{jj'} r - \frac{1}{2} l \pi) + \left(\frac{k_{jj}}{k_{j'j'}} \right)^{\frac{1}{2}} R^{jj'}(j'l; j'l') \cos(k_{jj'} r - \frac{1}{2} l' \pi), \quad G32$$

leads to a relation between the R and S matrices given by

$$S = (I - iR)^{-1} (I + iR). \quad G33$$

The elements $T^{jj'}(j'l; j'l')$, may be found and hence the cross sections may be calculated from G19.

Equations G7 consist of an infinite set of coupled differential equations. Practically we can only take the summation over a few of the possible states. Thus the close coupling approximation ignores coupling to any higher levels than the ones under consideration.

Expansion of potential function

The potential $V(r, \theta - \theta')$ may be expanded in a series of Legendre polynomials,

$$V(r, \theta - \theta') = \sum_{\mu} v_{\mu}(r) P_{\mu}(\hat{r} \cdot \hat{r}'). \quad G34$$

The matrix elements defined in G9 then involve terms such as

$$\langle \gamma' l'; J | P_\mu(\hat{r}, \hat{r}') | \gamma'' l''; J \rangle = \iint \gamma_{\gamma' l'}^M(\hat{r}, \hat{r}')^* P_\mu(\hat{r}, \hat{r}') \gamma_{\gamma'' l''}^M(\hat{r}, \hat{r}') d\hat{r} d\hat{r}' \quad G35$$

Substituting equation G3 and using the expansion

$$P_\mu(\hat{r}, \hat{r}') = \frac{4\pi}{2\mu+1} \sum_m Y_{\mu m}(\hat{r}) Y_{\mu m}^*(\hat{r}'), \quad G36$$

gives rise to the integrals evaluated by Rose (1957),

$$\int Y_{l_3 m_3}^*(\hat{r}) Y_{l_2 m_2}(\hat{r}) Y_{l_1 m_1}(\hat{r}) d\hat{r} = \left[\frac{(2l_1+1)(2l_2+1)}{4\pi(2l_3+1)} \right]^{\frac{1}{2}} (l_1, l_2, 0, 0 | l_1, l_2, l_3, 0) (l_1, l_2, m_1, m_2 | l_1, l_2, l_3, m_3) \quad G37$$

i.e.

$$\langle \gamma' l'; J | P_\mu(\hat{r}, \hat{r}') | \gamma'' l''; J \rangle = \left[(2l'+1)(2l''+1)(2\gamma'+1)(2\gamma''+1) \right]^{\frac{1}{2}} \times (l'' l' 0 0 | l'' l' \mu 0) (\gamma \gamma' 0 0 | \gamma \gamma' \mu 0) \times \frac{1}{(2\mu+1)^2} \times K, \quad G38$$

where

$$K = \sum_{m_2'} \sum_{m_{\gamma'}} \sum_{m_{\gamma''}} \sum_{m_{\gamma''}} \sum_m (-1)^{m+m'} (\gamma' l' m_{\gamma'} m_{\gamma''} | \gamma' l' J M) \times (\gamma'' l'' m_{\gamma''} m_{\gamma''} | \gamma'' l'' J M) (l'' l' + m_{\gamma''} - m_{\gamma'}, | l'' l' \mu m) \times (\gamma \gamma' + m_{\gamma''} - m_{\gamma'} | \gamma \gamma' \mu - m). \quad G39$$

Using formulae given by Racah (1942),

$$(\gamma_1, \gamma_2, m_1, m_2 | \gamma, \gamma_2, \gamma, m) = (-1)^{\gamma+m} (2\gamma+1)^{\frac{1}{2}} V(\gamma_1, \gamma_2, \gamma, m_1, m_2, -m)$$

and

$$\begin{aligned} & \sum_{\alpha\beta\gamma\delta\phi} (-1)^{f+\phi} V(a, b, e, \alpha, \beta, -\epsilon) V(a, c, f, -\alpha, \gamma, \phi) \\ & \quad \times V(b, d, f, -\beta, \delta, -\phi) V(c, d, g, \gamma, \delta, -\eta) \\ & = (-1)^{e+\epsilon+f+d-b} W(a, b, c, d; e, f) \delta(e, g) \delta(\epsilon, \eta) / (2\epsilon+1), \end{aligned}$$

then

$$K = (-1)^{\gamma+l'-l} W(\gamma'' l'' \gamma' l'; \gamma, \mu) / (2\gamma+1). \quad G40$$

Hence

$$\begin{aligned} & \langle \gamma' l'; \gamma | P_\mu(\hat{x}, \hat{x}') | \gamma'' l''; \gamma \rangle \\ & = \frac{(-1)^{\gamma''+\delta'-\gamma}}{2\mu+1} \left[(2\gamma'+1)(2\gamma''+1)(2l'+1)(2l''+1) \right]^{\frac{1}{2}} \\ & \quad \times (l'' l' 0 0 | l'' l' \mu_0) (\gamma'' \gamma' 0 0 | \gamma'' \gamma' \mu_0) \\ & \quad \times W(\gamma'' l'' \gamma' l'; \gamma, \mu) \\ & = f_\mu(\gamma' l'; \gamma'' l''; \gamma). \end{aligned}$$

From G41 it is easily shown that

$$f_0(j'l'; j''l''; J) = \begin{cases} 0 & j'' \neq j' & l'' \neq l' \\ 1 & j'' = j' & l'' = l' \end{cases} \quad \text{G42}$$

Thus from G42 it can be seen that no rotational transitions for a $V(\tau, \theta - \theta')$ having only a $\mu = 0$ term are possible.

If the rotator is symmetric, so that

$$V(\tau, \theta - \theta') = V(\tau, \pi - [\theta - \theta']),$$

then only even values of μ will appear in expansion G34.

For even values of μ ,

$$f_\mu(j'l'; j''l''; J) = 0,$$

unless $j' + j''$ and $l' + l''$ are both even. This means that for a homonuclear diatomic molecule, no rotational transitions can take place for which $\Delta \gamma$ is not even. If $V(\tau, \theta - \theta')$ is further restricted by truncating the series G34 after the term in $\mu = 2$, the only f_μ that are non-zero are those for which $j' = j'' \pm 2$ and $l' = l'' + 2$. This gives rise to the selection rule $\Delta \gamma = 0, \pm 2$, for a homonuclear diatomic molecule whose potential has only $\mu = 0$ and $\mu = 2$ terms when expanded as in G34.

Thus the double summation in G7 consists, in general, of nine terms.

CHAPTER H

Validity of the distorted wave approximation

The validity of the distorted wave approximation depends on the smallness of the off-diagonal matrix elements of the interaction energy. This will be investigated using an example given by Mott and Massey (1949).

It was shown in chapter G that the distorted wave approximation could be regarded as a first order approximation in an iteration procedure to solve the strongly coupled differential equations G7. The equations are here considered to be

$$\left[\nabla^2 + k_0^2 - \frac{2\mu}{\hbar^2} V_{00} \right] u_0 = \frac{2\mu}{\hbar^2} V_{0n} u_n, \quad \text{H1}$$

$$\left[\nabla^2 + k_n^2 - \frac{2\mu}{\hbar^2} V_{nn} \right] u_n = \frac{2\mu}{\hbar^2} V_{n0} u_0, \quad \text{H2}$$

with the assumption that $V_{on} = V_{no}$.

These equations represent the interaction between two waves, the incident and elastically scattered, and that scattered after excitation of the n^{th} stationary state.

In the case where the state given by 0 and n are nearly in resonance, the matrix element V_{on} will not be small and the distorted wave approximation would not be expected to yield good re-

sults. Both the distorted wave and close coupling approximations will be applied to this example and the respective expressions for the inelastic cross sections compared.

Writing $k_o^2 = k^2 = k_n^2$ and assuming that the field V_{oo} is the same as V_{nn} , equations H1, H2 become

$$\left[\nabla^2 + k^2 - \frac{2\mu}{\hbar^2} V_{oo} \right] u_o = \frac{2\mu}{\hbar^2} V_{on} u_n, \quad \text{H3}$$

$$\left[\nabla^2 + k^2 - \frac{2\mu}{\hbar^2} V_{oo} \right] u_n = \frac{2\mu}{\hbar^2} V_{on} u_o, \quad \text{H4}$$

The required solutions satisfy

$$u_o \sim e^{ikr} + \frac{1}{r} e^{ikr} f_o(\theta, \phi), \quad \text{H5}$$

$$u_n \sim \frac{1}{r} e^{ikr} f_n(\theta, \phi). \quad \text{H6}$$

Adding and subtracting H3 and H4 gives the equations

$$\left[\nabla^2 + k^2 - \frac{2\mu}{\hbar^2} (V_{oo} + V_{on}) \right] (u_o + u_n) = 0, \quad \text{H7}$$

$$\left[\nabla^2 + k^2 - \frac{2\mu}{\hbar^2} (V_{oo} - V_{on}) \right] (u_o - u_n) = 0. \quad \text{H8}$$

If the functions V_{oo} and V_{on} are spherically symmetric these equations may be solved to give

$$\mu_0 + \mu_m \sim \frac{1}{2} \left[e^{i k r} + e^{i k r} \sum_l \frac{(2l+1)}{2 i k r} \left(e^{2 i \eta_l} - 1 \right) P_l(\cos \theta) \right], \quad \text{H9}$$

$$\mu_0 - \mu_m \sim \frac{1}{2} \left[e^{i k r} + e^{i k r} \sum_s \frac{2s+1}{2 i k r} \left(e^{2 i \delta_s} - 1 \right) P_s(\cos \theta) \right], \quad \text{H10}$$

where the phase shifts η_l, δ_s are given by the equations

$$\left[\frac{d^2}{dr^2} + k^2 - \frac{l(l+1)}{r^2} - \frac{2\mu}{\hbar^2} (V_{00} + V_{0m}) \right] u = 0, \quad \text{H11}$$

$$\left[\frac{d^2}{dr^2} + k^2 - \frac{s(s+1)}{r^2} - \frac{2\mu}{\hbar^2} (V_{00} - V_{0m}) \right] u = 0, \quad \text{H12}$$

respectively.

Hence

$$\mu_m \sim \frac{1}{r} e^{i k r} \cdot \frac{1}{4 i k} \sum_l (2l+1) \left\{ e^{2 i \eta_l} - e^{2 i \delta_l} \right\} P_l(\cos \theta) \quad \text{H13}$$

and the differential scattering cross section corresponding to transfer of excitation will be

$$I_m(\theta) = \frac{1}{16 k^2} \left| \sum_l (2l+1) \left\{ e^{2 i \eta_l} - e^{2 i \delta_l} \right\} P_l(\cos \theta) \right|^2, \quad \text{H14}$$

so total cross section is given by

$$Q_m = \frac{\pi}{k^2} \sum_l (2l+1) \sin^2(\eta_l - \delta_l). \quad \text{H15}$$

Applying the distorted wave approximation to this problem gives the equations

$$\left[\nabla^2 + k^2 - \frac{2\mu}{\hbar^2} V_{00} \right] u_0 = 0, \quad \text{H16}$$

$$\left[\nabla^2 + k^2 - \frac{2\mu}{\hbar^2} V_{00} \right] u_m = \frac{2\mu}{\hbar^2} V_{0m} U_0(r, \theta), \quad \text{H17}$$

where $U_0(r, \theta)$ is that solution of H16 such that

$$U_0(r, \theta) \sim e^{iky} + \frac{1}{r} e^{ikr} f(\theta).$$

Then

$$u_m \sim -\frac{1}{4\pi} \frac{1}{r} e^{ikr} \int W_0(r', \pi - \Theta) \frac{2\mu}{\hbar^2} V_{0m} U_0(r', \theta') d\tau', \quad \text{H18}$$

where $\cos \Theta = \cos \theta \cos \theta' + \sin \theta \sin \theta' \cos(\phi - \phi')$,

and $W_0(r, \theta)$ is a solution of H17 with the right hand side set equal to zero. In this case

$$W_0(r, \theta) = U_0(r, \theta).$$

Using the expansions

$$U_0(r, \theta) = \frac{1}{k} \sum_l (2l+1) i^l \frac{1}{r} U^l(r) P_l(\cos \theta), \quad \text{H19}$$

$$U_0(r, \pi - \Theta) = \frac{1}{k} \sum_l (2l+1) i^{-l} \frac{1}{r} U^l(r) P_l(\cos \Theta), \quad \text{H20}$$

where $U^l(r)$ is that solution of

$$\left[\frac{d^2}{dr^2} + k^2 - \frac{l(l+1)}{r^2} - \frac{2\mu}{\hbar^2} V_{00} \right] U = 0, \quad \text{H21}$$

which is regular at the origin, and by expanding $P_l(\cos \Theta)$ and integrating over ϕ' , θ' and Θ , it follows that

$$Q_m = \frac{\pi}{k^2} \sum_l (2l+1) \left| \frac{4\mu}{k\hbar^2} \int V_{0m} \{U^l(r)\}^2 dr \right|^2. \quad \text{H22}$$

Now if η_l and δ_l are small they obey the relations

$$\eta_l = \frac{2\mu}{\hbar^2} \int (V_{0m} + V_{00}) \left\{ \sqrt{\frac{\pi r}{2}} J_{l+\frac{1}{2}}(kr) \right\}^2 dr, \quad \text{H23}$$

$$\delta_l = \frac{2\mu}{\hbar^2} \int (V_{00} - V_{0m}) \left\{ \sqrt{\frac{\pi r}{2}} J_{l+\frac{1}{2}}(kr) \right\}^2 dr. \quad \text{H24}$$

Hence

$$\eta_l - \delta_l = \frac{4\mu}{\hbar^2} \int V_{0m} \left\{ \sqrt{\frac{\pi r}{2}} J_{l+\frac{1}{2}}(kr) \right\}^2 dr. \quad \text{H25}$$

Thus the total cross section as given by H25 agrees with equation H15 if $\eta_l - \delta_l$ is small.

Thus the condition of validity of the method of distorted waves is that the integral, given in H25, should be small.

Effect of an increase in coupling

We now investigate the effect of replacing V_{on} by λV_{on} in the previous analysis. λ is a parameter which is taken to indicate the effective magnitude of V_{on} . As λ is increased the distorted wave approximation will become less and less valid and we may examine the manner in which it breaks down.

For the distorted wave approximation the effect on the total cross section is given by

$$Q_m = \frac{\pi}{k^2} \sum_l (2l+1) \lambda^2 \left\{ \frac{4\mu}{k\hbar^2} \int V_{on} \{U^l(r)\}^2 \right\}^2. \quad H26$$

Thus as λ increases, the cross section will increase as λ^2 .

In the close coupling approximation the effect of increased coupling can be seen from equations H11 and H12 with V_{on} replaced by λV_{on} . As λ increases the phase shift η_l will increase while the phase shift δ_l will decrease. Hence the difference, $\eta_l - \delta_l$, will increase and equation H15 shows that the cross section will increase from zero to some maximum value and then it will oscillate.

The distorted wave approximation is only valid in the region of initial increase in the cross section. It predicts a monotonic increase of cross section and will usually indicate too great a probability of the transfer process.

We might expect a similar situation to occur if resonance is not exact. To test if this is so we try some numerical calculations

on a particular collision.

The example considered is the $j = 0 \rightarrow j' = 2$ rotational excitation of a hydrogen molecule by an incident hydrogen atom. For this case we solve equations G7 with boundary conditions G10 using the formula defined in chapter I for the interaction potential between these two bodies. Three different cases were taken :

- (a) Energy 0.05 e.V. , $J = 0$;
- (b) Energy 0.25 e.V. , $J = 0$;
- (c) Energy 0.25 e.V. , $J = 25$.

(a) With total angular momentum $J = 0$ the only possible inelastically scattered wave corresponding to $j' = 2$ is given by $\ell' = 2$. Thus there are only two coupled equations corresponding to $\ell' = 0$ and $\ell' = 2$. The value of λ was varied and the graph of cross section, calculated by the distorted wave approximation (G27) and by the close coupling approximation (G19), plotted against λ . The results are shown in Fig 3. This shows that for low energies the distorted wave is a valid approximation, a result which was expected as the off-diagonal matrix elements, as given by the phase shifts, are small. This graph also shows very clearly the oscillatory nature of the cross section as given by the solution of the fully coupled equations.

(b) Again, with $J = 0$, there are only two equations corresponding to $\ell' = 0$ and $\ell' = 2$. In this case, using a much higher energy, the values of the cross section as calculated

from the two approximations differ considerably before $\lambda = 1$. In fact at $\lambda = 1$ the value given by the distorted wave approximation is 36% greater than that given by the close coupling approximation (see Fig 4).

- (c) Using an energy of 0.25 e.V. and $J = 25$ will give three inelastically scattered waves corresponding to $\mathcal{L}' = 23, 25, 27$.

Thus we have four coupled equations to solve and, in this case, the distorted wave approximation is again valid, the agreement being good out to large values of λ (in the range 0 - 9). Again this is because the phase shifts are small for these values of \mathcal{L}' . These results are shown in Fig 5.

Thus the distorted wave is a good approximation for low energies; it breaks down at high energies, for low values of J ; at these higher energy values it becomes more and more valid as J increases.

Another interesting way of demonstrating this last statement is to plot a graph of the contributions to the cross section from individual values of J against the J values. This was done for a set of energies 0.05, 0.10, 0.15, 0.25 e.V. All the curves had the same basic shape except that, as the energy increased, the difference between the maxima of the two approximations increased. Only the graph for $E = 0.25$ e.V. is reproduced here (Fig 6).

It can be seen just how the distorted wave approximation approaches the close coupling approximation as values of J increase. This graph will also show if enough J values have been taken so that contributions from higher values of J can be neglected.

FIGURE 3

Calculated values of the partial inelastic cross section $\sigma_0(0-2)$ versus coupling coefficient λ , for $E = 0.05$ e.V., using both the distorted wave (DW) and close coupling (CC) approximations.

FIG. 3.

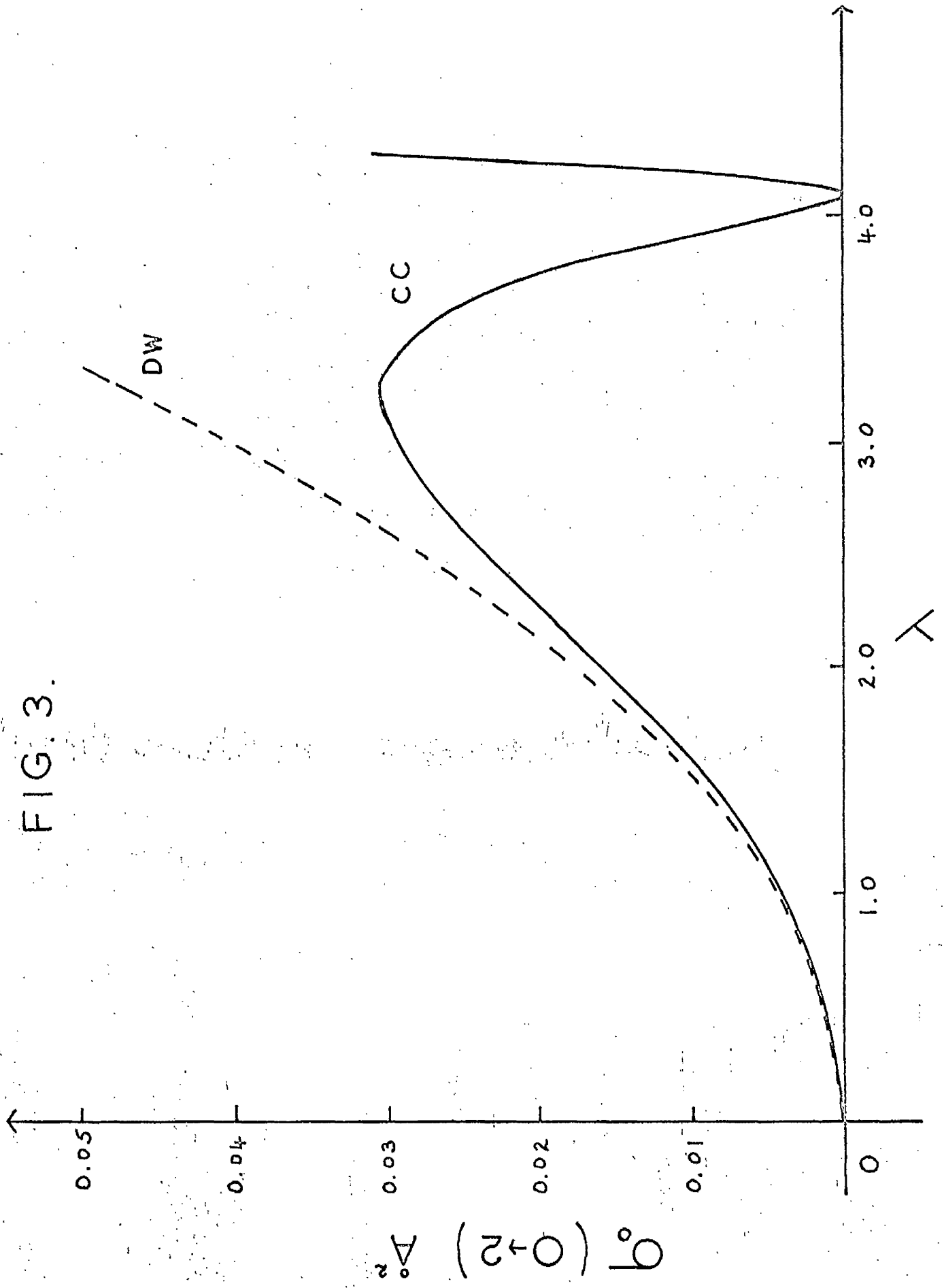


FIGURE 4

Calculated values of the partial cross section $\sigma_0^- (0 - 2)$ versus coupling coefficient λ for $E = 0.25$ e.V., using both the distorted wave (DW) and close coupling (CC) approximations.

FIG. 4.

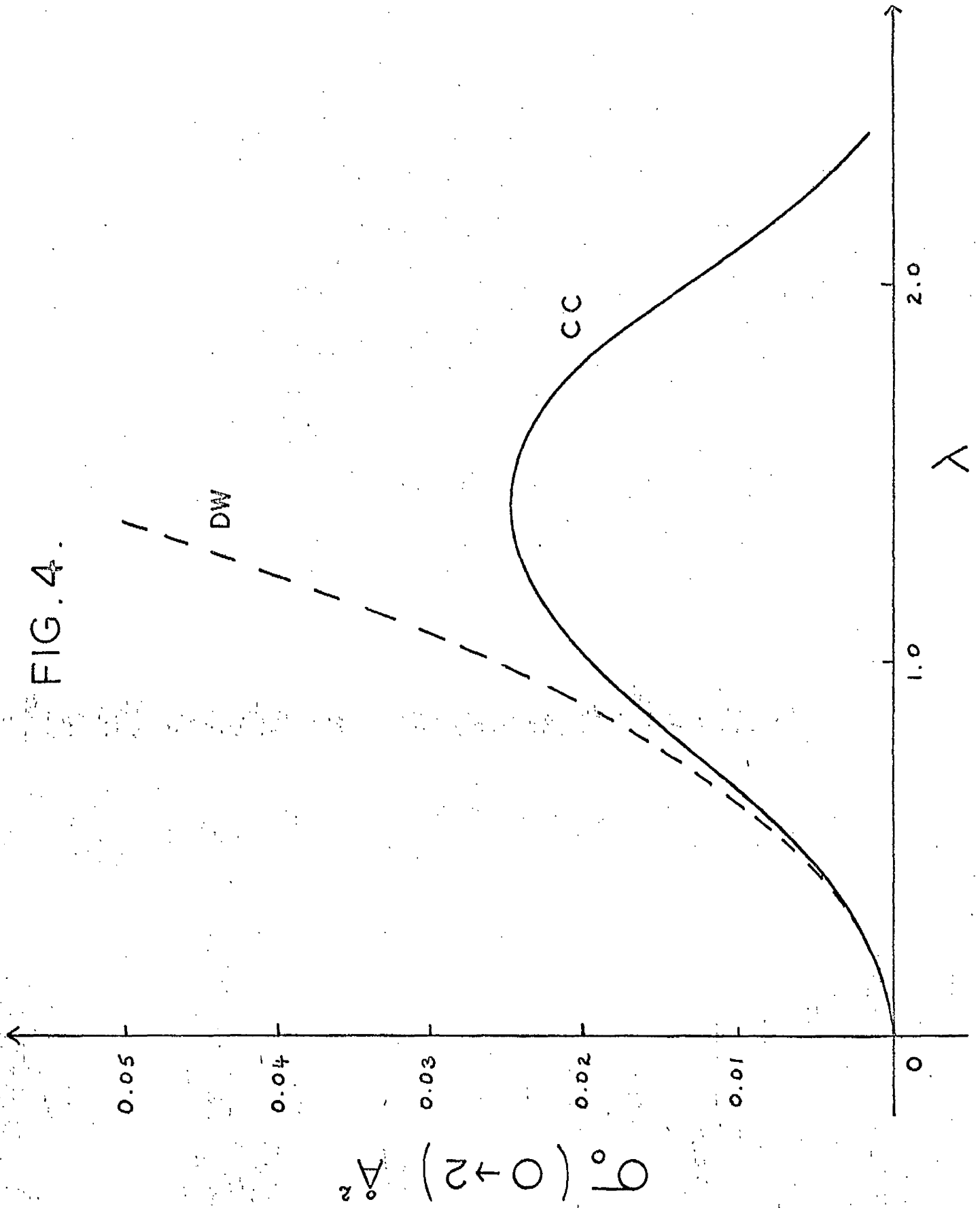


FIGURE 5

Calculated values of the partial cross section $\sigma_{25}(0-2)$ versus coupling coefficient λ for $E = 0.25$ e.V., using both the distorted wave (DW) and close coupling (CC) approximations.

FIG. 5.

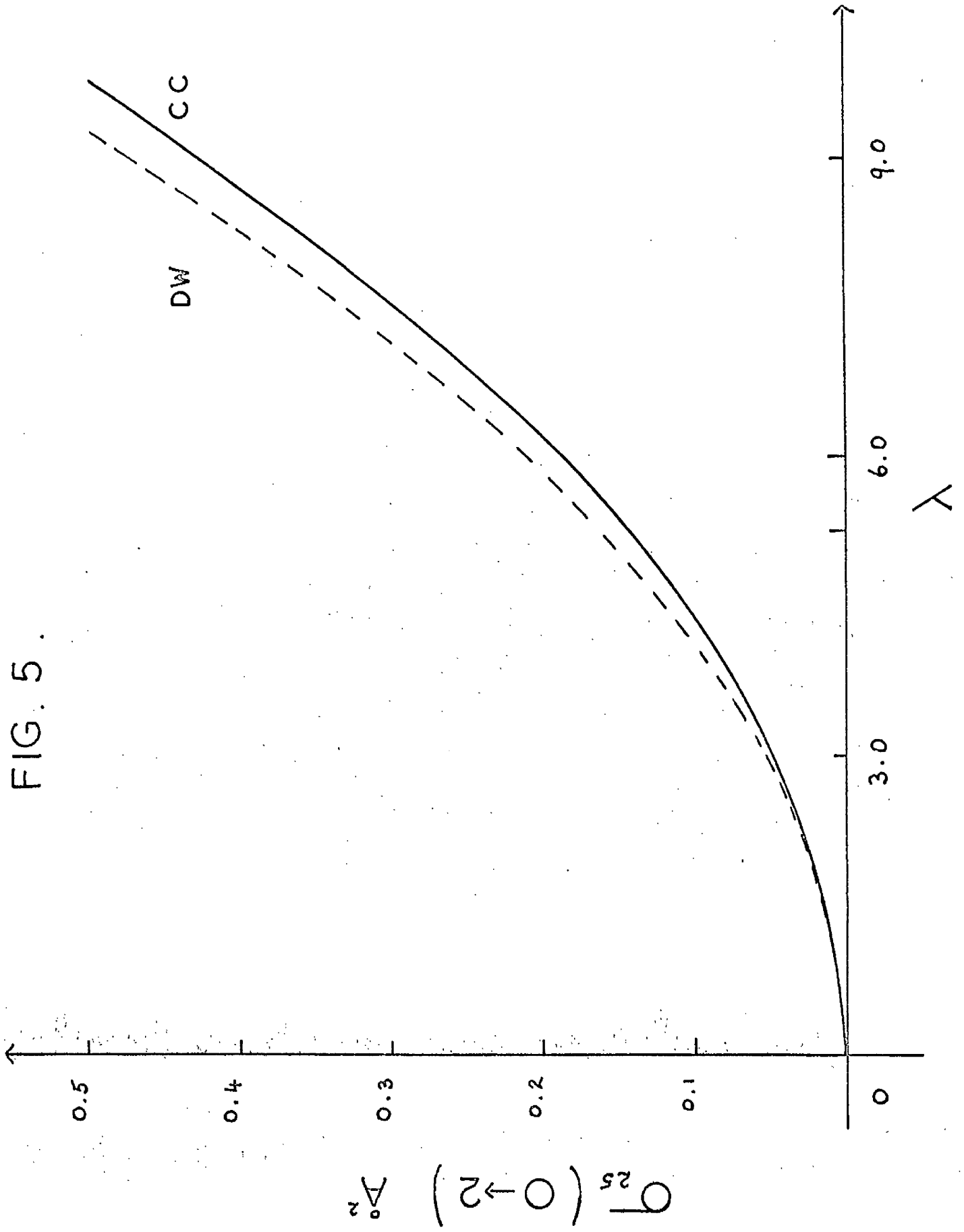
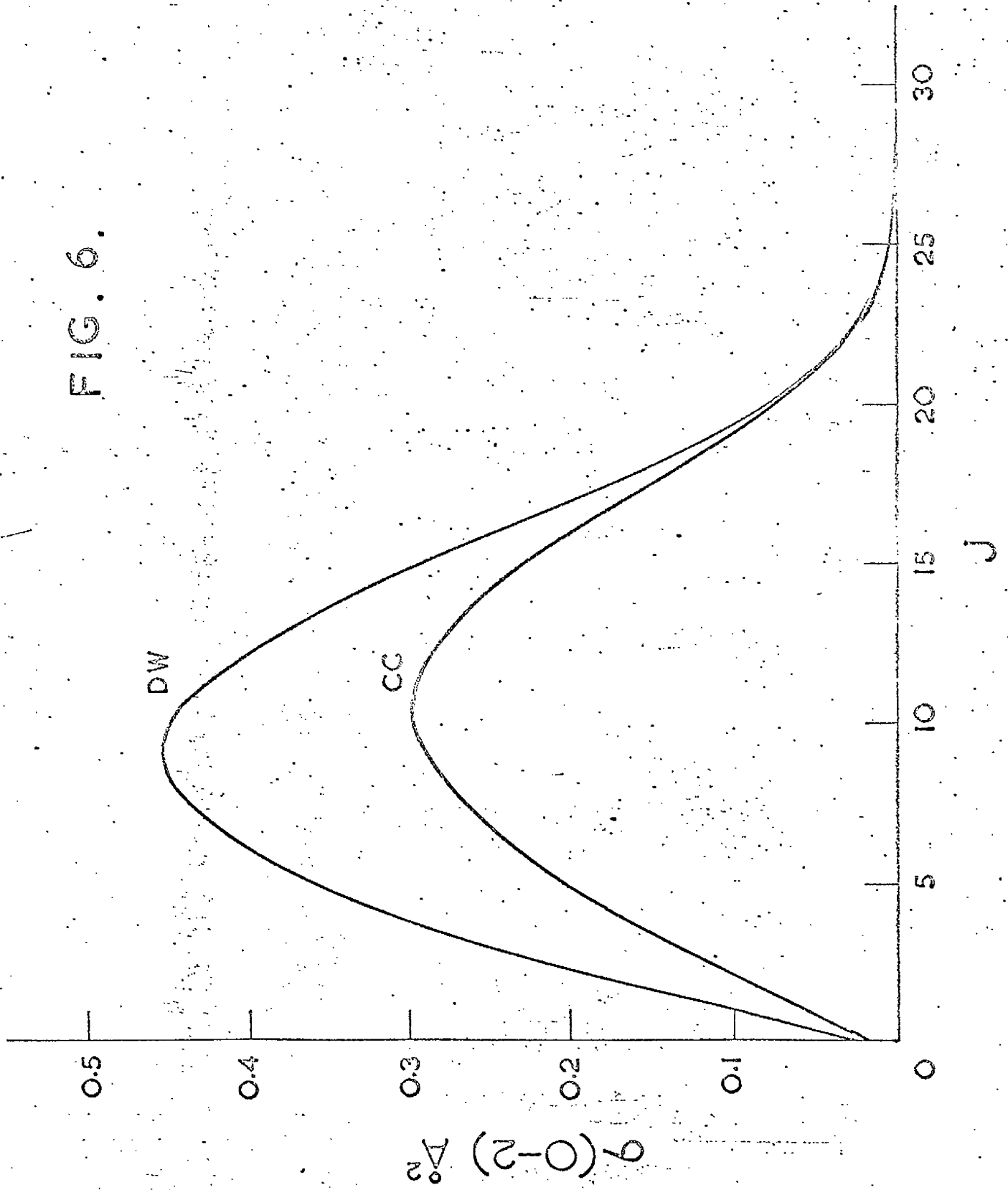


FIGURE 6

Comparison of the distorted wave (DW) and close coupling (CC) approximations as shown by the contribution to the inelastic cross section $\sigma(0-2)$ from various values of J , for $E = 0.25$ e.V.

FIG. 6.



CHAPTER I

Introduction

The theory and numerical methods of the previous chapters are now applied to some practical cases. We consider the rotational excitation of a hydrogen molecule by a hydrogen atom, a helium atom and another hydrogen molecule. With little extra effort we also include the rotational excitation of a deuterium molecule by a hydrogen atom. These collisions have already been studied using the distorted wave approximation (Takayanagi 1963, Roberts 1963, Davison 1963, 1964, Dalgarno and Henry 1964, Dalgarno, Henry and Roberts 1966). We have applied the close coupling approximation to these cases and have demonstrated the failure of the distorted wave approximation at high energy.

Calculations

The matrix element ,

$$\langle j' l'; J | V | j'' l''; J \rangle ,$$

given by equation G9 , connecting the different scattering channels is evaluated by expanding the interaction potential as in A17 ,

$$V(r) = \sum_{\mu} v_{\mu}(r) P_{\mu}(\cos \theta)$$

This equation has been truncated after $\mu = 2$ because Dalgarno and Henry (1965) have shown that higher order harmonics are unlikely to be important.

Hence

$$\langle j'l'; J | V | j''l''; J \rangle = \delta_{jj'} \delta_{ll'} V_0(r) + f_2(j'l', j''l''; J) V_2(r) \quad \text{I2}$$

and, as shown at the end of chapter G, the double summation in G7 consists, in general, of nine terms. The functions,

$$f_2(j'l', j''l''; J),$$

may be conveniently calculated from formulae given by Bernstein et al (1963).

Only collision processes in which the rotational quantum number j changed from zero to two were taken. In the case of scattering of a hydrogen molecule by another hydrogen molecule the incident molecule was not allowed to change its rotational level and was assumed to be in the state defined by $j = 0$ throughout the collision.

All coupling terms involving $j = 0$ were retained but the terms coupling $j = 2$ to higher rotational levels were neglected thereby reducing G7 to a set of four coupled differential equations.

Thus the scattering matrix $S^J(jl; j'l')$ is, in general, a four by four matrix defined by the transition $(jl; j'l')$

0J ; 0J	0J ; 2J-2	0J ; 2J	0J ; 2J+2
2J-2 ; 0J	2J-2 ; 2J-2	2J-2 ; 2J	2J-2 ; 2J+2
2J ; 0J	2J ; 2J-2	2J ; 2J	2J ; 2J+2
2J+2 ; 0J	2J+2 ; 2J-2	2J+2 ; 2J	2J+2 ; 2J+2

In the case of $J = 0$ this reduces to a two by two matrix obtained by deleting the second and third columns and rows while for $J = 1$ it gives a three by three matrix obtained by deleting the second row and column.

The elastic cross section $\sigma(0;0)$ and the inelastic cross section $\sigma(2;0)$ are calculated from equation G19. We also calculate the angular distribution defined by the relation

$$\mathcal{N}(\theta) = 2\pi \frac{d\sigma(\gamma'; \gamma | \hat{x})}{d\hat{x}} \sin \theta, \quad \text{I3}$$

where the differential scattering cross section $\frac{d\sigma(\gamma'; \gamma | \hat{x})}{d\hat{x}}$ is given by G16.

Equation G17 is not in a suitable form for computation and so, following Blatt and Biedenharn (1952), we write G17 in a form such that each term appears once only in the summation.

$$A_\lambda = \sum_{\mathcal{J}=0}^{\infty} \sum_{l=|\mathcal{J}-\gamma|}^{\mathcal{J}+\gamma} \sum_{l'=|\mathcal{J}-\gamma'|}^{\mathcal{J}+\gamma'} Z(l\mathcal{J}l\mathcal{J}; \gamma\lambda) Z(l'\mathcal{J}l'\mathcal{J}; \gamma'\lambda) \left| T^{\mathcal{J}}(\gamma l; \gamma' l') \right|^2$$

$$+ 2 \sum_{\mathcal{J}_1} \sum_{l_1} \sum_{l'_1} \left[\sum_{\mathcal{J}_2} \sum_{l_2} \sum_{l'_2} Z(l_1 \mathcal{J}_1 l_2 \mathcal{J}_2; \gamma \lambda) \right]$$

$$\begin{aligned}
& \times Z(l_1', J_1, l_2', J_2; \gamma' \lambda) \times \text{RP} [] \\
& + \sum_{l_2} \sum_{l_2'} Z(l_1, J_1, l_2, J_2; \gamma \lambda) \times Z(l_1', J_1, l_2', J_2; \gamma' \lambda) \\
& \quad \times \text{RP} [J_1 = J_2] + \sum_{l_2'} Z(l_1, J_1, l_1, J_1; \gamma \lambda) \\
& \quad \times Z(l_1', J_1, l_2', J_1; \gamma' \lambda) \times \text{RP} [J_1 = J_2, l_1 = l_2']
\end{aligned}$$

where $\text{RP} [.]$ denotes the real part of

$$T^{J_1}(\gamma l_1; \gamma' l_1')^* \cdot T^{J_2}(\gamma l_2; \gamma' l_2')$$

The actual number of terms in this expansion is reduced because of the restrictions that

$$l_1 + l_2 - \lambda, \quad l_1' + l_2' - \lambda, \quad l_1 + l_1', \quad l_2 + l_2'$$

must be even.

Rate coefficients (R) for a collision at temperature T° Kelvin in which the rotational quantum number changes from j to j' are defined by the equation

$$R = \left(\frac{16 k T}{2 \mu \hbar^2 \pi} \right)^{\frac{1}{2}} \langle Q_{j'j} \rangle,$$

15

where k is the Boltzmann constant and $\langle Q_{j'j} \rangle$ is the cross section for the $j \rightarrow j'$ transition averaged over the Maxwellian

distribution of incident energies,

i.e.

$$\langle Q_{j'j} \rangle = \int M(E) \sigma_E(j';j) dE, \quad I6$$

where

$$M(E) = \frac{E}{(kT)^2} \exp\left(-\frac{E}{kT}\right)$$

and $\sigma_E(j';j)$ is the inelastic cross section corresponding to impact energy E .

All calculations in this chapter are performed using values of energy in electron volts and measuring distance in angstroms with the exception of the rate coefficients which are in units of cm^3 / sec .

H - H₂

We have adopted the Buckingham (exp - 6) type of potential used by Dalgarno, Henry and Roberts (1966) for the interaction potential between a hydrogen atom and a hydrogen molecule,

$$V_0(r) = 511.09 \exp(-3.59r) - 5.523/r^6,$$

$$V_2(r) = 346.66 \exp(-3.779r) - 0.612/r^6.$$

For these particles

$$\frac{2\mu}{\hbar^2} = 321.82 \text{ (e.V. } \text{\AA}^2)^{-1}$$

and for the hydrogen molecule

$$\frac{\hbar^2}{2I} = 0.007564 \text{ e.V.}$$

Thus there is an energy difference of 0.0454 e.V. between the $j = 0$ and $j = 2$ rotational states of the hydrogen molecule.

Hence

$$\hbar^2_{j,j} = \frac{2\mu}{\hbar^2} E,$$

$$\hbar^2_{j',j} = \frac{2\mu}{\hbar^2} \left\{ E - 0.0454 \right\}.$$

The energy range taken was from 0.05 e.V., which lies just above the threshold of the $j = 2$ rotational level, up to 0.25 e.V. which lies below the first excited vibrational state at 0.353 e.V (Roberts 1963).

The criteria described in chapter E were applied to give an estimate of the initial and final intervals and these parameters were fed into the distorted wave program described in chapter D. The results of Dalgarno, Henry and Roberts (1966) were verified and the largest value of r required to give convergence of the phase shifts were printed out. This value was used to give an estimate of the position of the matching points in the close coupling program. We also noted the number of J values required so that the contribution to the inelastic cross section from higher values was

negligible. This value too was required by the close coupling program which was now used to repeat the previous calculations. A full list of the numerical parameters for the close coupling program is given in Table 6. The results are shown in Fig 7. Angular distributions, defined by I3, were calculated for a few values of energy and we also computed the rate coefficients from equations I5 and I6 for several values of temperature.

H - D₂

For this collision we used the same interaction potential as in the previous section.

In this case

$$\frac{2\mu}{\hbar^2} = 386.10 (\text{e.V. } \text{\AA}^2)^{-1}$$

and since the moment of inertia of the deuterium molecule is twice that of the hydrogen molecule, both being considered as rigid rotators,

$$\frac{\hbar^2}{2I} = 0.003782 \text{ e.V.}$$

Hence

$$k_{\gamma\gamma}^2 = \frac{2\mu}{\hbar^2} E,$$

$$k_{\gamma'\gamma}^2 = \frac{2\mu}{\hbar^2} \left\{ E - 0.0227 \right\},$$

where E is the kinetic energy of the incident hydrogen atom. Again the results of the distorted wave approximation were in complete agreement with Dalgarno, Henry and Roberts (1966). The numerical parameters used for the close coupling program are listed in Table 7. In this case the energies considered were restricted to the range 0.025 e.V. to 0.15 e.V. and our results are shown in Fig 8.

He - H₂

Roberts (1963) has used a purely repulsive potential in his distorted wave calculations of the scattering of a helium atom by a hydrogen molecule. We adopt the same potential which is defined by

$$V_0(r) = 470.10 \exp(-3.830r),$$

$$V_2(r) = 0.375 V_0(r).$$

For this collision

$$\frac{2\mu}{\hbar^2} = 643.47 (\text{e.V. } \text{\AA}^2)^{-1},$$

while again

$$\frac{\hbar^2}{2I} = 0.007564 \text{ e.V.}$$

The distorted wave program was used to verify the results of Roberts (1963) and to set up the parameters for the close coupling program (Table 8). Both sets of results are compared in Fig 9 for the energy range 0.05 e.V. to 0.20 e.V.

H₂ - H₂

The scattering of a hydrogen molecule by another hydrogen molecule has been studied by Davison (1963) and Roberts (1963) using the Morse potential derived by Takayanagi (1957),

$$V_0(r) = A \left(\exp[-2\alpha(r-r_0)] - 2 \exp[-\alpha(r-r_0)] \right),$$

$$V_2(r) = \beta A \exp[-2\alpha(r-r_0)],$$

where $A = 2.991_{10}^{-3}$,

$$\alpha = 1.767,$$

$$r_0 = 3.387,$$

$$\beta = 0.075.$$

From their independent calculations both Davison (1963) and Roberts (1963) conclude that the value of β is too small and a value of $\beta = 0.14$ is more realistic. Davison (1963) also considered the Buckingham (exp - 6) potential defined by

$$V_0(r) = A \exp[-2\alpha(r-r_0)] - B/r^6,$$

$$V_2(r) = \beta A \exp[-2\alpha(r-r_0)] - D/r^6,$$

where $B = 11.0$, $D = 0.8$ and $\beta = 0.14$. This was the potential used in our calculations. For these molecules,

$$\frac{2\mu}{\hbar^2} = 482.62 (\text{e.V. } \text{\AA}^2)^{-1},$$

while again

$$\frac{\hbar^2}{2I} = 0.007654 \text{ e.V.}$$

Elastic and inelastic cross sections are calculated over the energy range 0.05 e.V. to 0.3 e.V. using both the distorted wave and close coupling approximations. The numerical parameters are given in Table 9 and the results are illustrated in Fig 10.

Angular distributions over the same energy range are calculated together with the rate coefficients for several values of temperature.

Discussion

For the $j = 0$ to $j' = 2$ rotational transition of a hydrogen molecule by hydrogen impact, Dalgarno, Henry and Roberts (1966) noted

that departures of the distorted wave S matrix from unitarity became serious above energies of 0.15 e.V. and Fig 7 confirms their conclusion. At the highest energy investigated, 0.25 e.V., the distorted wave approximation overestimates the inelastic cross section by 50% and the error is increasing with increasing energy.

A similar comparison for the $0 \rightarrow 2$ excitation of deuterium by hydrogen impact is presented in Fig 8. Because of the closer rotational spacing in the deuterium molecule the distorted wave approximation becomes invalid at lower impact energies. At an energy of 0.15 e.V. it overestimates by 33%.

Fig 9 shows the cross sections for the $0 \rightarrow 2$ excitation of a hydrogen molecule by helium impact. The results show that the off-diagonal S matrix elements are becoming large at impact energy 0.10 e.V. and this is again demonstrated by a comparison with the close coupling results. Indeed at an energy of 0.15 e.V. the result of a semi-classical calculation by Lawley and Ross (1965), giving a value of 1.51 \AA^2 for the inelastic cross section, differs by less than 10% from the close coupling result, 1.38 \AA^2 , and is superior to the distorted wave values of 1.89 \AA^2 .

Fig 10 compares the cross sections for the $0 \rightarrow 2$ excitation of hydrogen by molecular hydrogen impact. The rotational cross sections are small and little error results from the use of the distorted wave approximation for energies up to 0.3 e.V.

The angular distributions and the elastic cross sections may be valuable in analyses of experimental data. The angular distributions

defined by equation 13 are shown in Figs 11, 12, 13, 14. They are all very similar; as the energy increased σ becomes more sharply peaked and the location of its maximum shifts slowly to lower angles.

The elastic cross sections are slowly varying functions of the impact energy, determined almost entirely by the spherical symmetric parts of the interaction potential. For $H - H_2$, $\sigma(0;0)$ varies from 46.7 \AA^2 at 0.05 e.V. to 39.7 \AA^2 at 0.25 e.V.; for $H - D_2$, $\sigma(0;0)$ varies from 48.5 \AA^2 at 0.025 e.V. to 41.0 \AA^2 at 0.17 e.V.; for $He - H_2$, $\sigma(0;0)$ varies from 53.9 \AA^2 at 0.05 e.V. to 47.4 \AA^2 at 0.20 e.V.; for $H_2 - H_2$, $\sigma(0;0)$ varies from 45.5 \AA^2 at 0.05 e.V. to 43.5 \AA^2 at 0.30 e.V.

The rotational excitation of hydrogen molecules by impact with slow hydrogen atoms and other hydrogen molecules may be an important cooling mechanism in interstellar space (Dalgarno, Henry and Roberts 1966). For this reason rate coefficients have been calculated in the two cases, $H - H_2$, $H_2 - H_2$, and these results are listed in Tables 10 and 11.

TABLE 6 Numerical Parameters for H - H₂

B₀ = 321.82 r₀ = 1.0 h = 0.006 I₁ = 100 I₂ = 50 I₃ = 250

E	p1	p2	k ₁ ²	k ₂ ²	ra	rb	h _f	J max
0.05	3	4	16.09	1.49	20.074	20.434	0.072	10
0.07	2	5	22.53	7.92	16.846	17.146	0.060	16
0.10	3	3	32.18	17.57	14.682	14.952	0.054	22
0.15	2	4	48.27	33.67	13.918	14.158	0.048	28
0.20	2	3	64.36	49.76	10.990	11.170	0.036	34
0.25	2	3	80.46	65.85	10.990	11.170	0.036	40

TABLE 7 Numerical Parameters for H - D₂

B₀ = 386.10 h = 0.01 I₁ = 100 I₂ = 150 I₃ = 400

E	p1	p2	k ₁ ²	k ₂ ²	r0	ra	rb	J max
0.025	2	5	9.653	0.891	1.5	44.91	45.41	10
0.035	2	4	13.514	4.752	1.3	36.83	37.23	15
0.050	2	4	19.305	10.544	1.0	36.53	36.93	20
0.070	2	3	27.027	18.266	1.0	28.65	28.95	25
0.100	2	3	38.610	29.849	1.0	28.65	28.95	27
0.120	2	3	46.332	37.571	1.0	28.65	28.95	30
0.150	2	2	57.915	49.154	1.0	19.77	19.77	35
0.170	2	2	65.637	56.876	1.0	19.77	19.77	35

TABLE 8 Numerical Parameters for He - H₂

B₀ = 643.47 h = 0.005 I₁ = 100 I₂ = 150 I₃ = 300

E	p1	p2	k ₁ ²	k ₂ ²	r0	ra	rb	J max
0.05	2	5	32.174	2.970	1.5	18.205	18.455	13
0.06	2	5	38.608	9.405	1.3	18.005	18.255	18
0.07	2	4	45.043	15.840	1.0	14.765	14.965	22
0.08	2	4	51.478	22.274	1.0	14.765	14.965	25
0.09	2	4	57.912	28.709	1.0	14.765	14.965	27
0.10	2	4	64.347	35.144	1.0	14.765	14.965	30
0.12	2	3	77.216	48.013	1.0	11.825	11.975	32
0.15	2	3	96.521	67.317	1.0	11.825	11.975	35
0.17	2	3	109.390	80.187	1.0	11.825	11.975	37
0.20	2	3	128.694	99.491	1.0	11.825	11.975	40

TABLE 9

Numerical Parameters for $H_2 - H_2$
 $B_0 = 482.62$ $h = 0.008$ $I_1 = 100$ $I_2 = 150$ $I_3 = 400$

E	p1	p2	k_1^2	k_2^2	r0	ra	rb	J max
0.05	2	4	24.131	2.228	1.4	29.824	30.144	12
0.06	2	4	28.957	7.054	1.2	29.624	29.944	15
0.07	2	4	33.783	11.880	1.0	29.424	29.744	17
0.08	2	3	38.610	16.706	1.0	23.120	23.360	20
0.09	2	3	43.436	21.533	1.0	23.120	23.360	22
0.10	2	3	48.262	26.359	1.0	23.120	23.360	25
0.12	2	3	57.914	36.011	1.0	23.120	23.360	27
0.15	2	3	72.393	50.490	1.0	23.120	23.360	30
0.17	2	2	82.045	60.142	1.0	16.016	16.176	32
0.20	2	2	96.524	74.621	1.0	15.216	15.376	35
0.25	2	2	120.660	98.757	1.0	15.216	15.373	37
0.30	2	2	144.790	122.880	1.0	15.216	15.376	40

TABLE 10

Rate Coefficients (R) for H - H₂ (cm³/sec.)

T(°K)	R
20	4.5 ₁₀ ⁻²³
30	4.0 ₁₀ ⁻¹⁹
40	3.5 ₁₀ ⁻¹⁷
50	5.1 ₁₀ ⁻¹⁶
60	3.1 ₁₀ ⁻¹⁵
70	1.1 ₁₀ ⁻¹⁴
80	3.1 ₁₀ ⁻¹⁴
90	6.8 ₁₀ ⁻¹⁴
100	1.3 ₁₀ ⁻¹³
200	3.1 ₁₀ ⁻¹²
300	1.1 ₁₀ ⁻¹¹
400	2.3 ₁₀ ⁻¹¹
500	3.7 ₁₀ ⁻¹¹

TABLE 11

Rate Coefficients (R) for $H_2 - H_2$ ($cm^3/sec.$)

T($^{\circ}$ K)	R
20	3.7_{10}^{-24}
30	3.3_{10}^{-20}
40	2.9_{10}^{-18}
50	4.3_{10}^{-17}
60	2.6_{10}^{-16}
70	9.7_{10}^{-16}
80	2.7_{10}^{-15}
90	6.0_{10}^{-15}
100	1.2_{10}^{-14}
200	3.2_{10}^{-13}
300	1.2_{10}^{-12}
400	2.7_{10}^{-12}
500	4.6_{10}^{-12}

FIGURE 7

Cross section for excitation of the 0 - 2 rotational transition in H_2 by H impact. DW, distorted wave results of Dalgarno, Henry and Roberts (1966); CC, close coupling results.

FIG. 7.

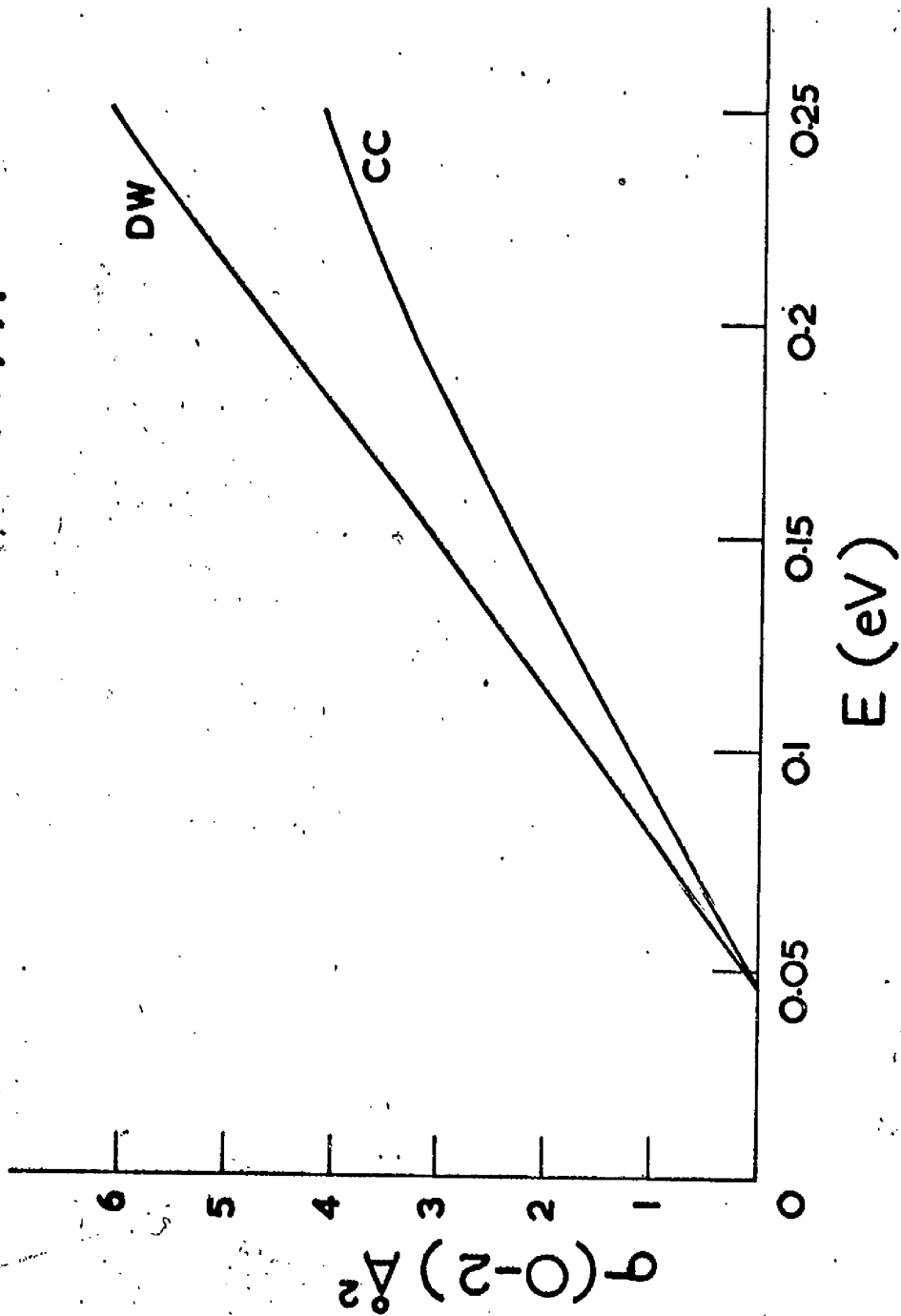


FIGURE 8

Cross section for excitation of the 0 - 2 rotational transition in D_2 by H impact. DW, distorted wave results of Dalgarno, Henry and Roberts (1966); CC, close coupling results.

FIG. 8.

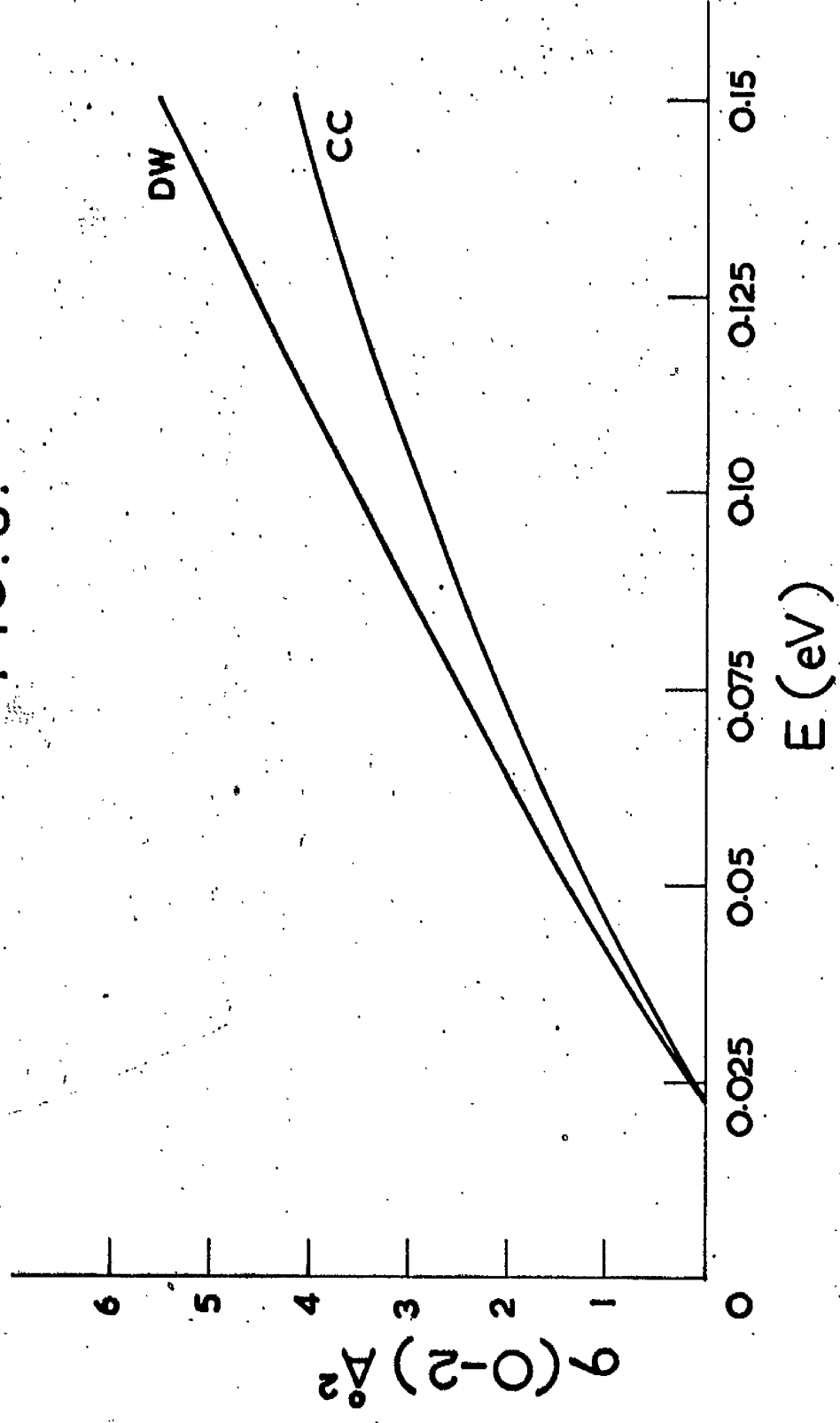


FIGURE 9

Cross section for excitation of the 0 - 2 rotational transition in H_2 by He impact. DW, distorted wave results of Roberts (1963); CC, close coupling results.

FIG. 9.

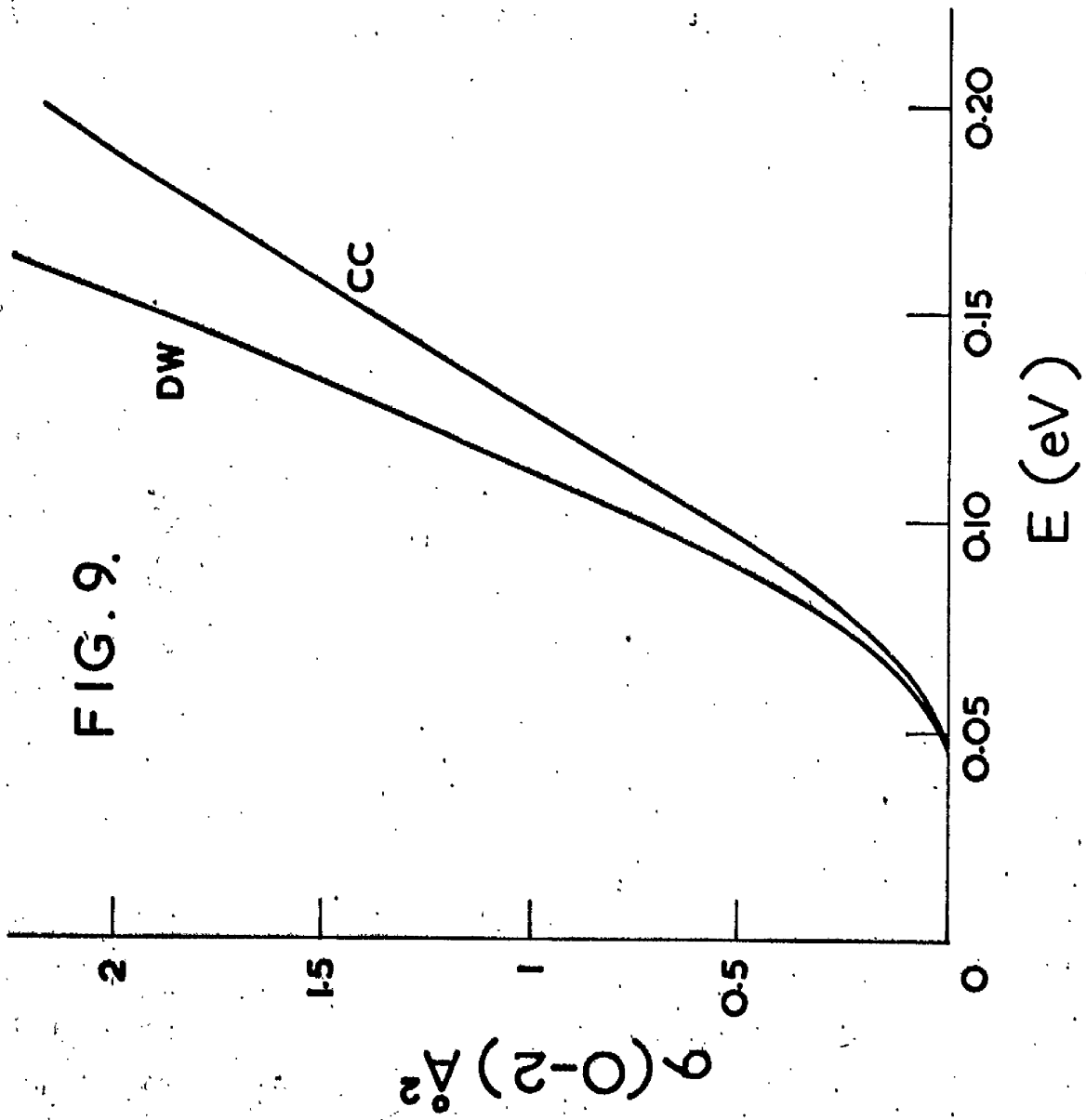


FIGURE 10

Cross section for excitation of the 0 - 2 rotational transition in H_2 by H_2 impact. DW, distorted wave results of Davison (1963); CC, close coupling results.

FIG. 10.

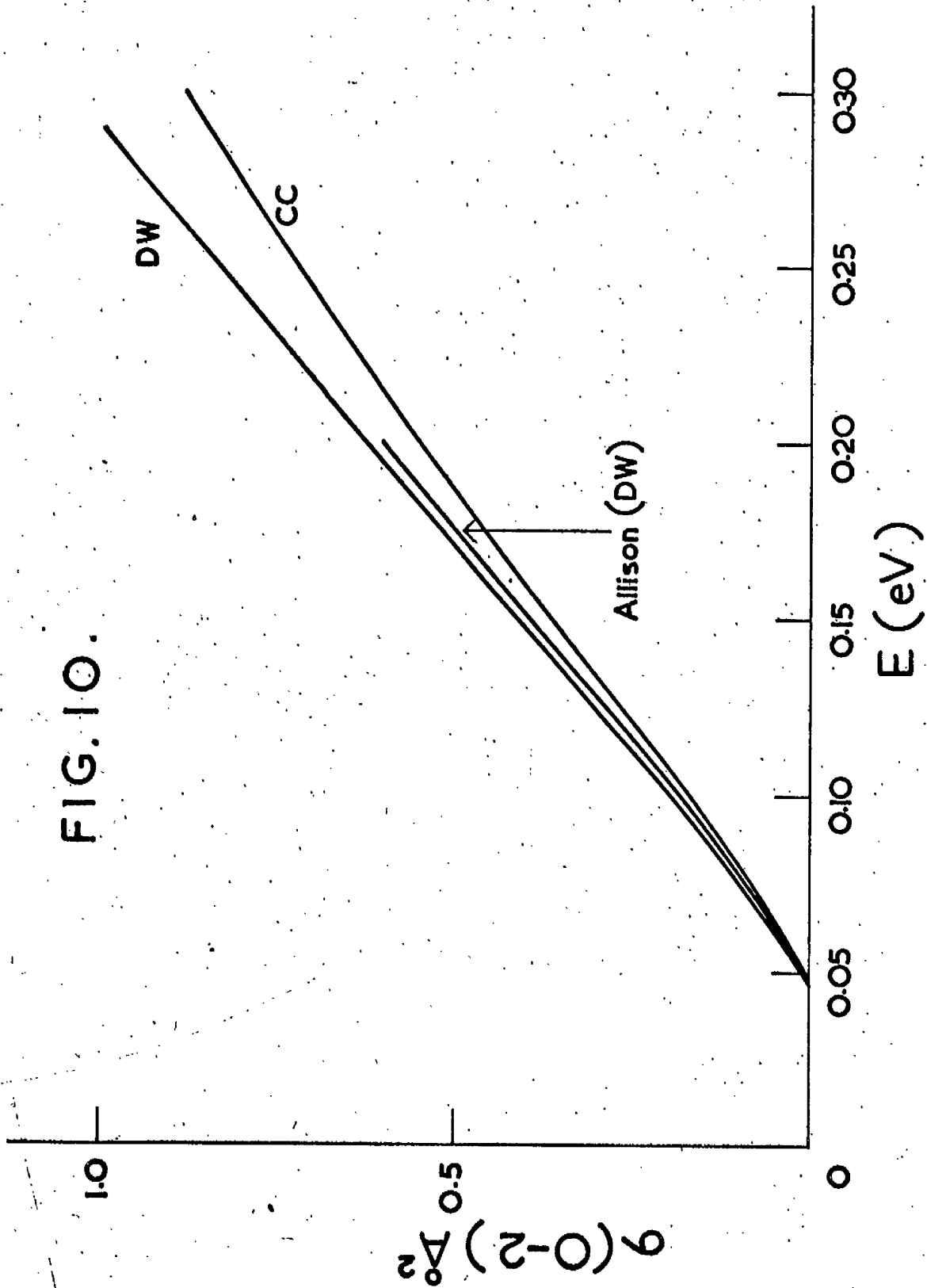


FIGURE 11

Angular distribution $\mathcal{N}(0-2)$ for H - H₂ .

FIG. 11.

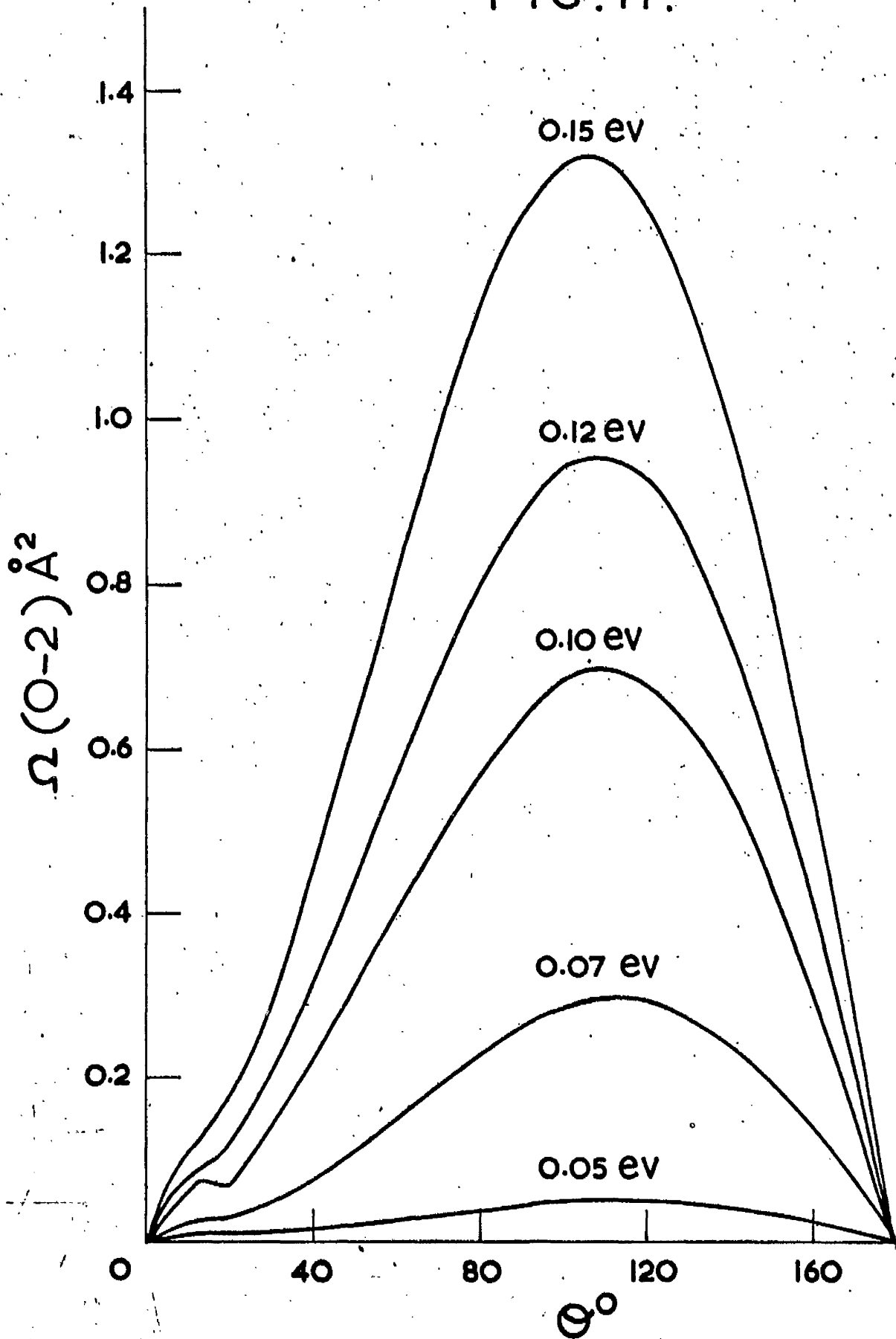


FIGURE 12

Angular distribution $\mathcal{N}(0 - 2)$ for H - D₂ .

FIG. 12.

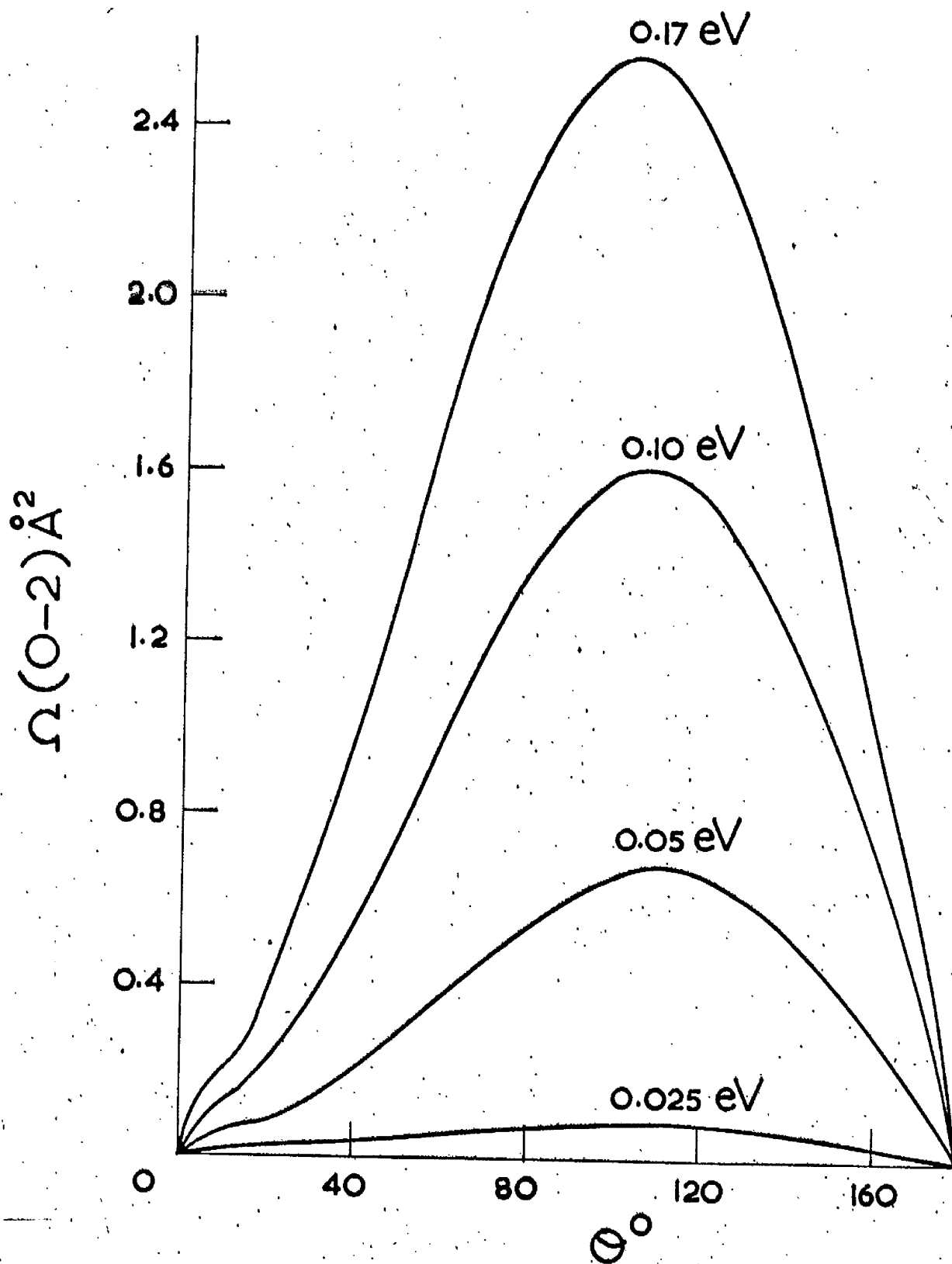


FIGURE 13

Angular distribution $\mathcal{N}(0-2)$ for He - H₂ .

FIG. 13.

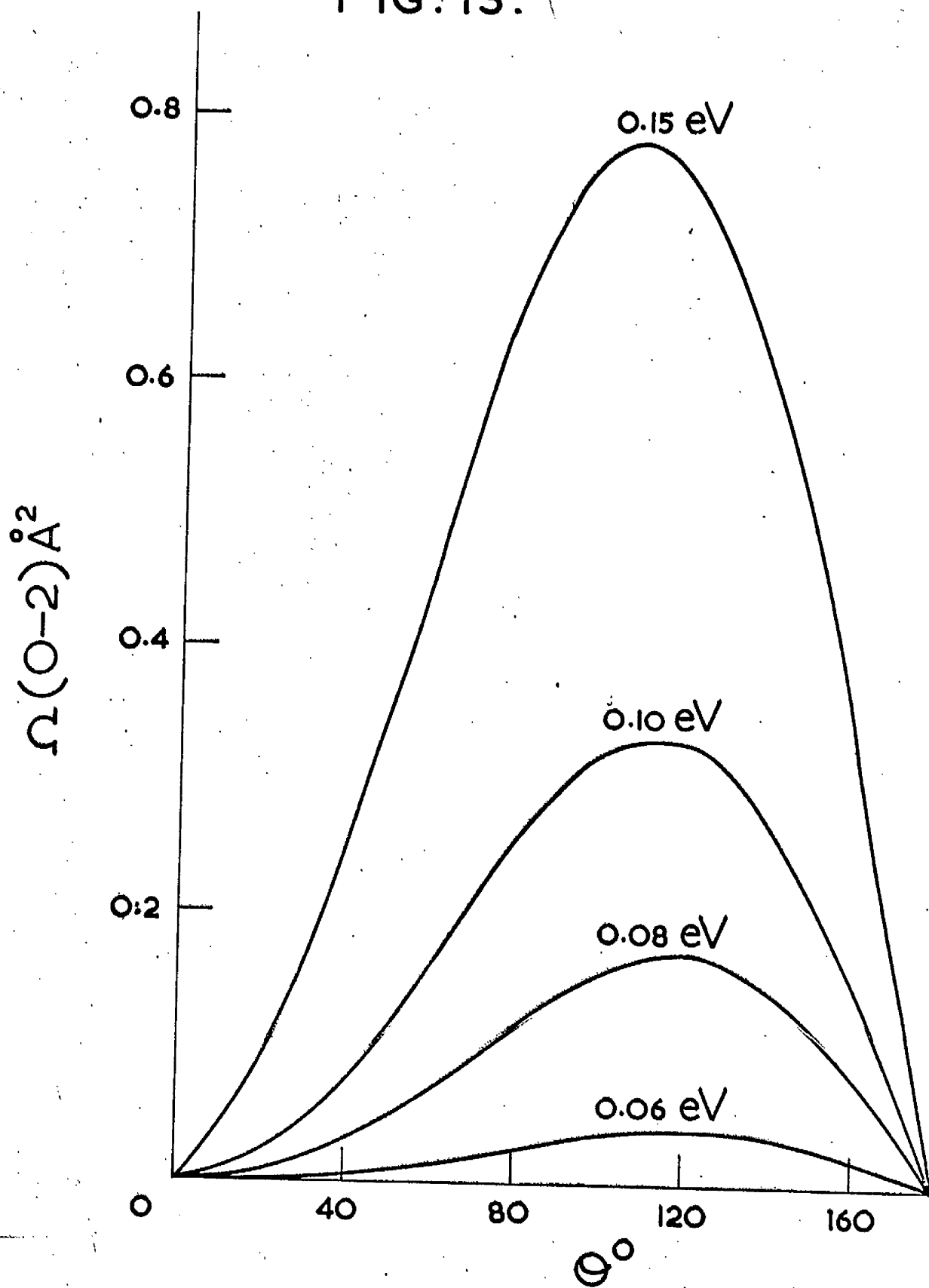
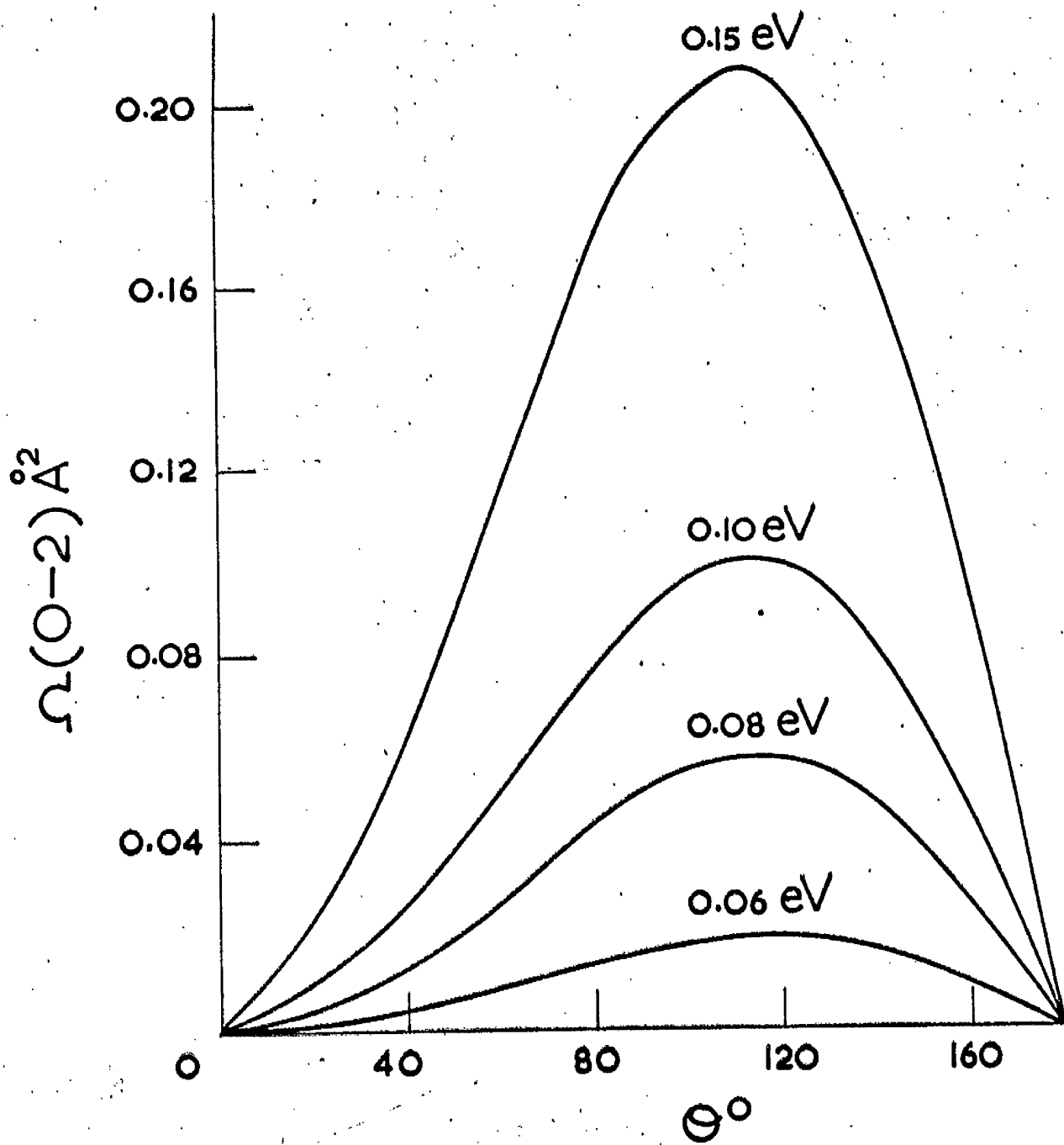


FIGURE 14

Angular distribution $\mathcal{N}(0-2)$ for $H_2 - H_2$.

FIG. 14.



CHAPTER J

We consider the effects which may arise in the elastic scattering when the impact energy is below the threshold value necessary to produce excitation to a higher level. In particular, we are looking for resonances, i.e. a sudden variation in the value of the elastic cross section.

A two state approximation is defined by equations G7 with $J = 0$. The equations can be written

$$\left[\frac{d^2}{dr^2} + k_0^2 - V_{00} \right] u_0 = V_{01} u_1, \quad J1$$

$$\left[\frac{d^2}{dr^2} + k_1^2 - \frac{6}{r^2} - V_{11} \right] u_1 = V_{10} u_0, \quad J2$$

and solutions u_0 and u_1 are required such that,

u_0 and u_1 are regular at the origin,

$$u_0 \sim \sin(k_0 r) + R \cos(k_0 r), \quad J3$$

$$u_1 \sim B \exp[-(Kr)], \quad J4$$

where k_1 is now complex and $k_1^2 = -K^2$, K being taken positive.

If V_{11} is attractive and sufficiently large in absolute magnitude then there will be a set of solutions of the equation

$$\left[\frac{d^2}{dr^2} - K^2 - \frac{6}{r^2} - V_{11} \right] u_1 = 0, \quad J5$$

corresponding to the eigenvalues $K_1^2 \dots K_n^2$. It is to be expected that variations in the elastic cross section will appear at values of k_0^2 such that K^2 is close to one of the values $K_1^2 \dots K_n^2$.

The matrix element T_{00} may be continued into the region where $k_1^2 < 0$ by replacing k_1 by iK . This is because outgoing waves of wave number k_1 are then replaced by exponentially decreasing functions as required.

This is not possible for R_{00} which instead is calculated, for $k_1^2 < 0$ from

$$T_{00} = 1 - e^{2i\gamma_0^0}$$

where γ_0^0 is the phase shift for elastic scattering from the ground state. Above the threshold γ_0^0 is complex but below it is real and equal to $\tan^{-1} R_{00}$.

Since T and R are both symmetric two by two matrices they may be expressed in terms of three variables (Mott and Massey 1965). One of these, c , is taken to be R_{00} above the threshold and the other two are defined in terms of T_{11} ,

$$T_{11} = 1 - e^{2i\gamma_0^1}$$

where γ_0^1 is the complex phase shift for elastic scattering of particles of wave number k_1 .

If we now assume that there is no change in angular momentum,
i.e. no term in $6/r^2$ in J_2 then

$$k_1 \cot \gamma_0' = -\frac{1}{a} = -\frac{1}{A - \lambda B}, \quad B > 0, \quad J7$$

and A and B define the other two variables.

Following Mott and Massey (1965),

$$T_{00} = -2 \left(\frac{1 + \lambda c}{1 - \lambda c} \right) \left(\frac{c}{1 + \lambda c} + \frac{\lambda k_1 B}{1 + \lambda k_1 a} \right), \quad J8$$

$$T_{01} = T_{10} = \frac{[k_1 B (1 + c^2)]^{\frac{1}{2}}}{(1 - ic)(1 + \lambda k_1 a)}, \quad J9$$

$$R_{11} = k_1 (Bc - A), \quad J10$$

$$R_{01} = R_{10} = [k_1 B (1 + c^2)]^{\frac{1}{2}}, \quad J11$$

where R matrix elements only apply above the threshold. The
elastic cross section is given by

$$\frac{\pi}{k_0^2} \cdot |T_{00}|^2,$$

and, for $k_1^2 > 0$,

$$|T_{00}|^2 = 4 \left| \frac{c}{1 + ic} + \frac{\lambda k_1 B}{1 + \lambda k_1 a} \right|^2. \quad J12$$

Expanding in powers of k_1 , we see that, just above the threshold,

$$|\tau_{00}|^2 = \frac{4c^2}{1+c^2} (1 - 2Bk_1) \quad \text{J13}$$

To obtain the corresponding formula just below the threshold we replace k_1 by iK in J12 to give

$$|\tau_{00}|^2 = \frac{4c^2}{1+c^2} \left(1 - 2B \frac{K}{c}\right) \quad \text{J14}$$

Since $B > 0$ it follows that the elastic cross section falls at least initially in passing above the threshold. In passing below the threshold it will rise or fall depending on the sign of c . In either case the cross section has an infinite derivative at the threshold. This is expected since from J9 the cross section for inelastic collisions rises as k_1 and

$$\frac{d\sigma_{inel}}{dk_0} \propto \frac{dk_1}{dk_0} = \frac{d}{dk_0} (k_0^2 - \lambda)^{\frac{1}{2}} = \frac{k_0}{k_1} \xrightarrow{k_1 \rightarrow 0} \infty \quad \text{J15}$$

Thus we would expect the onset of the inelastic processes with infinite derivative with respect to k_0 to have a similar effect on the elastic cross section.

We now consider the case where the incident and inelastically scattered waves are associated with different angular quantum numbers, i.e. the term $6/r^2$, corresponding to $\ell = 2$ is included in equation J2. In this case,

$$T_{01} \propto k_1^{l+\frac{1}{2}}$$

J16

provided $r^{l+2} V_{01} \rightarrow 0$ as $r \rightarrow \infty$,

J17

and hence the inelastic cross section will rise as k_1^{2l+1} for small k_1 .

Thus

$$\begin{aligned} \frac{\delta \sigma_{inel}}{\delta k_0} &= \frac{\delta k_1^{2l+1}}{\delta k_0} = \frac{\delta}{\delta k_0} \left(k_0^2 - \lambda \right)^{l+\frac{1}{2}} \\ &= k_0 (2l+1) k_1^{l-\frac{1}{2}} \rightarrow 0 \text{ as } k_1 \rightarrow 0. \end{aligned} \quad \text{J18}$$

Thus the cross section for inelastic collisions no longer possesses an infinite derivative with respect to k_0 at the threshold and we would expect no anomalous behaviour. Further confirmation of this last statement can be obtained by extending the previous method.

This has been verified numerically in the case of rotational excitation of a hydrogen molecule by a hydrogen atom. Using the potential defined in chapter I we find that condition J17 is satisfied since V_{01} goes off asymptotically as $1/r^2$.

The behaviour of the cross section is manifested in the variation of the phase shift defined in J3.

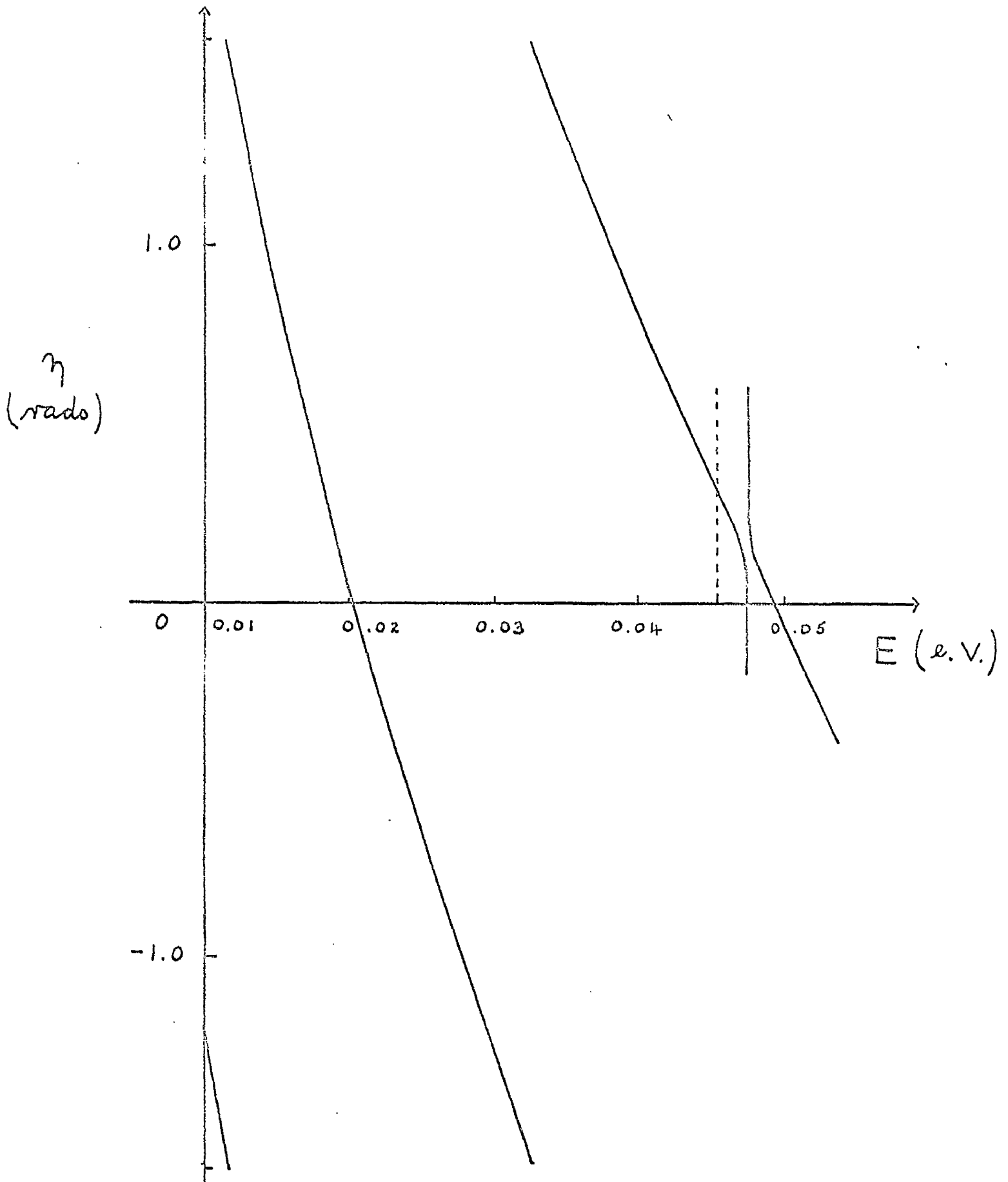
The equations J1 and J2 are solved subject to the boundary conditions J3 and J4, using the program described in chapter F.

The phase shifts are printed out for values of energy below the threshold of 0.045 e.V. Values of the phase shift above the threshold, where both channels are open, are calculated by the usual close coupling program of chapter E. The results are shown in Fig 15. It is clear that no abnormal behaviour occurs just below the threshold, the phase shift varying smoothly to match up with the values above the threshold. The discontinuity at an energy of 0.0473 e.V. is the same type of singularity as described at the end of chapter E. Thus these results confirm that a resonance is not likely to be found in any case in which there is an internal change in angular momentum.

FIGURE 15

Graph of η_1 versus energy E (e.V.) showing smooth behaviour through the threshold.

FIG. 15.



CHAPTER KIntroduction

Rotational excitation of homonuclear diatomic molecules by slow electrons has been extensively studied in the past. The first attempts to treat rotational excitation of these molecules failed to obtain cross sections large enough to explain the observed energy losses (Morse 1953, Carson 1954). In these investigations all long range effects were neglected.

Gerjuoy and Stein (1955 a, b) pointed out that the long range interaction between an electron and the quadrupole moment of the molecule would account for these large energy losses. There are discrepancies between their calculations, based on the Born approximation, and analyses of experimental values (Engelhardt and Phelps, 1963). Dalgarno and Moffet (1963) showed that polarisation of the molecule by the incident electron would result in an additional long range force which would increase the cross section for molecular hydrogen. It was found that while inclusion of the polarisation correction improved the agreement in the case of H_2 , the results were still too small. This last discrepancy was resolved by considering distortion of the wave function describing the scattered electron by the electron-molecule interaction. Investigations have been carried out using the distorted wave approximation, by Mjølness

120

and Sampson (1965), Takayanagi and Geltman (1964, 1965) and Dalgarno and Henry (1965) with the result that the cross sections obtained are in fair agreement with experiment. A major uncertainty in the $e - H_2$ scattering problem is the manner of including the polarisation interaction. At low energy this is usually accomplished by cutting off the asymptotic form of the potential at some value of r determined by fitting the calculated elastic cross section to the experimental values.

In this chapter the close coupling approximation is applied to the rotational excitation of a hydrogen molecule by a slow electron. The program described in chapter E has been altered to include the more complicated potential function and also the initial step has been modified so that, for $l = 0$, the integration effectively starts at the origin.

The choice of parameters involved in the inclusion of the polarisation term is discussed and the results are compared with the equivalent distorted wave approximation and the work of other authors.

Potential function for $e - H_2$

The potential used to represent the interaction between a hydrogen molecule and an incident slow electron is that given by Dalgarno and Henry (1965).

The potential is expanded as in A17,

$$V(r, \theta) = - \sum_{\mu=0}^2 \left\{ v_{\mu}^N(r) - v_{\mu}^E(r) \right\} P_{\mu}(\cos \theta), \quad K1$$

where

$$v_0^N(r) = \begin{cases} \frac{2}{r} & , \quad r > 0.7 ; \\ 2.857 & , \quad r < 0.7 ; \end{cases} \quad K2$$

$$v_2^N(r) = \begin{cases} \frac{0.98}{r^3} & , \quad r > 0.7 ; \\ 5.831 r^2 & , \quad r < 0.7 ; \end{cases} \quad K3$$

$$v_0^E(r) = \frac{2}{r} \sum_{\gamma=1}^3 \left[\sum_{\lambda=1}^{14} A_{\lambda\gamma} r^{\lambda-1} \exp(-a_{\lambda\gamma} r) - A_{1\gamma} \right], \quad K4$$

$$v_2^E(r) = \frac{2}{r^3} \sum_{\gamma=1}^5 \left[\sum_{\lambda=1}^{12} B_{\lambda\gamma} r^{\lambda-1} \exp(-b_{\lambda\gamma} r) - B_{1\gamma} \right], \quad K5$$

r being measured in units of Bohr radius and $v(r)$ is in atomic units. Atomic units will be used throughout this chapter.

The coefficients A_{ij} , a_j , B_{ij} , b_j are listed in Tables 12, 13 to six decimal places. The functions

$$v_{\mu}(r) = v_{\mu}^N(r) - v_{\mu}^E(r), \quad \mu = 0, 2;$$

are illustrated in Fig 16.

In the present form equations K4 and K5 are not in a suitable form for computation.

e.g. for $r > 0.7$,

$$N_0(r) = \frac{2}{r} + \frac{2}{r} \sum \left[A_{\lambda\gamma} - \sum A_{\lambda\gamma} r^{\lambda-1} \exp(-a_\gamma r) \right], \quad K6$$

and since the asymptotic form of $v_0(r)$ does not involve terms in $1/r$ these must cancel. The coefficients A_{ij} are only tabulated to six decimal places so rounding error will bring in a contribution from the $1/r$ term. Using the fact that $\sum_{\gamma=1}^3 A_{1j} = -1$ this formula may be rewritten for $r > 0.7$,

$$N_0(r) = -\frac{2}{r} \sum_{\gamma=1}^3 \sum_{\lambda=1}^{14} A_{\lambda\gamma} r^{\lambda-1} \exp(-a_\gamma r),$$

which may be evaluated without the previous trouble.

In the case of $v_2(r)$, for $r < 0.7$,

$$N_2(r) = 5.831 r^2 + \frac{2}{r^3} \sum_{\gamma=1}^5 \left[B_{1\gamma} - \sum_{\lambda=1}^{12} B_{\lambda\gamma} r^{\lambda-1} \exp(-b_\gamma) \right] \quad K7$$

and from symmetry conditions (Geltman and Takayanagi 1965) $v_2(r)$ is zero at $r = 0$. Hence all the coefficients of $1/r^s$, $s = 0, 1, 2, 3$ must vanish. Again rounding errors will occur and the term in $1/r^3$ will dominate the value of $v_2(r)$ as r tends to zero.

The computed values begin this spurious increase for values of $r < 0.3$. Thus it was decided to replace the entire expression K7 for $v_2(r)$ by a function of the form Pr^2 which will give the correct behaviour at the origin. Here P is a constant.

At large values of r , $v_0(r)$ falls off exponentially and $v_2(r)$ as $-0.447 / r^3$. Dalgarno and Moffet (1963) have calculated the quadrupole moment of a hydrogen molecule to be 0.473 so the computed $v_2(r)$ has been increased by a factor 1.058 to give the correct asymptotic behaviour $-\frac{0.473}{r^3}$.

This potential has ignored the long range terms due to the polarisation interaction and these are included asymptotically as

$$-\frac{\alpha_\mu}{2\pi^4} \text{ in } v_\mu(r).$$

α_0 was taken as $5.33 a_0^3$ and α_2 as $1.25 a_0^3$ (Takayanagi and Geltman 1965). This form would dominate the potential for small values of r so it is cut off near the origin by multiplying by a factor

$$(1 - \exp[-(\beta r)^4]),$$

(Mjølness and Sampson 1965) where β is an arbitrary parameter which controls the effective strength of the polarisation. The final values of the potential are then obtained by adding

$$-\frac{\alpha_\mu}{2\pi^4} (1 - \exp[-(\beta r)^4])$$

K8

to the functions $v_\mu(r)$.

Discussion of results

Arthurs and Dalgarno (1960) showed that for collisions of slow electrons with molecules the major contribution to the elastic cross section comes from values of J near to values of j corresponding to low values of ℓ . Thus to calculate the elastic cross section given by $j = j' = 0$ the important equation is that with $\ell = 0$. For the inelastic scattering defined by $j = 0, j' = 2$ the equation with $\ell = 1, \ell' = 1$ for $J = 1$ gives the largest contribution.

If the polarisation terms were neglected, i.e. $\beta = 0$ in K8 then the values of the elastic cross section obtained were very much greater than the experimental values. As the parameter β was increased so the elastic cross section decreased while the inelastic cross section increased (Fig 17). A value of $\beta = 0.6$ gave elastic cross sections over the energy range up to 1 e.V. which fitted reasonably well with the experimental values calculated by Engelhardt and Phelps (1963). At an energy of 1 e.V. the inelastic cross section increased by a factor four, as β varied from 0 to 0.6, showing that inclusion of the polarisation term is of major importance in these calculations. This investigation of a suitable choice of β was done using the distorted wave approximation. The calculations were repeated using the close coupling approximation (Fig 18). In all cases the inelastic cross section as given by the close coupling approximation was about 10% higher than that given by the distorted wave approximation. At

first glance this seems surprising considering the argument of chapter H. However, if the off-diagonal matrix elements are small, it is possible, initially, for the close coupling results to be greater than those given by the distorted wave. This has been confirmed by comparing the inelastic cross section for different values of λ , where λ is a constant multiplying the off-diagonal matrix elements. The behaviour is illustrated in Fig 19 which is consistent with the conclusions of chapter H.

Also, it was apparent that the $j = 0$ elastic cross section for scattering in the energy range below 1 e.V. was sensitive to the coupling with an inelastic channel. For example, the $j = 0$ elastic cross section was reduced from $65 a_0^2$ to $56 a_0^2$ at $E = 1$ e.V. by including coupling with the $j' = 2$ state.

In the final graph, Fig 20, we compare our results, using a value of $\beta = 0.6$, with those of previous workers, over the energy range less than 1 e.V. Dalgarno and Henry (1965) used the distorted wave approximation with the same potential given in equation K1 but omitting the polarisation terms. Their results are denoted DH and are smaller than all the others which include the polarisation. Dalgarno and Moffet (1963) included the polarisation term and, using the Born approximation, obtained an extension of the theoretical formulae derived by Gerjuoy and Stein (1955 a,b). This formula gives values (DM) which are larger than in the previous case.

Takayanagi and Geltman (1965) have applied the distorted wave to the asymptotic form of the potential,

$$V(r) = -\frac{\alpha}{2r^4} - \left(\frac{Q}{r^3} + \frac{\alpha'}{2r^4} \right) P_2(\cos\theta), \quad K9$$

and they took $Q = 0.464$, $\alpha = 5.3$, $\alpha' = 1.25$. This asymptotic form was cut off at some value of r (say R), the non-spherical part was taken to zero proportional to r^2 and the spherical part retained the value $-\alpha/2R^4$ for $r < R$. They chose the cut off value $R = 1.2$ as that value which gave the best fit to the experimental values of the elastic cross section. This choice brings in rather more of the polarisation than we have taken and hence their results give larger inelastic cross sections (TG).

Mjolness and Sampson (1965) also considered only the asymptotic form of the potential but they used a more sophisticated method of determining the cut off parameter. They included the polarisation term with both a non-exponential cut off in which r^4 is replaced by $r^4/(r_0^2 + r^2)^2$ and an exponential cut off,

$$1 - \exp \left[- \left(r/r_0 \right)^4 \right].$$

The exponential cut off proved to be more satisfactory in the case of the hydrogen molecule so this is the case we quote. The parameter r_0 is chosen such that agreement with the experimental values of the elastic cross section is obtained. Their value of $r_0 = 1.8$ compares favourably with our value of $\beta = 0.6$. An additional parameter r_c is also introduced at which point the contribution from the quadrupole term is sharply cut off. r_c is chosen to be

1 a₀ for a hydrogen molecule. Their potential is

$$V(r) = -\frac{\alpha}{2r^4} G(r) - \frac{Q}{r^3} D(r) P_2(\cos \theta), \quad \text{K10}$$

where

$$D(r) = \theta(r) + \frac{\alpha'}{2Qr} G(r),$$

and $G(r) = 1 - \exp\left[-\left(\frac{r}{r_0}\right)^4\right],$

$$\begin{aligned} \theta(r) &= 1 \quad \text{if } r > r_c, \\ &= 0 \quad \text{if } r < r_c. \end{aligned}$$

They took the values $Q = 0.49$, $\alpha = 5.5$, $\alpha' = 1.38$.

The problem of finding a potential which represents the long range forces correctly, includes a minimum number of arbitrary parameters and is easy to handle, is difficult. In these respects our potential which includes the cut off of the quadrupole term in the definition of the short range terms and which only includes the one cut off parameter appears to be the most satisfactory of the potentials described.

The results published in this chapter are in good agreement with similar calculations recently carried out by Lane and Geltman (1967).

TABLE 12

Coefficients A_{ij} and a_{ij} for e - H₂ potential.

i	A_{i1}	A_{i2}	A_{i3}
1	-0.99963	-0.00034	-0.00003
2	-3.16654	-0.00381	-0.00048
3	-4.54009	-0.02122	-0.00368
4	-3.75910	-0.07770	-0.01863
5	-1.86801	-0.20975	-0.07017
6	-0.66033	-0.44262	-0.20930
7	-0.28954	-0.75373	-0.51385
8	-0.24780	-1.04861	-1.06440
9	+0.03922	-1.17911	-1.88985
10	0.0	-1.00688	-2.89977
11	0.0	-0.47909	-3.84426
12	0.0	+0.14033	-4.34352
13	0.0	+2.73735	-3.99879
14	0.0	0.0	-2.54867

a_1	a_2	a_3
4.14286	12.42857	16.57143

TABLE 13

Coefficients B_{ij} and b_{ij} for e - H₂ potential.

i	B_{i1}	B_{i2}	B_{i3}	B_{i4}	B_{i5}
1	-0.26498	-0.00139	-0.00008	-0.00003	-0.00001
2	-1.09777	-0.01152	-0.00097	-0.00039	-0.00011
3	-2.27396	-0.04772	-0.00600	-0.00283	-0.00095
4	-3.14024	-0.13179	-0.02487	-0.01370	-0.00527
5	-3.25239	-0.27300	-0.07727	-0.04966	-0.02185
6	-2.48435	-0.44978	-0.19190	-0.14396	-0.07241
7	-0.11533	-0.01498	-0.39568	-0.34719	-0.19977
8	0.0	+0.15209	-0.69283	-0.71485	-0.47130
9	0.0	-0.08320	-0.08131	-1.27733	-0.96840
10	0.0	-0.05082	-0.03954	-1.99882	-1.75415
11	0.0	0.0	-0.02352	-0.25251	-2.82053
12	0.0	0.0	0.0	-0.04941	-4.03232
	b_1	b_2	b_3	b_4	b_5
	4.14286	8.28571	12.42857	14.50000	16.57143

FIGURE 16

Potential function $V(r)$ used in the $e^- - H_2$ collision.

FIG. 16.

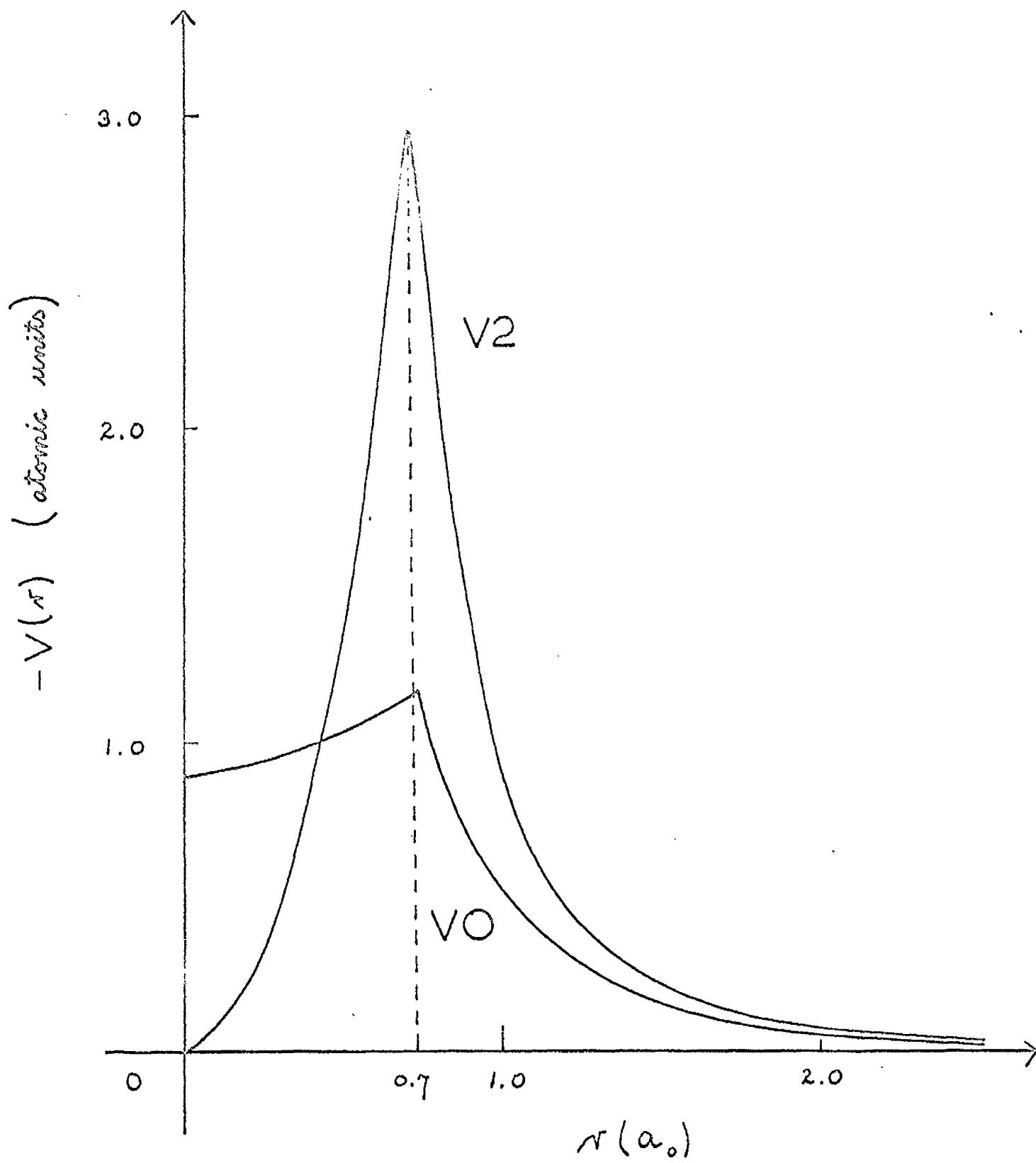


FIGURE 17

Variation in the elastic cross section $\sigma^-(0-0)$ and the inelastic cross section $\sigma^-(0-2)$ depending on the value of the cut-off parameter β , for energy $E = 1.0 \text{ e.V.}$

FIG. 17.

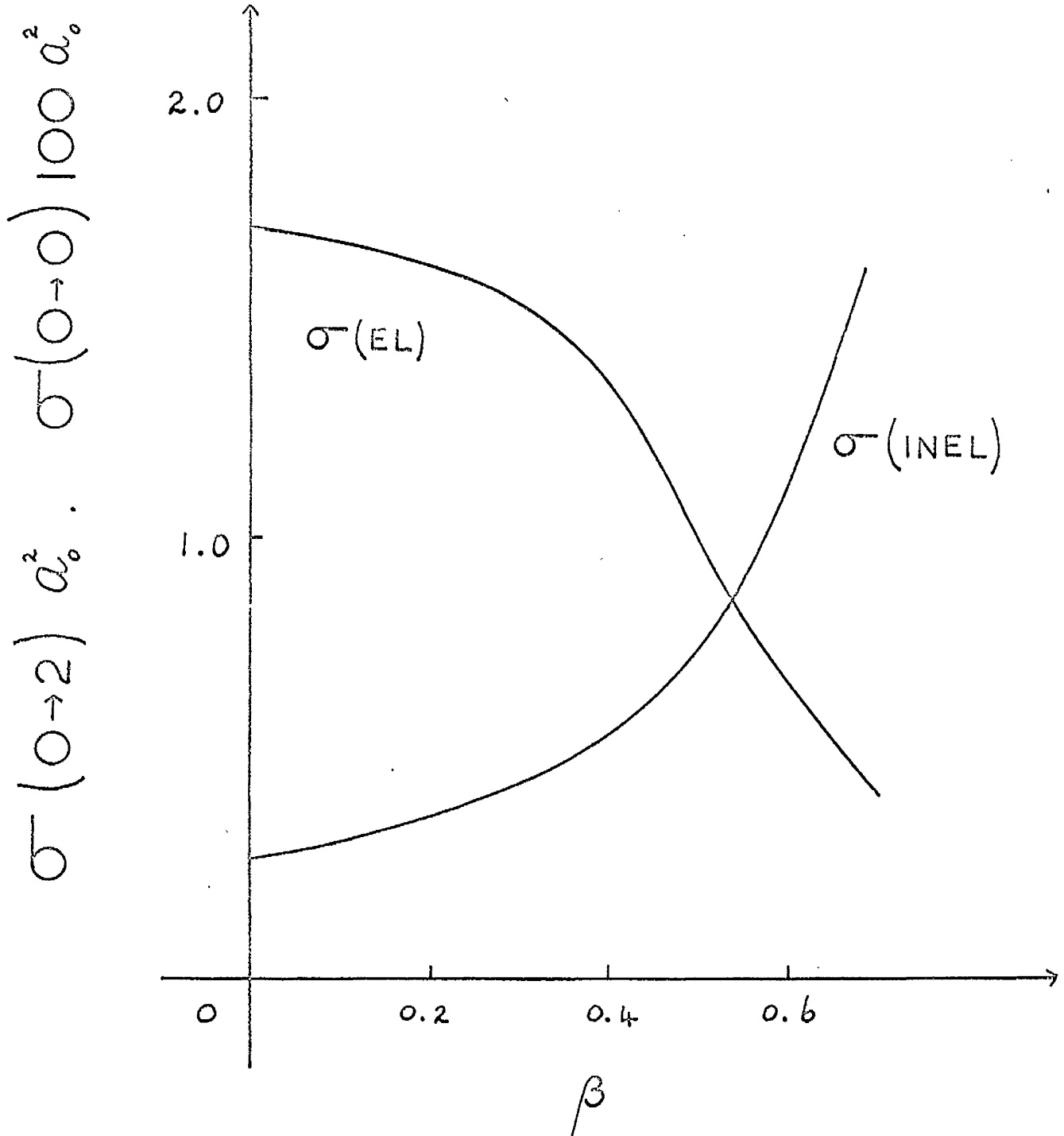


FIGURE 18

Comparison of the inelastic cross section $\sigma_{(0-2)}$ versus energy E (e.V.) for several values of $\beta = 0.2, 0.4, 0.6$, using both the distorted wave (DW) and close coupling (CC) approximations.

FIG. 18.

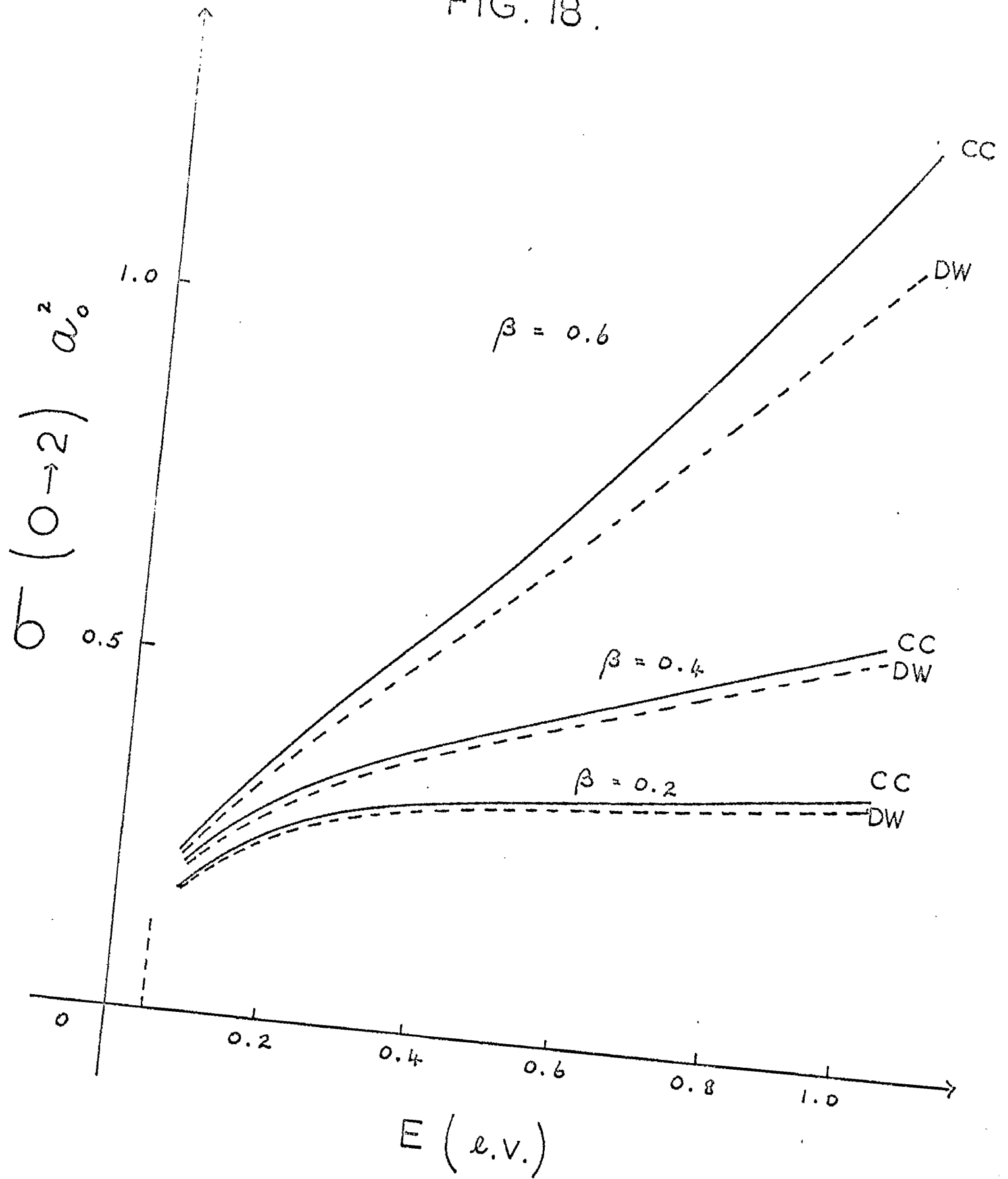
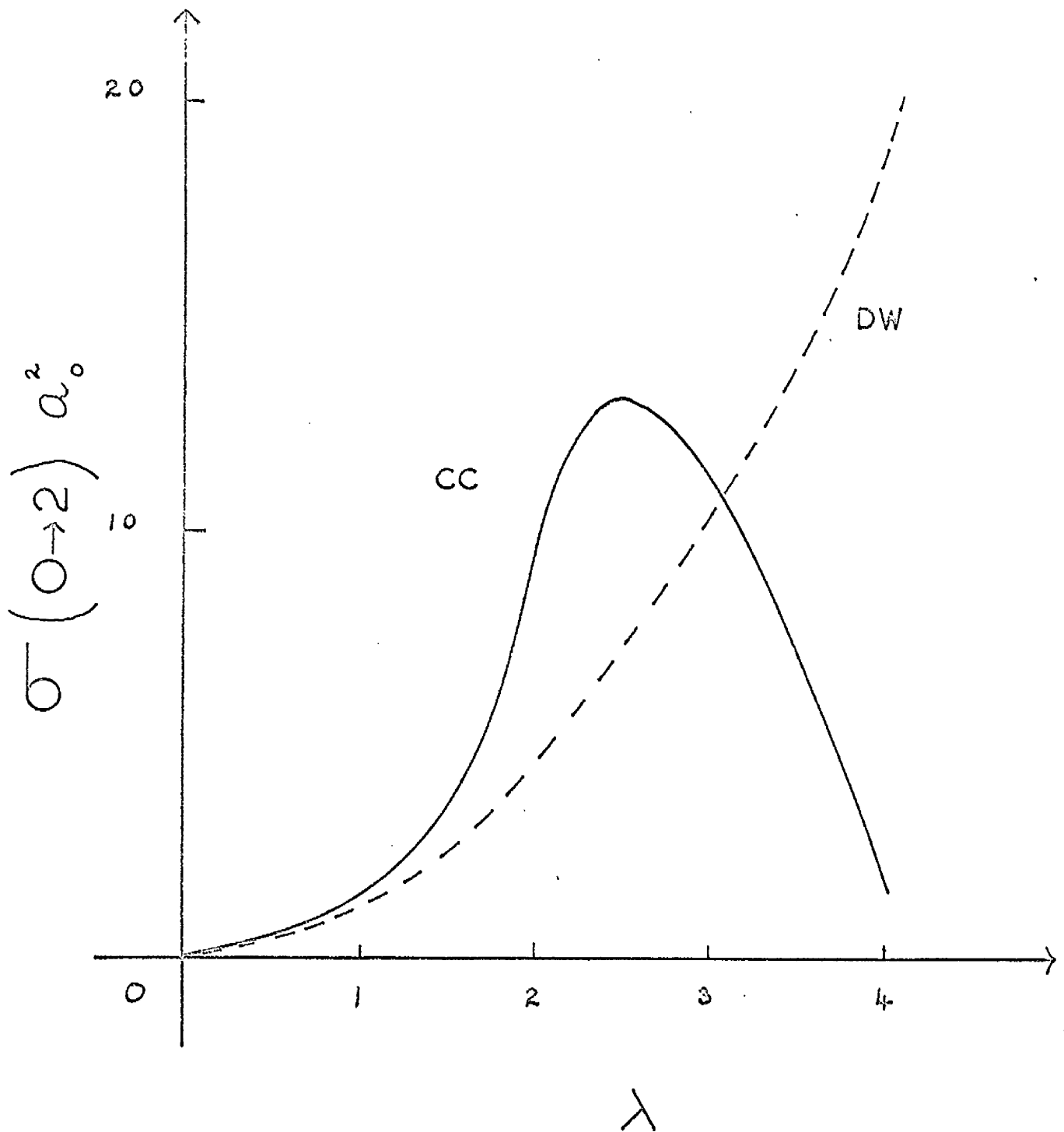


FIGURE 19

Calculated values of the inelastic cross section $\sigma(0-2)$ versus coupling coefficient λ , for $E = 1.0$ e.V., using both the distorted wave (DW) and close coupling (CC) approximations.

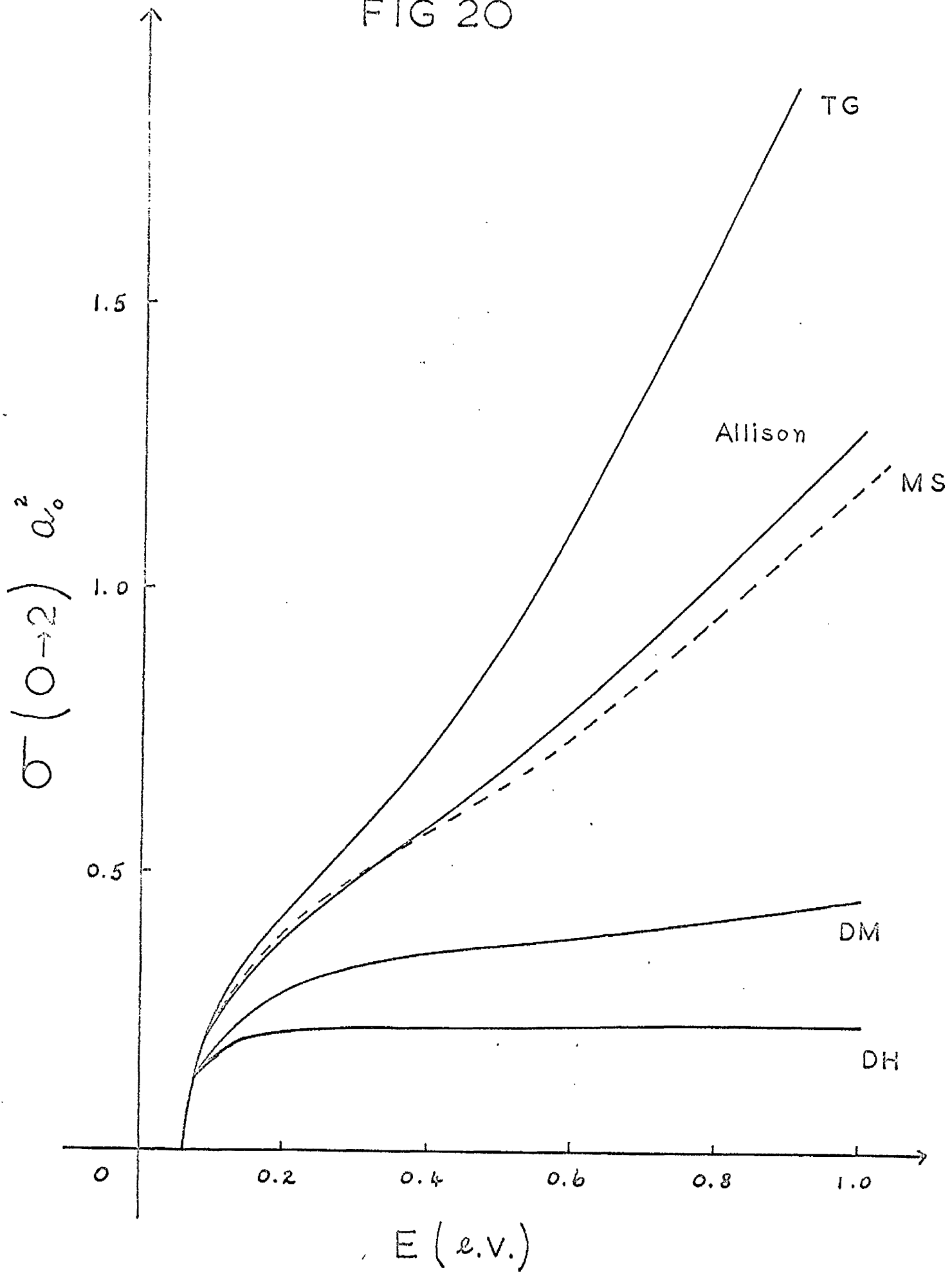
FIG. 19



F I G U R E 20

Comparison of the inelastic cross section $\sigma(0-2)$ calculated in this thesis with the work of previous authors : (DH) Dalgarno and Henry, (DM) Dalgarno and Moffet, (MS) Mjølness and Sampson, (TG) Takayanagi and Geltman.

FIG 20



REFERENCES

- Allison, A.C., and Dalgarno, A., 1967, Proc. Phys. Soc., 90, 609.
- Arthurs, A.M., and Dalgarno, A., 1960, Proc. Roy. Soc., A, 256, 540.
- Barnes, L.L., Lane, N.F., and Lin, C.C., 1965, Phys. Rev., 137, A 388.
- Berstein, R.B., Dalgarno, A., Massey, H.S.W., and Percival, I.C.,
1963, Proc. Roy. Soc., A, 274, 427.
- Biedenharn, L.C., Blatt, J.M., and Rose, M.E., 1952, Rev. Mod. Phys.,
24, 249.
- Blatt, J.M., and Biedenharn, L.C., 1952, Rev. Mod. Phys., 24, 258.
- Buckingham, R.A., 1960, Planet. Space. Sci., 3, 295.
- Buckingham, R.A., 1962, Numerical Solution of Ordinary and Partial
Differential Equations (Ed. L. Fox), Pergamon Press.
- Buckingham, R.A., and Massey, H.S.W., 1942, Proc. Roy. Soc., A, 179, 123.
- Burke, P.G., and Smith, K., 1962, Rev. Mod. Phys., 34, 458.
- Carson, T.R., 1954, Proc. Phys. Soc., A67, 909.
- Condon, E.U., and Shortley, G.H., 1935, Theory of Atomic Spectra, Cambridge University Press.
- Dalgarno, A., 1963, Rev. Mod. Phys., 35, 611.
- Dalgarno, A., and Henry, R.J.W., 1964, Atomic Collision Processes,
Ed. M.R.C. McDowell (Amsterdam: North Holland),
914.
- Dalgarno, A., and Henry, R.J.W., 1965, Proc. Phys. Soc., 85, 679.
- Dalgarno, A., and Moffet, R.J., 1963, Proc. Nat. Acad. Sci. India, A, 33, 5
511.

- Dalgarno, A., Henry, R.J.W., and Roberts, G.S., 1966, Proc. Phys. Soc. 88, 611.
- Davison, W.D., 1963, Disc. Faraday Soc., 33, 71.
- Davison, W.D., 1964, Proc. Roy. Soc., A, 280, 227.
- De Vogelaere, R., 1955, J. Res. Nat. Bur. Stand., 54, 119.
- Engelhardt, A.G., and Phelps, A.V., 1963, Phys. Rev., 131, 2115.
- Fox, L., 1962, Numerical Solution of Ordinary and Partial Differential Equations (Ed. L. Fox), Pergamon Press.
- Fox, L., and Goodwin, E.T., 1949, Proc. Camb. Phil. Soc., 45, 373.
- Gerjuoy, E., and Stein, S., 1955a, Phys. Rev., 97, 1671.
- Gerjuoy, E., and Stein, S., 1955b, Phys. Rev., 98, 1848.
- Hartree, D.R., 1957, The Calculation of Atomic Structures (New York: John Wiley).
- Hirschfelder, J.O., Curtiss, C.F., and Bird, R.B., 1954, Molecular Theory of Gases and Liquids (New York: John Wiley).
- Kopal, Z., 1955, Numerical Analysis (London: John Wiley).
- Lane, N.F., and Geltman, S., 1967 (unpublished).
- Lawley, K.P., and Ross, J., 1965, J. Chem. Phys., 43, 2930.
- Mayers, D.F., 1962, Numerical Solution of Ordinary and Partial Differential Equations (Ed. L. Fox), Pergamon Press.
- Modern Computing Methods, 1961, Notes on Applied Science, No. 16 (H.M.S.O.)
- Morse, P.M., 1953, Phys. Rev., 90, 51.
- Mott, N.F., 1952, Elements of Wave Mechanics (Camb. Univ. Press).

- Mott, N.F., and Massey, H.S.W., 1949, *The Theory of Atomic Collisions* (Oxford: Clarendon, 2nd. edit.).
- Mott, N.F., and Massey, H.S.W., 1965, *The Theory of Atomic Collisions* (Oxford: Clarendon, 3rd. edit.).
- Mjolness, R.C., and Sampson, D.H., 1965, *Phys. Rev.*, 140, A1466.
- Percival, I.C., 1960, *Proc. Phys. Soc.*, 76, 206.
- Racah, G., 1942, *Phys. Rev.*, 62, 438.
- Roberts, C.S., 1963, *Phys. Rev.*, 131, 209.
- Robertson, H.H., 1956, *Proc. Camb. Phil. Soc.*, 52, 538.
- Rose, M.E., 1957, *Elementary Theory of Angular Momentum* (London: Chapman and Hall).
- Schwarz, R.N., and Herzfeld, K.F., 1954, *J. Chem. Phys.*, 22, 767.
- Seaton, M.J., 1961, *Proc. Phys. Soc.*, 77, 174.
- Smith, K., Henry, R.J.W., and Burke, P.G., 1966, *Phys. Rev.*, 147, 21.
- Smith, K., 1965 (unpublished).
- Tables of Spherical Bessel Functions, 1947, *Nat. Bur. Stand.* (New York: Columbia Univ. Press).
- Takayanagi, K., 1952, *Prog. Theor. Phys.*, 8, 497.
- Takayanagi, K., 1957, *Proc. Phys. Soc.*, A70, 348.
- Takayanagi, K., 1963, *Prog. Theor. Phys.*, Japan (Suppl.), 25, 1.
- Takayanagi, K., and Geltman, S., 1964, *Phys. Letters*, 13, 135.
- Takayanagi, K., and Geltman, S., 1965, *Phys. Rev.*, 138, A1003.

Watson, G.N., 1944, Theory of Bessel Functions (Camb. Univ. Press).

Wu, T.Y., and Ohmura, T., 1962, Quantum Theory of Scattering (London: Prentice-Hall).

Zener, C., 1931, Phys. Rev., 37, 556.